

GEOLOGY AND SULFIDE MINERALIZATION OF THE  
DULUTH COMPLEX - VIRGINIA FORMATION CONTACT  
MINNAMAX DEPOSIT, ST. LOUIS COUNTY, MINNESOTA

A THESIS

SUBMITTED TO THE FACULTY OF THE GRADUATE SCHOOL  
OF THE UNIVERSITY OF MINNESOTA

BY

WILLIAM FULLER MATLACK

IN PARTIAL FULFILLMENT OF THE REQUIREMENTS

FOR THE DEGREE OF

MASTER OF SCIENCE

AUGUST, 1980

ABSTRACT

The Minnamax deposit, near Babbitt, Minnesota, is a large, low-grade magmatic iron-copper-nickel sulfide deposit at the contact of the Duluth Complex and the Virginia Formation. The Virginia Formation consists of pelitic hornfels with locally abundant calc-silicate pods and contains diabase intrusions - all have been deformed and metamorphosed to the pyroxene hornfels facies by the Duluth Complex. The Duluth Complex, emplaced as a crystal mush, consists of sulfide-bearing troctolitic rocks, commonly noritic near the contact, which contain barren gabbro to peridotite xenoliths. The Duluth Complex - Virginia Formation contact is highly irregular, characterized by numerous Duluth Complex apophyses and Virginia Formation xenoliths. Granite to diorite dikes cut all lithologies.

Sulfide mineralization, consisting of pyrrhotite, pentlandite, chalcopyrite, and cubanite, is primarily disseminated in the troctolitic rocks within 1000 feet of the contact. Sulfide veins fill fractures and breccia zones in both the Duluth Complex and the Virginia Formation. Pelitic hornfels adjacent to the veins and the sulfide-bearing troctolitic rocks commonly is replaced by sulfides. In one area the veins are sufficiently concentrated to form a high-grade sulfide body, the Local Boy deposit. The veins probably formed by filter-pressing of sulfide liquid from the troctolitic rocks into fractures. Some distinctly chalcopyrite-cubanite rich veins appear to have formed by separation of a copper-rich liquid from a pyrrhotite solid solution at magmatic temperatures. Late stage hydrothermal solutions deposited sulfides and gangue along fractures and in calc-silicate pods.

## ACKNOWLEDGEMENTS

AMAX Exploration, Inc. granted permission to study the Minnamax deposit, and provided logistical and financial support. Stanley N. Watowich, James E. Kulas, and Tony J. Nemgar introduced the writer to the geology and sulfide mineralization at Minnamax, and provided insights into the nature of the deposit. While the writer benefitted greatly from their knowledge and ideas, he assumes responsibility for interpretations and assumptions presented herein.

Dr. Ralph W. Marsden and Dr. James A. Grant were advisors to this thesis. Their interest in the study and critical review of its results are greatly appreciated. Mark H. Kirstein provided information about the petrology of calc-silicate pods within the deposit. The writer was recipient of an AMAX Fellowship during much of the period of study.

## TABLE OF CONTENTS

ABSTRACT . . . . .	i
ACKNOWLEDGEMENTS . . . . .	ii
TABLE OF CONTENTS . . . . .	iii
ILLUSTRATIONS . . . . .	vi
TABLES . . . . .	ix
INTRODUCTION . . . . .	1
Location . . . . .	1
REGIONAL GEOLOGY . . . . .	3
PREVIOUS INVESTIGATIONS IN THE MINNAMAX AREA . . . . .	6
Rock Units . . . . .	6
Biwabik Iron Formation . . . . .	6
Virginia Formation . . . . .	8
Metadiabase . . . . .	8
Duluth Complex . . . . .	9
Inclusions . . . . .	10
Conditions of Metamorphism . . . . .	11
Structure . . . . .	12
PRESENT INVESTIGATION AND METHODS OF STUDY . . . . .	14
GEOLOGY AND SULFIDE MINERALIZATION OF THE DULUTH COMPLEX - VIRGINIA FORMATION CONTACT . . . . .	16
LITHOLOGIES . . . . .	20
Virginia Formation . . . . .	20
Pelitic Hornfels . . . . .	20
Biotite-rich Pelitic Hornfels and Biotite Schist . . . . .	23

## TABLE OF CONTENTS (cont.)

Graphite Schist . . . . .	23
Mafic Hornfels . . . . .	23
Calc-silicate Pods . . . . .	26
Interpretation . . . . .	27
Metadiabase . . . . .	30
Interpretation . . . . .	32
Duluth Complex . . . . .	33
Sulfide-bearing Troctolitic Rocks . . . . .	33
Gabbro to Peridotite Xenoliths . . . . .	37
Interpretation . . . . .	43
Granite to Diorite Dikes . . . . .	45
Interpretation . . . . .	49
SULFIDE MINERALIZATION . . . . .	50
General Occurrence and Distribution . . . . .	50
Disseminated Sulfides in the Troctolitic Rocks . . . . .	50
Sulfide Veins . . . . .	53
Fe-Cu-Ni Sulfide Veins . . . . .	53
Late Stage Veins . . . . .	56
Interstitial Sulfides in the Virginia Formation . . . . .	59
Stratiform Sulfides . . . . .	59
Sulfides in Pelitic Hornfels Adjacent to the Sulfide-bearing Troctolitic Rocks and Fe-Cu-Ni Sulfide Veins . . . . .	59
Sulfides in the Calc-silicate Pods . . . . .	62
Mineragraphy . . . . .	62
Pyrrhotite . . . . .	62
Pentlandite . . . . .	62

## TABLE OF CONTENTS (cont.)

Cubanite-Chalcopyrite . . . . .	65
Ilmenite and Magnetite. . . . .	68
GENESIS OF THE SULFIDE MINERALIZATION . . . . .	70
Syngenetic, Sedimentary Sulfides in the Virginia Formation	70
Magmatic Sulfides. . . . .	70
Hydrothermal Sulfides. . . . .	73
SUMMARY AND CONCLUSIONS . . . . .	74
APPENDIX I: SAMPLES. . . . .	76
APPENDIX II: EXPERIMENTAL WORK IN THE Cu-Fe-S AND Cu-Fe-Ni-S SYSTEMS AND ITS APPLICATION TO THE SULFIDES AT MINNAMAX . . .	82
REFERENCES CITED. . . . .	88

## ILLUSTRATIONS

Figure	Page
1. INDEX MAP OF THE MINNAMAX AREA. . . . .	2
2. GENERAL GEOLOGIC MAP OF NORTHEASTERN MINNESOTA. . . . .	4
3. LOCATIONS OF DRILL CORES STUDIED IN PREVIOUS INVESTIGATIONS. . . . .	11
4. STRUCTURE CONTOUR MAP OF THE TOP OF THE BIWABIK IRON FORMATION. . . . .	13
5. INTERPRETATIVE GEOLOGIC SECTION OF THE STUDY AREA . . . . .	17
6. INTERPRETATIVE BLOCK DIAGRAM OF THE DULUTH COMPLEX - VIRGINIA FORMATION CONTACT IN THE STUDY AREA. . . . .	18
7. INTERPRETATIVE PLAN VIEW OF THE DULUTH COMPLEX - VIRGINIA FORMATION CONTACT ON THE 1700 LEVEL. . . . .	19
8. VIRGINIA FORMATION IN THE MINNAMAX DEPOSIT. . . . .	21
9. PHOTOMICROGRAPH OF PELITIC HORNFELS . . . . .	21
10. PLASTIC DEFORMATION OF THE VIRGINIA FORMATION . . . . .	22
11. PHOTOMICROGRAPH OF ORTHOCLASE POIKILOBLASTS . . . . .	22
12. PHOTOMICROGRAPH OF BIOTITE SCHIST . . . . .	24
13. PHOTOMICROGRAPH OF GRAPHITE SCHIST. . . . .	24
14. PHOTOMICROGRAPH OF MAFIC HORNFELS . . . . .	25
15. BEDDING IN MAFIC HORNFELS . . . . .	25
16. PHOTOMICROGRAPH OF BEDDING CONTACT IN MAFIC HORNFELS. . . . .	26
17. ACF DIAGRAM OF MINERAL ASSEMBLAGES IN THE VIRGINIA FORMATION. . . . .	28
18. PHOTOMICROGRAPH OF METADIABASE. . . . .	31
19. PORPHYRITIC METADIABASE . . . . .	31
20. CLASSIFICATION SCHEME FOR MAFIC IGNEOUS ROCKS . . . . .	35

## ILLUSTRATIONS (cont.)

Figure	Page
21. PHOTOMICROGRAPH OF SULFIDE-BEARING NORITE. . . . .	36
22. PHOTOMICROGRAPH OF OPHITIC AUGITE. . . . .	38
23. CONTACT BETWEEN SULFIDE-BEARING GABBRO AND A TROCTOLITIC XENOLITH . . . . .	38
24. DIKE OF SULFIDE-BEARING TROCTOLITE IN FELDSPATHIC PERIDOTITE XENOLITH. . . . .	40
25. PHOTOMICROGRAPH OF CONTACT BETWEEN SULFIDE-BEARING GABBRO AND PICRITE XENOLITH. . . . .	40
26. PHOTOMICROGRAPH OF A PERIDOTITE XENOLITH . . . . .	42
27. PHOTOMICROGRAPH OF AN ANORTHOSITIC TROCTOLITE XENOLITH. . . . .	44
28. PHOTOMICROGRAPH OF AN OLIVINE GABBRO XENOLITH. . . . .	44
29. GRANITE DIKE IN SULFIDE-BEARING TROCTOLITE . . . . .	47
30. GRANITE DIKE SPECIMEN. . . . .	47
31. PHOTOMICROGRAPH OF GRAPHIC GRANITE . . . . .	48
32. PHOTOMICROGRAPH OF MESOPERTHITE IN A GRANITE DIKE. . . . .	48
33. TEXTURES OF DISSEMINATED SULFIDE MINERALIZATION IN THE TROCTOLITIC ROCKS . . . . .	52
34. PHOTOMICROGRAPH OF A MYRMEKITIC INTERGROWTH OF CUBANITE-CHALCOPYRITE AND HYPERSTHENE IN TROCTOLITE. . . . .	52
35. CHALCOPYRITE-CUBANITE VEIN . . . . .	54
36. Fe-Cu-Ni SULFIDE VEIN IN THE SULFIDE-BEARING TROCTOLITE. . . . .	54
37. Fe-Cu-Ni SULFIDE VEIN IN SULFIDE-BEARING TROCTOLITE. . . . .	55
38. PHOTOMICROGRAPH OF CHALCOPYRITE-CUBANITE VEIN. . . . .	55
39. PHOTOMICROGRAPH OF AN Fe-Cu-Ni SULFIDE VEIN. . . . .	57
40. PHOTOMICROGRAPH OF A BIOTITE-RICH Fe-Cu-Ni SULFIDE VEIN. . . . .	57
41. PHOTOMICROGRAPH OF THE CONTACT BETWEEN AN Fe-Cu-Ni SULFIDE VEIN AND A GRANITE DIKE . . . . .	58

## ILLUSTRATIONS (cont.)

Figure	Page
42. CHALCOPYRITE-RICH LATE STAGE VEIN. . . . .	58
43. LATE STAGE VEIN MINERALIZATION IN FAULT BRECCIA. . . . .	60
44. PHOTOMICROGRAPH OF INTERSTITIAL SULFIDES IN THE PELITIC HORNFELS. . . . .	60
45. PHOTOMICROGRAPH OF INTERSTITIAL CHALCOPYRITE IN MAFIC HORNFELS. . . . .	61
46. SULFIDE-RICH ZONE IN THE PELITIC HORNFELS. . . . .	63
47. SULFIDE MINERALIZATION IN A CALC-SILICATE POD. . . . .	63
48. PHOTOMICROGRAPH OF PYRRHOTITE REPLACED BY CUBANITE . . . . .	64
49. PHOTOMICROGRAPH OF AN EXSOLUTION INTERGROWTH OF TROILITE AND PYRRHOTITE . . . . .	64
50. PHOTOMICROGRAPH OF PENTLANDITE . . . . .	66
51. PHOTOMICROGRAPH OF PENTLANDITE REPLACED BY CHALCOPYRITE . . . . .	66
52. PHOTOMICROGRAPH OF EXSOLVED CUBANITE-CHALCOPYRITE. . . . .	67
53. PHOTOMICROGRAPH OF A MYRMEKITIC INTERGROWTH OF PYRRHOTITE AND HYPERSTHENE IN TROCTOLITE . . . . .	67
54. PHOTOMICROGRAPH OF INTERGROWN CHALCOPYRITE AND BORNITE IN NORITE. . . . .	69
55. PHOTOMICROGRAPH OF ILMENITE IN SULFIDE-BEARING NORITE. . . . .	69
56. PHASE RELATIONS IN THE Cu-Fe-S SYSTEM. . . . .	83
57. PHASE RELATIONS IN THE Cu-Fe-Ni-S SYSTEM AT 1000 <sup>o</sup> C. . . . .	84
58. PHASE RELATIONS IN THE Cu-Fe-S SYSTEM. . . . .	85
59. PHASE RELATIONS IN THE Cu-Fe-S SYSTEM. . . . .	86
 Plate	
1. GEOLOGY OF UNDERGROUND DRIFTS, 1700 LEVEL, MINNAMAX DEPOSIT . . . . . (in pocket)	

## TABLES

Table	Page
1. MODAL ANALYSES (VOLUME PERCENT) OF THE SULFIDE-BEARING TROCTOLITIC ROCKS. . . . .	34
2. MODAL ANALYSES (VOLUME PERCENT) OF PERIDOTITE TO GABBRO XENOLITHS . . . . .	39
3. MODAL ANALYSES (VOLUME PERCENT) OF GRANITE TO DIORITE DIKES . . . . .	46
4. MODEL ORE COMPOSITIONS FOR THE BASAL SULFIDE-BEARING TROCTOLITIC ROCKS AND FOR Fe-Cu-Ni SULFIDE VEIN-RICH ZONES . . . . .	51
5. COMPOSITIONS OF THE MAJOR SULFIDE MINERALS . . . . .	65

## INTRODUCTION

The Minnamax deposit, near Babbitt, Minnesota, is one of several large, low-grade iron-copper-nickel sulfide deposits in the basal zone of the Duluth Complex. Sulfide mineralization in these deposits is primarily disseminated in inclusion-bearing troctolitic intrusions. Sulfides are locally concentrated at contacts with underlying country rocks, which include the Virginia Formation, the Biwabik Iron Formation, and the Giants Range batholith.

The Minnamax deposit occurs at the contact of the Duluth Complex and the Virginia Formation. The Virginia Formation, a thick sequence composed primarily of argillites, was deformed and metamorphosed to the pyroxene hornfels facies by troctolitic intrusions of the Duluth Complex. Metamorphism and assimilation of the Virginia Formation locally altered the composition of these intrusions (Bonnichsen, 1972); sulfur isotope studies identify the Virginia Formation as an important source of sulfur in similar nearby deposits (Mainwaring and Maldrett, 1977; Ripley, 1978).

This study examines the geology and sulfide mineralization of the Duluth Complex - Virginia Formation contact in a portion of the Minnamax deposit. Objectives are to determine the petrology and space-time relationships of the major rock units, and controls of the distribution of sulfide mineralization. The contact zone is outlined by extensive drilling, and is well exposed in 3800 feet of underground drifts.

### Location

The Minnamax deposit is located 5 miles south of Babbitt, Minnesota,

immediately southeast of the taconite mining operations of Reserve Mining Company. The study area is on the 1700 feet level of the deposit, and covers a 1500 feet by 1300 feet zone in sections 28, 29, 32, and 33, T. 60 N., R. 12 W. (Figures 1 and 3).

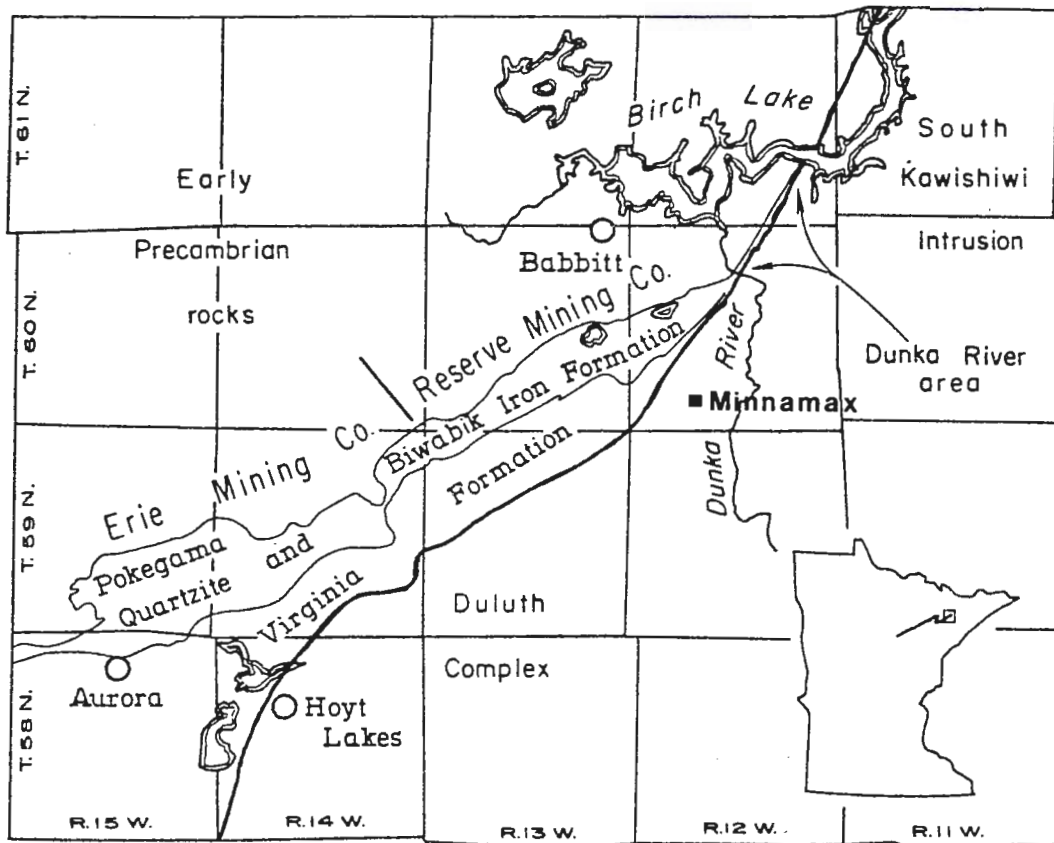


Figure 1. INDEX MAP OF THE MINNAMAX AREA showing the location of the Minnamax deposit in relation to other features in the region (from Bonnicksen, 1968).

Fig 3

## REGIONAL GEOLOGY

The Minnamax deposit is located in the Eastern Mesabi region, near the southern edge of the Superior Province of the Canadian Shield. Rocks in the region are Early, Middle, and Late Precambrian in age. Major unconformities separate the three groups. The regional geology is shown in Figures 1 and 2.

Early Precambrian greenstone and granite terranes are exposed in the northwest portion of the region. Metavolcanic and metasedimentary rocks of the Ely Greenstone, Soudan Iron Formation, and Knife Lake Group form an east-west trending greenstone belt which dips steeply north. The Giants Range batholith, a granitic complex formed by multiple intrusions, extends for 100 miles along the stratigraphic base of this thick volcanic-sedimentary sequence. The batholith intruded the greenstone belt during the Algoman orogeny, 2.6 b.y. ago (Sims and Viswanathan, 1972). In the Eastern Mesabi region the Giants Range batholith forms the basement on which Middle Precambrian sediments of the Animikie Group were deposited.

The Animikie Group consists of three conformable formations. These are, from oldest to youngest, the Pokegama Quartzite, the Biwabik Iron Formation, and the Virginia Formation. The Pokegama Quartzite, consisting of impure quartzite and argillite, is as much as 150 feet thick, but thins eastward and pinches out at the eastern end of the Mesabi Range (White, 1954). The Biwabik Iron Formation, a ferruginous chert containing 25 to 35% iron, ranges in thickness from 800 feet in the Main Mesabi region to 200 feet in the Eastern Mesabi region (Bonnichsen, 1968). The Virginia Formation, a thick argillite sequence, is the uppermost Animikie unit in

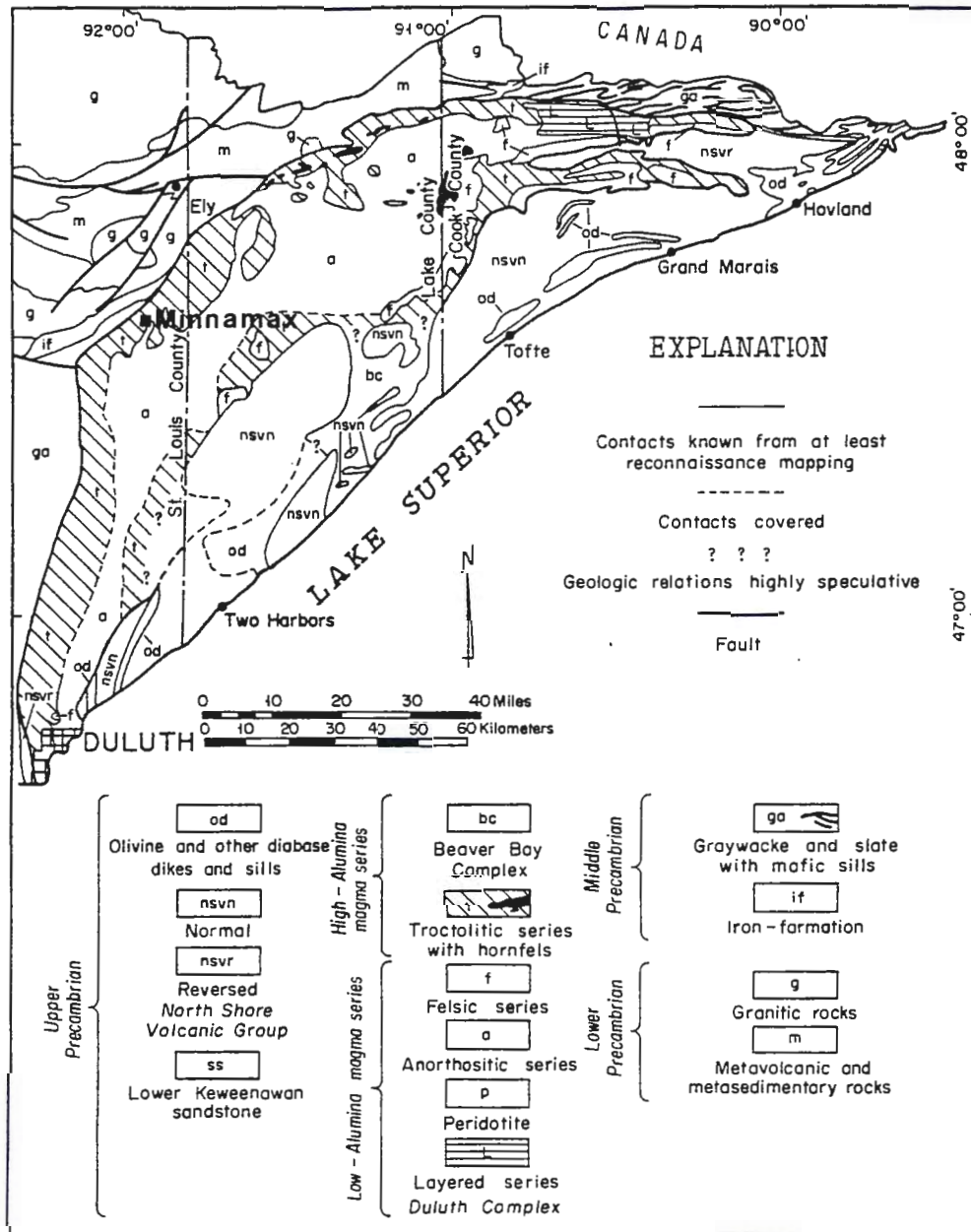


Figure 2. GENERAL GEOLOGIC MAP OF NORTHEASTERN MINNESOTA (from Weiblen and Morey, 1975).

the region. Animikie strata generally dip 5 to 10 degrees southeast. Near their contact with the Duluth Complex they are metamorphosed to the pyroxene hornfels facies and dip up to 50 degrees southeast.

Metadiabase dikes and sills, which were metamorphosed by the Duluth

Complex, occur in Animikie strata in close proximity to the Duluth Complex contact (Grout and Broderick, 1919; Gundersen and Schwartz, 1962; Bonnichsen, 1968).

The Late Precambrian Duluth Complex, a mafic igneous body composed of multiple intrusions, truncates the Early and Middle Precambrian rocks to the east. The complex forms an arcuate belt which extends 150 miles northeastward from Duluth to Hovland, Minnesota. It intruded genetically related mafic volcanic rocks of the North Shore Volcanic Group during a Keweenawan rifting event 1.1 b.y. ago (Weiblen and Morey, 1975). Rocks of the Duluth Complex are divided into an anorthositic series and a younger troctolitic series by field and petrographic criteria (Taylor, 1964). The troctolitic series consists primarily of troctolite, olivine gabbro, gabbro, and oxide gabbro intrusions, and is the host to copper-nickel mineralization in the Duluth Complex. It was emplaced along the basal contact of the complex, and is the predominant Duluth Complex lithology in the Eastern Mesabi region (Weiblen and Morey, 1975).

Pleistocene glaciation deposited a thin veneer of drift which covers and obscures much of the Precambrian geology in the region.

PREVIOUS INVESTIGATIONS IN  
THE MINNAMAX AREA

The Duluth Complex and its contact rocks near Minnamax have been the subject of numerous investigations. Grout and Broderick (1919) first mapped the area and developed its geological framework. The Duluth Complex - Virginia Formation contact trends northeast and dips 5 to 50 degrees southeast. The Biwabik Iron Formation conformably underlies the Virginia Formation in close proximity to the Duluth Complex contact. Metadiabase dikes and sills, which were metamorphosed by the Duluth Complex, occur in the Virginia Formation and the upper portion of the Biwabik Iron Formation. Due to poor bedrock exposure, only a general geological framework has been established for the area.

Rock Units

Biwabik Iron Formation

The Biwabik Iron Formation is approximately 350 feet thick near Minnamax. It is subdivided into four members, from oldest to youngest: Lower Cherty, Lower Slaty, Upper Cherty, and Upper Slaty (Wolff, 1917). These stratigraphic divisions were established in relatively unmetamorphosed portions of the iron formation, where slaty members consist primarily of fine-grained, finely laminated taconite and cherty members consist mainly of granular taconite. They are recognized in more metamorphosed portions of the iron formation by relict textures and key beds. The base of the iron formation either rests unconformably on the Giants Range batholith or conformably on the Pokegama Quartzite, and the top, a 10 feet thick calcite-rich calc-silicate horizon, is conformable with the

overlying Virginia Formation (Grout and Broderick, 1919). A transition zone a few feet thick occurs locally between the iron formation and the Virginia Formation. It consists of interlayered beds of quartzite, marble, calc-silicate granofels, and feldspar-pyroxene hornfels (Bonnichsen, 1968).

The Biwabik Iron Formation is metamorphosed within several miles of the Duluth Complex. French (1968) delineated four mineralogic zones in the iron formation as one approaches the Duluth Complex:

1. fine-grained "unaltered" taconite: consists of quartz, magnetite, hematite, siderite, ankerite, talc, and the iron silicates chamosite, greenalite, minnesotaite, and stilpnomelane.
2. a transition zone, mineralogically identical to zone 1.
3. moderately metamorphosed taconite: characterized by the development of cummingtonite-grunerite and the disappearance of ankerite, siderite, and iron phyllosilicates.
4. highly metamorphosed taconite: consists primarily of quartz, magnetite, and orthopyroxene, with fayalite, Ca-pyroxene, cummingtonite-grunerite, and hornblende present locally due to variations in the chemical environment of the iron formation during metamorphism.

Calc-silicate horizons consist mainly of calcite, diopside, andradite, and idocrase (Bonnichsen, 1968). Texturally, the iron formation is highly recrystallized and relatively coarse-grained.

Near Minnamax, the Biwabik Iron Formation is characteristic of zone 4. Metamorphism was isochemical, except for the loss of original  $H_2O$  and  $CO_2$ . Diffusion occurred between adjacent chemically incompatible horizons (French, 1968; Bonnichsen, 1968). Pegmatite dikes, consisting primarily of quartz, hornblende, alkali-feldspar, and graphic quartz and alkali-feldspar intergrowths, occur in the upper portion of the iron

formation and formed during emplacement of the Duluth Complex (Grout and Broderick, 1919; Gundersen and Schwartz, 1962).

#### Virginia Formation

Limited exposure of the Virginia Formation has restricted studies of its geology to drilling and mining information obtained during exploration and development of the Biwabik Iron Formation. The Mesabi Deep Drilling Project provides the most complete section of the Virginia Formation (Pfleider et al, 1968). Where unmetamorphosed, the formation consists primarily of interlayered argillaceous siltstone, silty argillite, and fissile carbonaceous argillite. Graywacke, graphite-rich argillite, and carbonate beds occur locally. Carbonate beds or lenses are abundant near the base of the formation.

The Duluth Complex truncates the Virginia Formation in the Minnamax area. Only the lowermost several hundred feet of the formation remain. Mineral assemblages within the pelitic rocks and calc-silicate rocks are indicative of the pyroxene hornfels facies of metamorphism (Bonnichsen, 1968, 1972; Hardyman, 1969; Renner, 1969; Kirstein, 1979). Whole rock chemical analysis of selected samples by Bonnichsen (1972) indicates that the pelitic rocks within a few hundred feet of the Duluth Complex are substantially lower in  $\text{SiO}_2$ ,  $\text{K}_2\text{O}$ , and  $\text{Na}_2\text{O}$ . Bonnichsen suggests that these constituents contaminated the basal Duluth Complex and possibly formed granitic dikes which are common in the contact zone.

#### Metadiabase

Metadiabase dikes and sills occur within the Virginia Formation and the Upper Slaty member of the Biwabik Iron Formation near the Duluth Complex (Grout and Broderick, 1919; Gundersen and Schwartz, 1962; Bonnichsen, 1968). These intrusions, which were metamorphosed by the Duluth Complex, are younger than the Virginia Formation and older than the Duluth Complex.

The dikes and sills are 5 to 35 feet thick where exposed within the iron formation, and commonly can be traced for at least one mile (Grout and Broderick, 1919).

The dikes and sills are termed "metadiabase" on the basis of mineralogy and texture. They are dark gray with a fine-grained diabasic texture, which commonly was obliterated where the rock was highly metamorphosed. Plagioclase phenocrysts, as much as 5 cm long, are locally concentrated in the upper halves of the sills. The metadiabase contains essential plagioclase feldspar, hypersthene, and augite (Gundersen and Schwartz, 1962; Bonnicksen, 1968).

#### Duluth Complex

Detailed mapping by Phinney (1969) and Bonnicksen (1972) established that troctolitic rocks are the dominant Duluth Complex lithology in the Minnamax area. Several intrusions were identified. Relationships within and between the intrusions are obscured by glacial cover, and thus are poorly understood.

Discovery of disseminated copper and nickel bearing sulfides near Ely, Minnesota in 1948 brought attention to the economic potential of basal rocks of the Duluth Complex. Mining companies commenced land acquisition and exploration along the basal portion of the complex between Ely and Hoyt Lakes. In 1953 the U.S. Bureau of Mines drilled 3 holes near Ely which confirmed the presence of substantial amounts of disseminated copper-nickel sulfides. Schwartz and Davidson (1952), Grosh et al (1955), and Anderson (1956) summarize the results of this early work.

Bear Creek Mining Company acquired the property that is now the Minnamax deposit in 1951. Following extensive geophysical evaluation, surface holes were drilled between 1958 and 1971. This drilling delineated the Bathtub, Tiger Boy, and Local Boy deposits which form the

Minnamax deposit (Figure 4). AMAX Exploration, Inc. assumed management of the project in 1974 to evaluate the deposit for mining. Surface drilling continued through 1977 and totals 560,000 feet.

Results of this exploration have provided abundant information about the geology and sulfide mineralization of the Minnamax deposit (Watowich, 1978). Tyson and Chang (1978) describe a major sulfide-bearing troctolitic intrusion found in drill cores from the deposit. The intrusion, which contains xenoliths of rhythmically layered picrite and troctolite, has several repetitive cryptic layers and contains disseminated iron-copper-nickel sulfides. Its basal portion is characterized by symplectite intergrowths of hypersthene and plagioclase, epitaxial biotite, plagioclase and olivine enriched in Na and Fe, respectively, and a marked increase in sulfide content.

Major sulfide minerals in the troctolitic rocks are pyrrhotite (38%), cubanite (38%), chalcopyrite (18%), and pentlandite (6%) (Watowich, 1978). The sulfides constitute disseminated ore within several hundred feet of the Virginia Formation contact. Watowich notes a sulfide zonation where pyrrhotite and cubanite increase relative to chalcopyrite toward the footwall. Lower grade "cloud zones", 30 to 400 feet thick, occur 100 to 1000 feet above the basal sulfide zone and consist primarily of chalcopyrite. Sulfides are concentrated locally at the footwall contact and in the underlying Virginia Formation. Locations of detailed studies of the sulfide mineralogy by Hardyman (1969) and Boucher (1975) are shown in Figure 3.

#### Inclusions

Inclusions, ranging up to hundreds of feet in extent, are abundant in the basal zone of the Duluth Complex. Locally the base of the complex is considered an intrusive breccia (Wager et al, 1969). Inclusion lithol-

ogies include the Virginia Formation, the Biwabik Iron Formation, the G-ants Range batholith, mafic volcanic rocks, and xenoliths of earlier Duluth Complex intrusions (Wager et al, 1969; Bonnicksen, 1972; Boucher, 1975; Tyson and Chang, 1978).

#### Conditions of Metamorphism

Contact rocks of the Duluth Complex were metamorphosed to the pyroxene hornfels facies. Studies of the metamorphism of the Biwabik Iron Formation by Perry and Bonnicksen (1966) and Perry et al (1973), using  $O^{18}$  to  $O^{16}$  ratios, indicate that the maximum temperature attained was 650

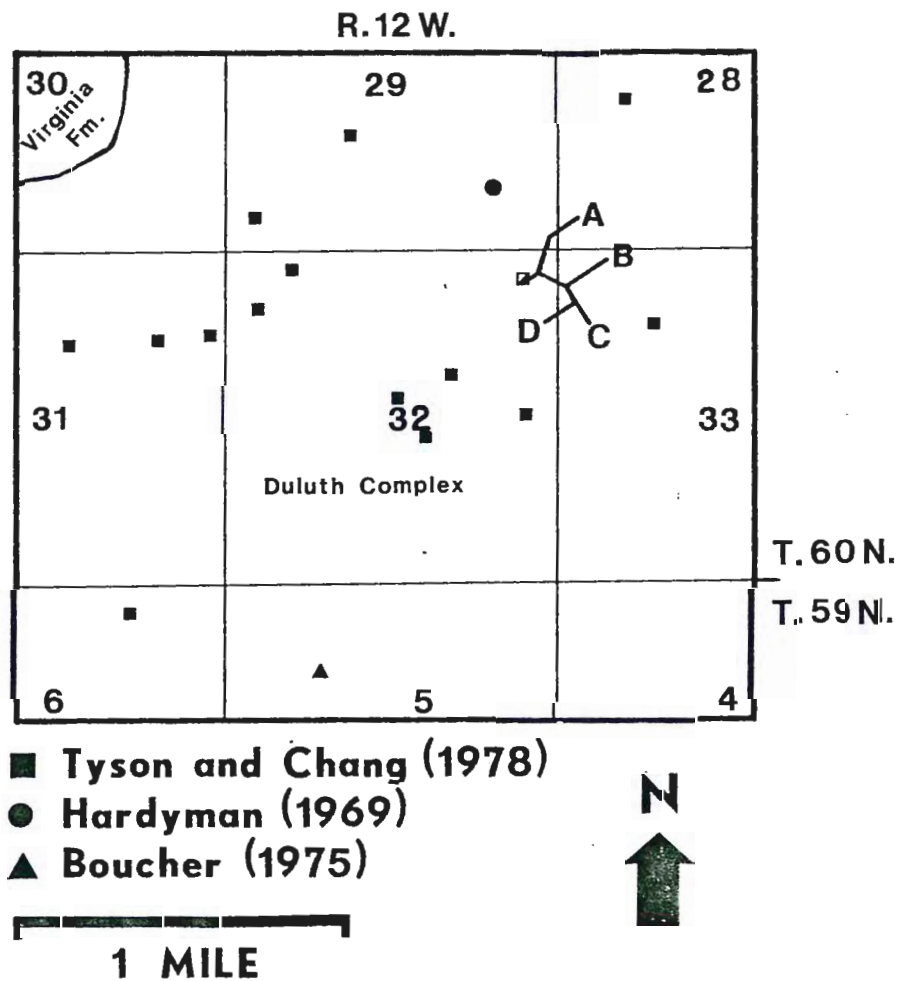


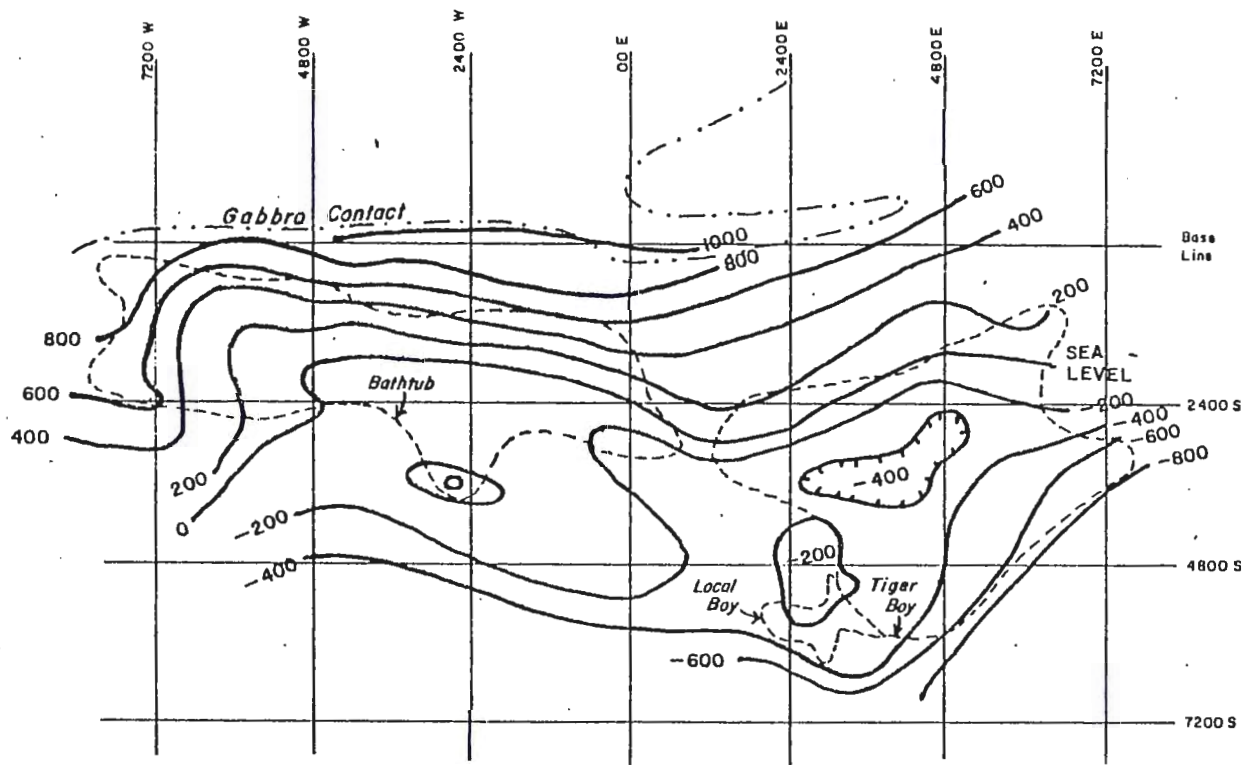
Figure 3. LOCATIONS OF DRILL CORES STUDIED IN PREVIOUS INVESTIGATIONS. Map shows collar locations of the vertical drill holes with respect to the underground workings.

to 750° C. Mineral assemblages of calc-silicate pods in the Virginia Formation suggest similar temperatures (Kirstein, 1979). Kirstein estimates a lithostatic pressure of 2 kilobars during metamorphism based on the assumption that contact rocks were no deeper than the maximum 20,000 feet thickness of the then overlying North Shore Volcanic Group. During metamorphism, substantial amounts of H<sub>2</sub>O and CO<sub>2</sub> were lost from the Biwabik Iron Formation (Bonnichsen, 1968, 1975; French, 1968); and H<sub>2</sub>O, CO<sub>2</sub>, K<sub>2</sub>O, Na<sub>2</sub>O, and SiO<sub>2</sub> were lost from the Virginia Formation (Bonnichsen, 1971, 1972).

### Structure

Surface drilling on 400 feet centers, magnetics, and taconite mine pits of the Reserve and Erie mining companies provide most of the limited information available on the structure of the Minnamax area. The large scale relationships are relatively simple. The Animikie strata strike northeast and dip southeast. The characteristically shallow dips of these formations steepen to as much as 50 degrees near the Duluth Complex, where at depths of 1600 to 2000 feet they flatten to form platforms and locally reverse to form troughs (Watowich, 1978) (Figure 4).

Mancuso and Dolence (1970) propose that emplacement of the Duluth Complex was controlled by pre-existing structure of the Biwabik Iron Formation. By this model the intrusions generally rode above the iron formation and cut the weaker Virginia Formation, which was highly deformed and incorporated within the Duluth Complex as xenoliths. Evidence presented in support of this model is that the basal contact of the Duluth Complex reflects pre-complex faults and folds in the iron formation.



--- outline of deposits **MINNAMAX PROJECT**  
 Structure Contours  
 Top of Biwabik Iron Formation.

Scale 0 1000 2000 feet

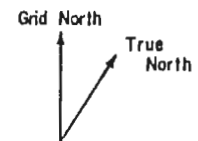


Figure 4. STRUCTURE CONTOUR MAP OF THE TOP OF THE BIWABIK IRON FORMATION. Note locations of the Bathtub, Tiger Boy, and Local Boy deposits (from Watowich, 1978).

## PRESENT INVESTIGATION AND

## METHODS OF STUDY

In 1977 AMAX Exploration, Inc. sunk a 1700 feet test shaft and drifted 3800 feet along the Duluth Complex - Virginia Formation contact. Sixty thousand feet of underground drilling were completed in 1977 and 1978. The underground workings and drill cores provide an unprecedented view of the geology and sulfide mineralization of the contact zone and form the basis of this study.

Investigation of the Duluth Complex - Virginia Formation contact included underground mapping and sampling, drill core examination and sampling, compilation of drilling information, thin section and polished section studies, and x-ray identification of minerals. Underground mapping occurred over 12 days in April, May, June, and October, 1978. Thirty eight hundred feet of drifts were mapped at a 1:240 scale. Drift walls were mapped to provide two-dimensional relationships. Cross-sections of the drilling were combined to develop a three-dimensional view of the geology of the contact zone.

Laboratory work and compilation of data began in the summer of 1978 and continued into 1980. 150 thin sections were examined to detail the mineralogy, texture, and alteration of the rock units. Plagioclase and olivine compositions were approximated by the Michel-Levy method and by estimation of 2V, respectively (Heinrich, 1965). Thin section heels were etched in HF, and stained with sodium cobaltinitrate and amarand to identify potassium and plagioclase feldspars, respectively. Intrusive rocks were point counted and classified on the basis of mineral modes. X-ray

diffraction was used to positively identify cordierite and laumontite. 42 polished sections were examined to detail the opaque mineralogy and textures.

GEOLOGY AND SULFIDE MINERALIZATION OF THE  
DULUTH COMPLEX - VIRGINIA FORMATION  
CONTACT

The geology and sulfide mineralization of the Duluth Complex - Virginia Formation contact zone are shown in Figures 5, 6, and 7. The Virginia Formation consists of pelitic hornfels with locally abundant calc-silicate pods and contains diabase intrusions. The Duluth Complex consists of sulfide-bearing troctolitic rocks, commonly noritic near the contact, which contain barren gabbro to peridotite xenoliths. Granite to diorite dikes cut all lithologies.

In the underground drift area, the contact forms a structural platform which reflects the structure of the underlying Biwabik Iron Formation. Here the contact is highly irregular, characterized by numerous Duluth Complex apophyses and Virginia Formation xenoliths, up to 150 feet in maximum dimension. Contacts between the sulfide-bearing troctolitic rocks and the Virginia Formation are sharp and regular to highly irregular. The troctolitic rocks are not chilled. A small number of post-Duluth Complex faults, of relatively minor displacement, contain zones, up to 5 feet thick, of breccia, gouge, and material sheared and slickensided to chlorite or serpentine schist.

Sulfide mineralization is primarily disseminated in the troctolitic rocks within 1000 feet of the contact. Sulfide veins fill fractures and breccia zones in both the Duluth Complex and the Virginia Formation. Pelitic hornfels adjacent to the veins commonly contains sulfides. In the Local Boy deposit (Figure 5) the veins are sufficiently concentrated to

N33°W

## MINNAMAX DEPOSIT - 3200 EAST

S33°E

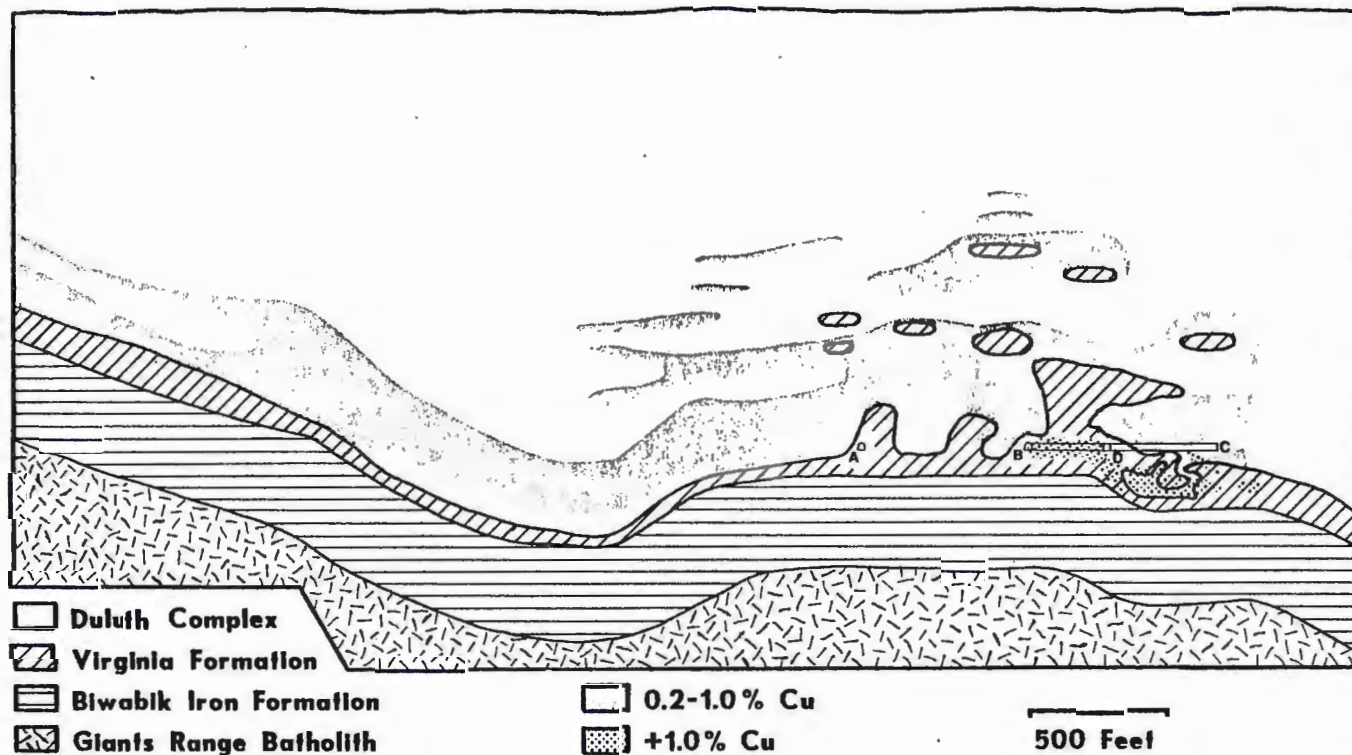


Figure 5. INTERPRETATIVE GEOLOGIC SECTION OF THE STUDY AREA based on surface drill holes (spaced approximately 400 feet) and extensive underground ring drilling. The Duluth Complex - Virginia Formation contact continues to the left at uniform dip to the surface. As suggested by Mancuso and Dolence (1970), emplacement of the Duluth Complex appears to have been controlled by the structure of the underlying Biwabik Iron Formation. Intrusions rode above the iron formation and cut the weaker Virginia Formation, which was highly deformed and incorporated within the Duluth Complex.

form a high-grade sulfide zone. Late stage sulfide mineralization and gangue occurs along post-Duluth Complex fractures.

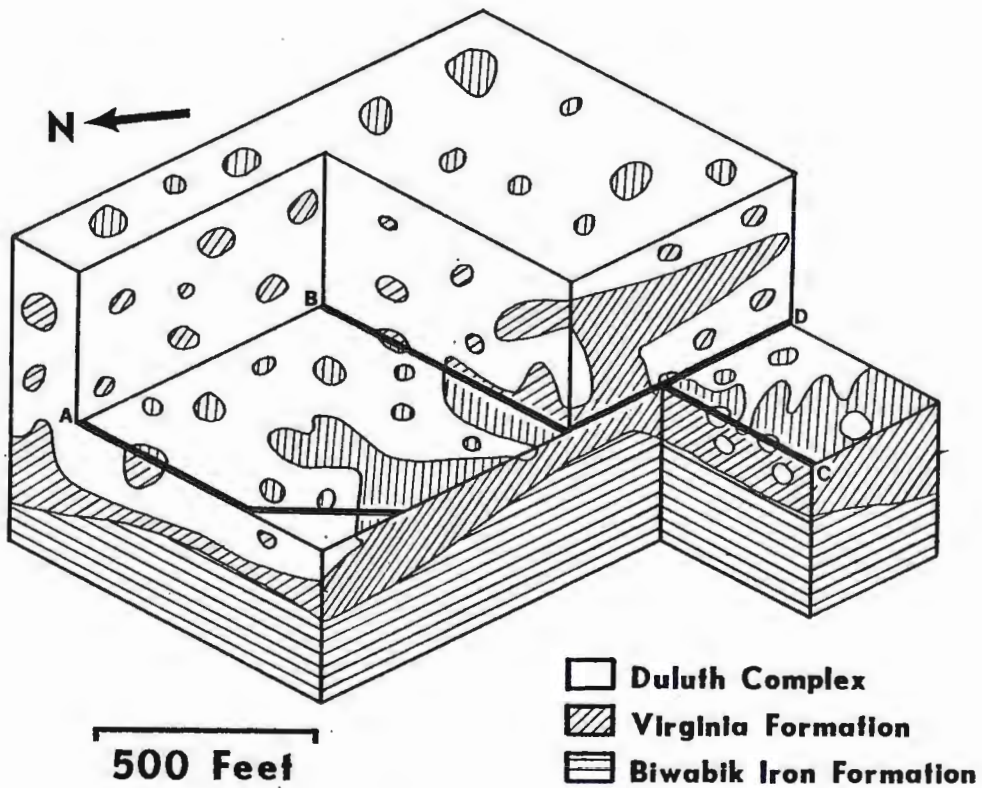


Figure 6. INTERPRETATIVE BLOCK DIAGRAM OF THE DULUTH COMPLEX - VIRGINIA FORMATION CONTACT IN THE STUDY AREA based on the geology in underground drifts and extensive underground drilling. Drifts are labelled.

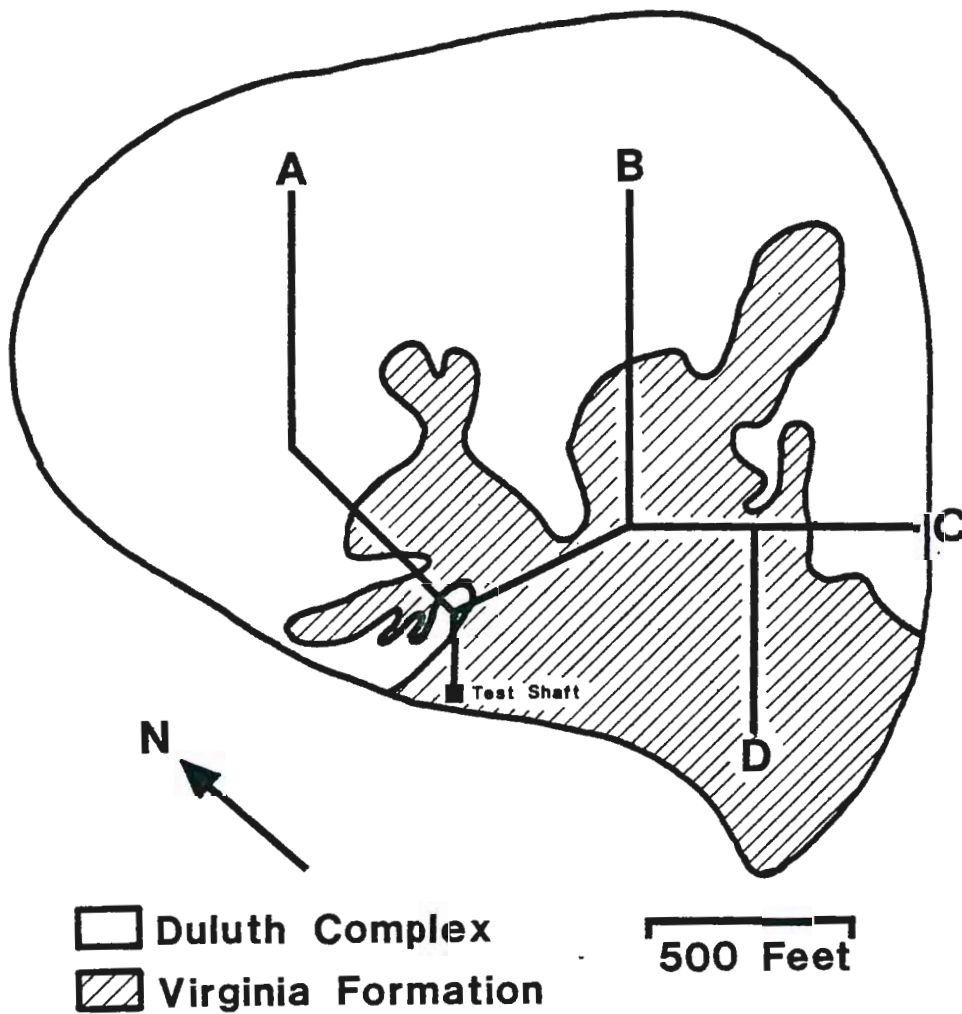


Figure 7. INTERPRETATIVE PLAN VIEW OF THE DULUTH COMPLEX - VIRGINIA FORMATION CONTACT ON THE 1700 LEVEL based on the geology in underground drifts and underground drilling. Drifts are labelled.

## LITHOLOGIES

Virginia Formation

The Virginia Formation consists primarily of pelitic hornfels with locally abundant calc-silicate pods (Figure 8). Minor lithologies include graphite schist, biotite schist and biotite-rich pelitic hornfels, and mafic hornfels.

Pelitic Hornfels

The pelitic hornfels is typically medium to dark gray, fine to medium grained (0.5 to 2 mm), granoblastic, and unaltered (Figures 8 and 9). It is commonly massive, but subtle bedding, some of which is highly contorted, occurs locally (Figure 10). The pelitic hornfels consists primarily of plagioclase feldspar (30 to 60%), cordierite (10 to 20%), and hypersthene (20 to 33%). Minor, locally abundant minerals include orthoclase (0 to 30%), biotite (tr.), graphite (1 to 4%), ilmenite-magnetite (tr. to 4%), apatite (tr.), and sulfides. The plagioclase and cordierite are typically untwinned and granoblastic. Some plagioclase crystals contain albite, carlsbad, and pericline twinning. The cordierite rarely displays sector twinning and commonly can only be identified by x-ray diffraction. The hypersthene is anhedral and commonly is subpoikiloblastic to poikiloblastic, enclosing plagioclase and cordierite. The orthoclase forms anhedral grains and poikiloblasts, up to 10 mm in diameter, with abundant plagioclase and orthoclase inclusions (Figure 11). Ilmenite-magnetite forms minute, equant, and rod-shaped inclusions in the silicates. Ragged graphite blades occur in 2 to 3 mm clumps in many samples. Red to brown biotite forms plates which are commonly poikilitic.



Figure 8. VIRGINIA FORMATION IN THE MINNAMAX DEPOSIT. Dark gray pelitic hornfels contains locally abundant calc-silicate pods. Both homogeneous and layered pods are present. A drift-924 feet.

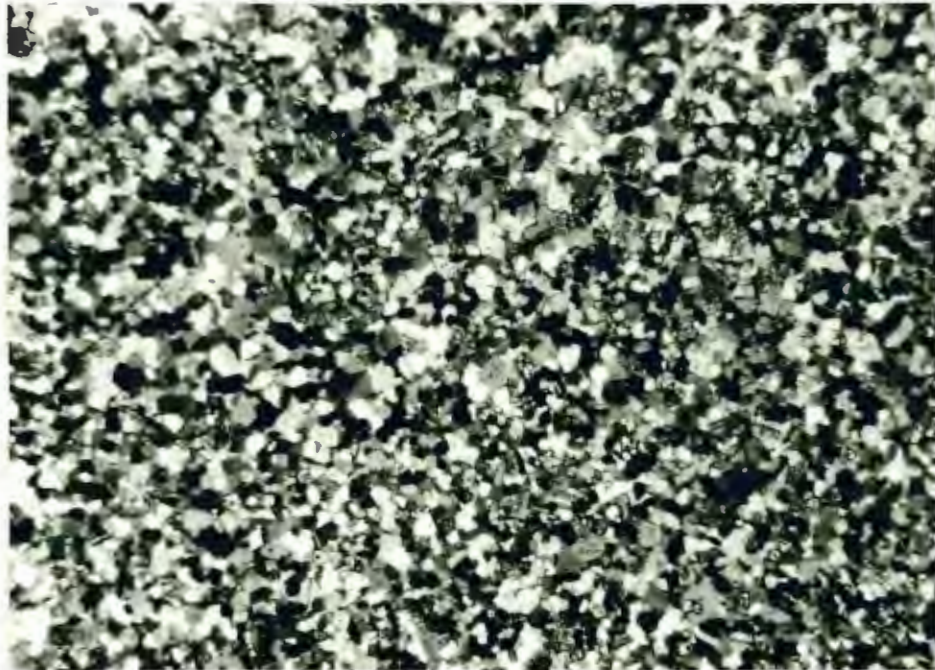


Figure 9. PHOTOMICROGRAPH OF PELITIC HORNFELS consisting of granoblastic plagioclase feldspar (low relief), cordierite (low relief), and hypersthene (high relief). Sample MM-A-27. Transmitted light, crossed polars. 6.25 mm across.



Figure 10. PLASTIC DEFORMATION OF THE VIRGINIA FORMATION.  
Note folded relict bedding and calc-silicate pod.  
B drift-727 feet.

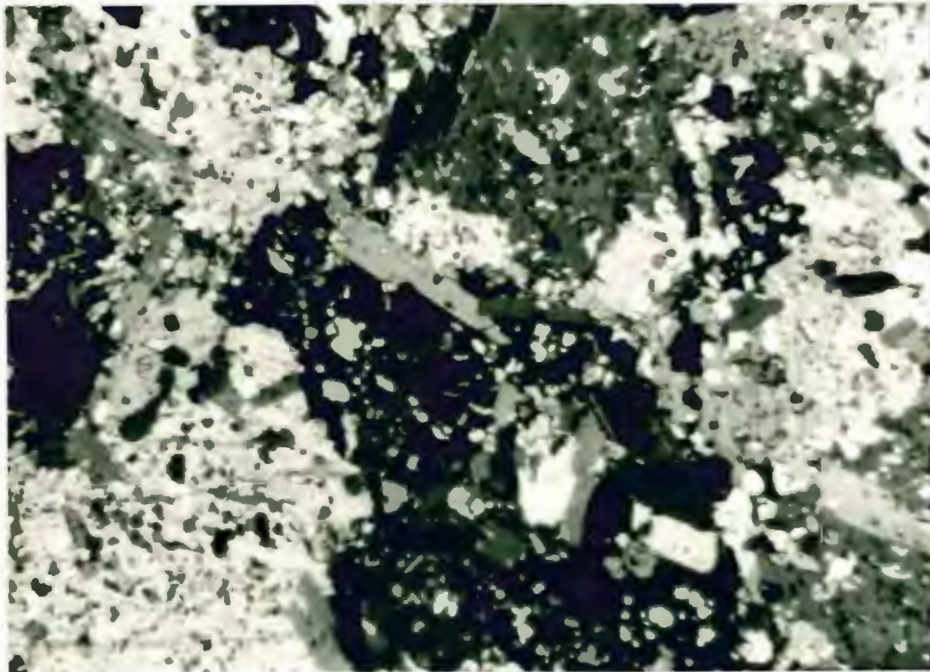


Figure 11. PHOTOMICROGRAPH OF ORTHOCLASE POIKILOBLASTS.  
Note abundant minute inclusions of plagioclase feldspar  
and cordierite, and biotite plates. Sample MM-A-29.  
Transmitted light, crossed polars. 6.25 mm across.

Euhedral apatite forms minute inclusions.

Biotite-rich Pelitic Hornfels  
and Biotite Schist

Biotite-rich pelitic hornfels and biotite schist occur locally in the pelitic hornfels, and are relatively abundant near contacts with the Duluth Complex and in xenoliths. These lithologies are recognized by their abundant fine to medium grained biotite plates (10 to 30%) which are commonly foliated (Figure 12). Orthoclase poikiloblasts are common. Otherwise, the lithologies are similar to the typical pelitic hornfels.

Graphite Schist

Graphite schist, found in the C and D drifts, is a variety of the pelitic hornfels which contains essential foliated graphite (15 to 30%) (Figure 13). It is fine-grained and has a dark gray metallic sheen. Biotite in some samples parallels the graphite foliation, while in others it is clearly later and overgrows this foliation. Locally the graphite schist is finely laminated, with alternating light and dark (graphite and pyrrhotite rich) bands 1 to 3 mm thick. Interestingly, sample MM-D-7 contains what appear to be recrystallized, graphite-free rock fragments which contain hypersthene in a graphite-rich, hypersthene barren matrix.

Mafic Hornfels

Mafic hornfels, found in the B and D drifts, is fine-grained and granoblastic (Figure 14). It is bedded, with alternating light and dark bands (grays, pinks, and purples) 3 to 15 mm thick formed by biotite and hypersthene concentrated in distinct layers (Figures 15 and 16). The mafic hornfels consists primarily of plagioclase feldspar (28 to 60%) and augite (15 to 65%). Minor minerals include hypersthene (0 to 20%), biotite (tr. to 7%), sphene (tr.), graphite (0 to 4%), and ilmenite-magnetite (tr.). The plagioclase is typically untwinned, granoblastic,



Figure 12. PHOTOMICROGRAPH OF BIOTITE SCHIST containing foliated biotite (black), hypersthene (gray, high relief), and plagioclase feldspar and cordierite (white, low relief). Sample MM-D-10. Transmitted light, uncrossed polars. 6.25 mm across.



Figure 13. PHOTOMICROGRAPH OF GRAPHITE SCHIST containing foliated graphite blades (black), hypersthene (gray, high relief), and plagioclase feldspar and cordierite (white, low relief). Sample MM-C-14. Transmitted light, uncrossed polars. 6.25 mm across.

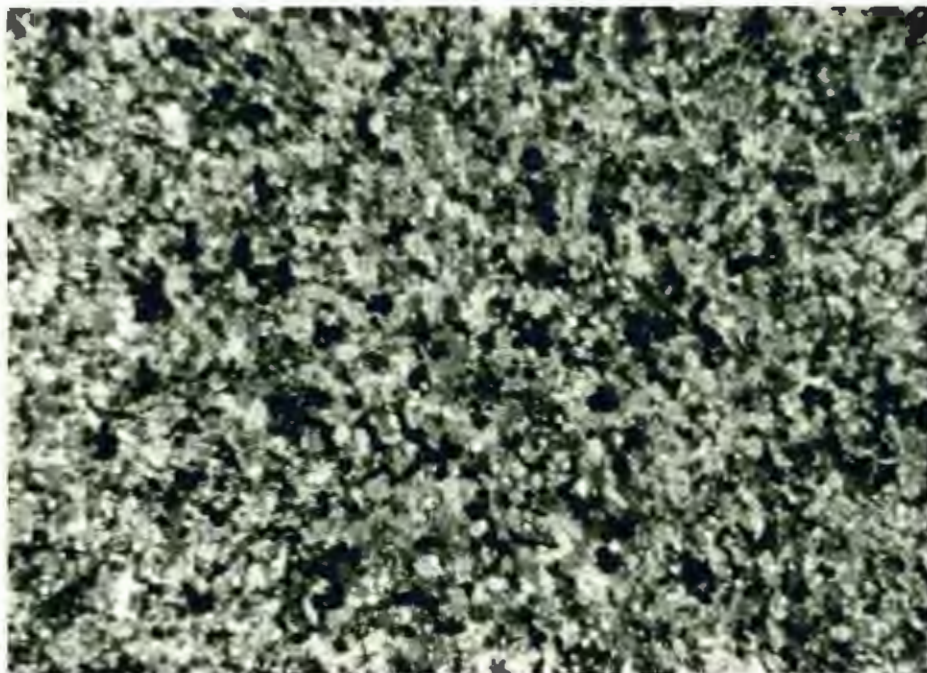


Figure 14. PHOTOMICROGRAPH OF MAFIC HORNFELS consisting of granoblastic plagioclase feldspar (low relief) and augite (high relief). Sample AX-26. Transmitted light, crossed polars. 6.25 mm across.



Figure 15. BEDDING IN MAFIC HORNFELS. Dark bands are due to concentration of biotite and hypersthene. Sample X-1.

and highly sericitized. The augite and hypersthene, which is commonly uralitized, are anhedral and typically subpoikiloblastic to poikiloblastic, enclosing plagioclase. Light brown biotite forms anhedral grains and ragged subhedral plates. The ilmenite-magnetite and graphite form randomly oriented rods and ragged blades, respectively.

#### Calc-silicate Pods

Calc-silicate pods in the pelitic hornfels are spherical to ellipsoidal, and range up to 8 feet in maximum dimension (Figure 8). The pods are generally randomly oriented, but locally they are subparallel. Some pods are angular, and one pod is folded (Figure 10). The pods are either homogeneous or layered (Figure 8). Layered varieties have alternating light and dark bands, up to 2 cm thick, which represent mineralogic zones. Bands are either concentric with the shape of the pods or

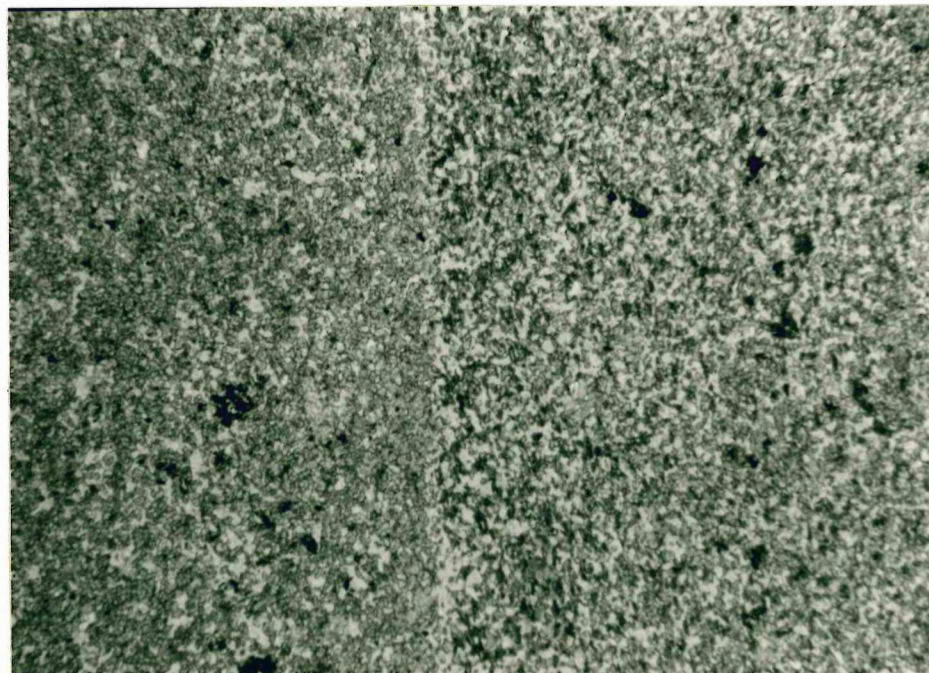


Figure 16. PHOTOMICROGRAPH OF BEDDING CONTACT IN MAFIC HORNFELS. Biotite in bed to left gives the bed its dark color. Sample X-1. Transmitted light, uncrossed polars. 6.25 mm across.

aligned with the pods' long dimensions.

The pods are light gray to pink, fine to coarse grained, and granoblastic. Poikiloblastic minerals occur locally. Diopside (40 to 60%) is ubiquitous, and wollastonite (0 to 50%), plagioclase feldspar (anorthite) (0 to 40%), grossular garnet (1 to 40%), idocrase (a major constituent of one sample), and sphene (0 to 3%) are common. Pink to green anhedral grains of diopside, 0.5 to 2 mm across, are concentrated at the rims of the pods. The wollastonite forms anhedral grains to subhedral blades 0.5 to 4 mm in length, and rarely forms poikiloblasts up to 1 cm across. The anorthite forms anhedral to subhedral grains 0.5 to 2 mm across that may display carlsbad and albite twinning. The grossular garnet forms light green to white, anhedral to subhedral grains 1 to 4 mm across. The idocrase is light green, anhedral, and poikiloblastic around calcite. The sphene forms brown, anhedral, interstitial grains (Kirstein, 1979).

Dark gray, fine-grained "reaction rims", 3 to 8 cm wide, occur at contacts between the calc-silicate pods and the pelitic hornfels. Mineralogic layers in the pods abut against the "reaction rims". The "reaction rims" completely enclose angular calc-silicate pods which appear to be fractured. The "reaction rims" are granoblastic and finer-grained than the pelitic hornfels. They consist of untwinned to poorly twinned plagioclase feldspar (50 to 70%), hypersthene (10 to 20%), and poikiloblastic augite (10 to 20%) (Kirstein, 1979).

#### Interpretation

Mineral assemblages in the pelitic hornfels, mafic hornfels, "reaction rims", and calc-silicate pods are characteristic of the pyroxene hornfels facies of metamorphism. These assemblages are generalized in Figure 17.

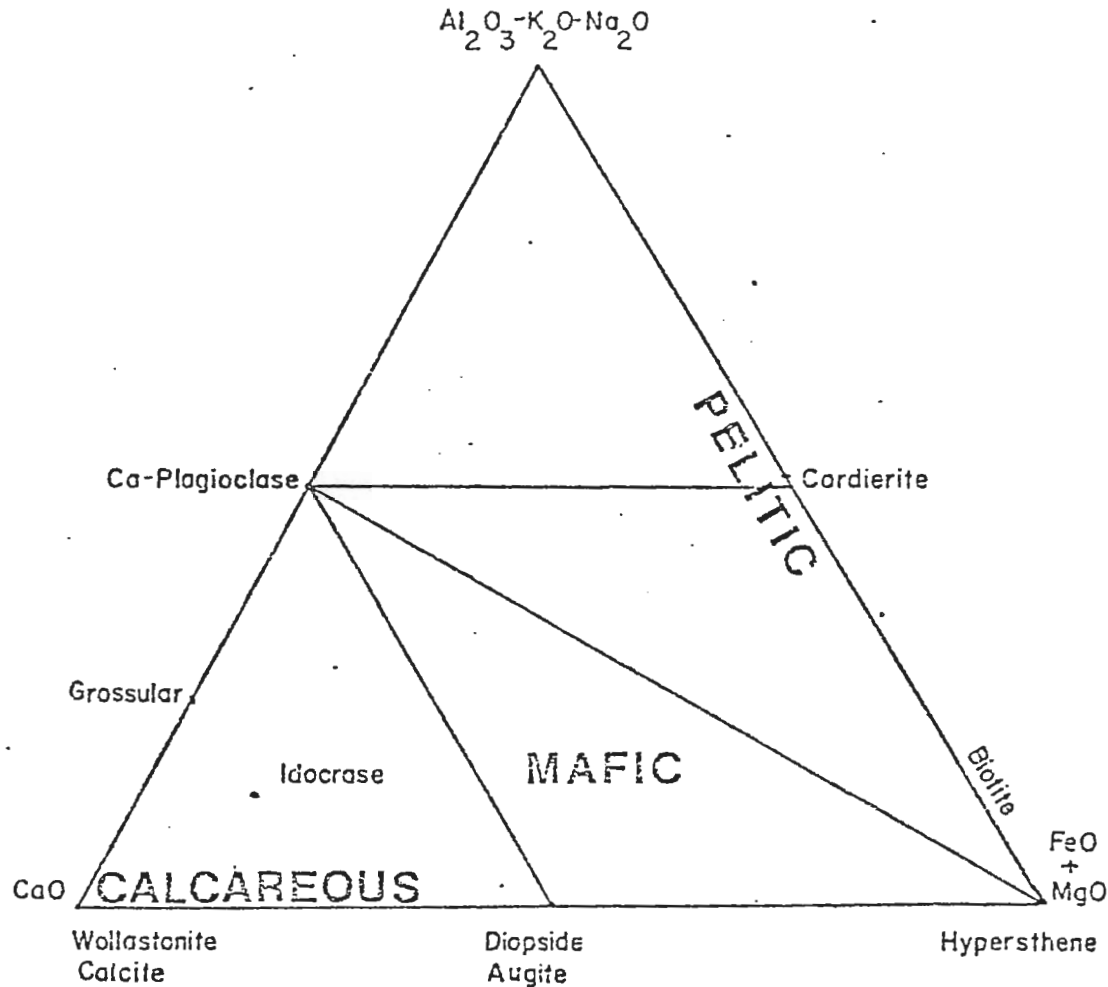


Figure 17. ACF DIAGRAM OF MINERAL ASSEMBLAGES IN THE VIRGINIA FORMATION. Assemblages include minerals in the pelitic hornfels (pelitic field); mafic hornfels and "reaction rims" (mafic field); and calc-silicate pods (calcareous field).

The mineral assemblage plagioclase-hypersthene-cordierite, typical of the pelitic hornfels, indicates a composition low in aluminum relative to calcium, iron, and magnesium, evidenced by the abundance of plagioclase and cordierite and the absence of aluminosilicate. This suggests that the protolith of the hornfels is a calcareous pelitic sediment. The mafic hornfels probably formed from a particularly calcareous clastic sediment. Potassium (biotite and orthoclase) rich rocks occur

in narrow zones in the pelitic hornfels, and are particularly common near the Duluth Complex contact and in xenoliths. On the basis of this distribution, the potassium rich rocks appear to have formed by the concentration of  $K_2O$  and  $H_2O$  along fractures during deformation and metamorphism of the Virginia Formation. The graphite schists have a carbonaceous pelitic sediment protolith.

Calc-silicate pods in the pelitic hornfels have the primary mineral assemblage diopside-garnet-wollastonite-plagioclase-sphene. This assemblage is characteristic of a dolomitic protolith, and indicates a temperature of formation between 650 and 750<sup>o</sup> C. at an estimated 2 kilobars pressure (Kirstein, 1979). Kirstein could find no evidence to explain why homogeneous and layered types formed. They occur together and have no major mineralogic differences. The calc-silicate pods appear to be metamorphic equivalents of calcareous concretions observed in the Thomson Formation, an equivalent of the Virginia Formation to the south, and described in the Virginia Formation by Pfleider et al (1968). Some calc-silicate bodies may be fractured portions of dolomitic beds of the transition zone between the Virginia Formation and the Biwabik Iron Formation.

"Reaction rims" between the pelitic hornfels and calc-silicate pods have the mineral assemblage plagioclase-clinopyroxene-hypersthene which is intermediate to the assemblages of the hornfels and the pods. Because the "reaction rims" surround both undeformed and angular calc-silicate pods, the rims do not appear to be sedimentary features of the Virginia Formation, but rather appear to have formed after deformation of the pods and during the main metamorphic event. Kirstein (1979) suggests that the "reaction rims" formed by diffusion of calcium from the calc-silicate pods into the pelitic hornfels.

Plastic and brittle deformation of the Virginia Formation accompanied emplacement of the Duluth Complex. This deformation is characterized by tight folds, the random orientation of calc-silicate pods, fractures and breccia zones filled by sulfides and granite to diorite dikes, and numerous xenoliths of the Virginia Formation and apophyses of the Duluth Complex.

#### Metadiabase

Metadiabase in the underground drifts is dark gray with a fine to medium grained (0.5 to 2 mm) diabasic texture (Figure 18). Locally abundant euhedral plagioclase feldspar phenocrysts form clear to milky white, randomly oriented laths up to 3 cm long in the metadiabase (Figure 19). The milky white color is due to corrosion and resorption along internal fractures. Major minerals in the metadiabase are plagioclase (43 to 55%), hypersthene (18 to 43%), and augite (0 to 23%). Minor, locally significant minerals include apatite (tr. to 10%), ilmenite-magnetite (3 to 8%), biotite (tr. to 5%), cummingtonite (tr. to 3%), quartz (0 to 5%), and olivine (0 to 18%). Plagioclase ( $An_{55-73}$ ) forms laths which give the rock its characteristic diabasic texture. The laths are typified by albite and carlsbad twinning, and by cloudy cores with abundant minute inclusions. Edges of the laths are commonly corroded and resorbed. Locally, trace amounts of sericite and carbonate occur along fractures in the plagioclase. The hypersthene is anhedral to subhedral, and commonly is replaced along cleavages by cummingtonite. Locally, the hypersthene forms poikiloblasts, up to 7 mm across, which contain sets of augite exsolution lamellae with various orientations. This textural relationship suggests that the hypersthene poikiloblasts formed by fusion of a group of adjacent pigeonite grains, each with a set of augite exsolution lamellae, during the inversion of pigeonite to

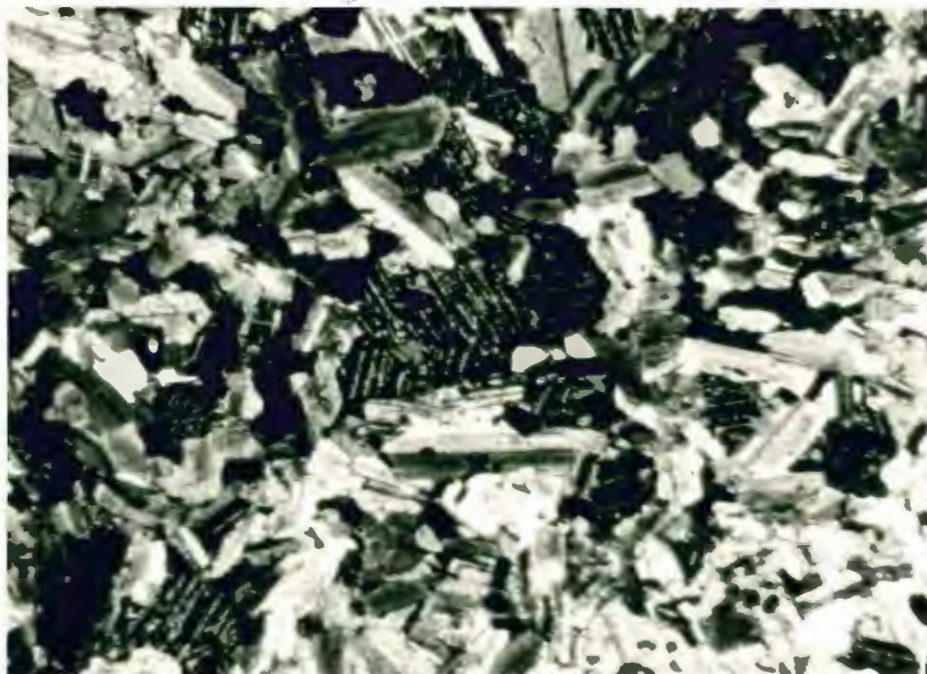


Figure 18. PHOTOMICROGRAPH OF METADIABASE. Note the diabasic texture, the cloudy appearance of plagioclase feldspar laths, and the ophitic hypersthene with randomly oriented sets of augite exsolution lamellae. Sample MM-D-17. Transmitted light, crossed polars. 6.25 mm across.



Figure 19. PORPHYRITIC METADIABASE (dark gray) with plagioclase phenocrysts (white). Red is paint. B drift-485 feet.

hypersthene. The augite forms fine, anhedral grains with well-developed cleavage. The olivine, found only in samples MM6 and MM7, is anhedral to subhedral. Interstitial quartz occurs locally. Euhedral apatite is ubiquitous as minute inclusions in the plagioclase and hypersthene, and forms 10% of sample AX-24. The biotite locally forms poikiloblasts up to 4 mm in length, and is ubiquitous as small, anhedral grains associated with hypersthene and ilmenite-magnetite. The ilmenite-magnetite forms equant to elongate sections and is locally skeletal. Trace amounts of ragged, bladed graphite occur locally.

The diabasic texture of the metadiabase was destroyed to varying degrees during metamorphism. The metadiabase is difficult or impossible to distinguish from the pelitic hornfels in underground workings, except where the plagioclase phenocrysts occur. Contacts between the metadiabase and the pelitic hornfels are difficult to recognize, and the extent of the metadiabase within the underground area can not be accurately determined. The contacts observed are sharp. The metadiabase does not appear chilled. Metadiabase bodies mapped in the drifts range in width of exposure from 10 to 150 feet. Near the end of the D drift, plagioclase phenocrysts in the metadiabase are concentrated within two feet of a conformable contact with the Virginia Formation. This relationship is reported to be characteristic of sills within the Biwabik Iron Formation (Grout and Broderick, 1919). Large, angular metadiabase bodies occur within the Virginia Formation. One such body has a thin rim of granitic material. Generally the metadiabase is less fractured than the Virginia Formation.

#### Interpretation

The metadiabase intrusions are similar in mineralogy and texture to metadiabase dikes and sills in Animikie strata in the region. Their

high degree of metamorphism and the fact that they do not cut the Duluth Complex are evidence that the metadiabase is pre-Duluth Complex. The absence of chilled metadiabase contacts, both at Minnamax and in the adjacent Reserve Mining Company taconite pit, indicates relatively high temperatures for the Virginia Formation during emplacement of the metadiabase.

If the assumption is made that the metadiabase at Minnamax is similar to metadiabase reported elsewhere in the region, speculation can be made about the extent and structural relationships of metadiabase in the underground workings. The metadiabase at Minnamax probably had considerable continuity before deformation. The large angular bodies of metadiabase observed could have formed by fracturing and dispersion of a few metadiabase intrusions during deformation of the Virginia Formation. Dikes are certainly present at Minnamax, and the concentration of plagioclase phenocrysts near the apparently conformable contact of a metadiabase body and the Virginia Formation suggests that sills are present as well.

#### Duluth Complex

The Duluth Complex in the underground workings consists of sulfide-bearing troctolitic rocks which contain barren gabbro to peridotite xenoliths.

#### Sulfide-bearing Troctolitic Rocks

The sulfide-bearing rocks are characteristically troctolitic, but are commonly noritic near the Virginia Formation contact (See Figure 20 for an explanation of the nomenclature for mafic igneous rocks). Modes of selected samples (Table 1) show the variations in composition of the sulfide-bearing rocks. The rocks are typically dark gray, medium to coarse grained, and hypidiomorphic. Locally they are pegmatitic, with

SAMPLES	Oliv.	Plag.	Aug.	Hyp.	Orth.	Amph.	Opaq.	Serp.	Biot.	Apat.	Ser.- Ural.	Rock Type
AX-3	16.6	68.2	7.8	1.5	tr.	-	3.3	0.6	1.8	0.1	tr.	anorthositic troctolite
MM-A-24	12.0	53.2	-	1.6	-	tr.	27.8	2.3	2.7	0.2	0.3	anorthositic troctolite
AX-8	7.9	71.7	6.9	2.4	5.0	1.0	1.4	0.2	2.8	0.1	2.0	troctolitic anorthosite
AX-1	3.8	91.4	2.2	1.2	-	-	0.3	0.3	0.8	-	-	anorthosite
AX-14	10.6	59.2	12.3	6.0	2.0	tr.	9.0	0.1	tr.	0.5	0.4	gabbro
AX-32	4.9	55.0	12.6	5.9	1.5	0.2	13.4	3.1	2.3	0.3	1.0	gabbro
MM-A-3	tr.	52.1	11.0	18.3	-	0.2	3.1	1.7	9.2	0.2	4.0	norite
MM-A-7	-	61.9	7.3	24.4	1.1	-	4.9	-	0.3	0.1	tr.	norite
MM-A-11	-	48.9	1.9	39.0	-	tr.	9.8	-	0.1	0.3	tr.	norite
MM-A-14	9.3	66.3	0.1	20.9	-	-	3.4	0.1	tr.	tr.	-	norite
MM-B-7	3.0	64.2	1.1	26.3	2.2	0.5	tr.	0.7	0.1	0.4	1.5	norite

Table 1. MODAL ANALYSES (VOLUME PERCENT) OF THE SULFIDE-BEARING TROCTOLITIC ROCKS. 1000 points were counted per thin section. For purposes of rock nomenclature, serpentine is considered an alteration product of olivine, sericite-uralite an alteration product of plagioclase feldspar, and amphibole an alteration product of hypersthene.

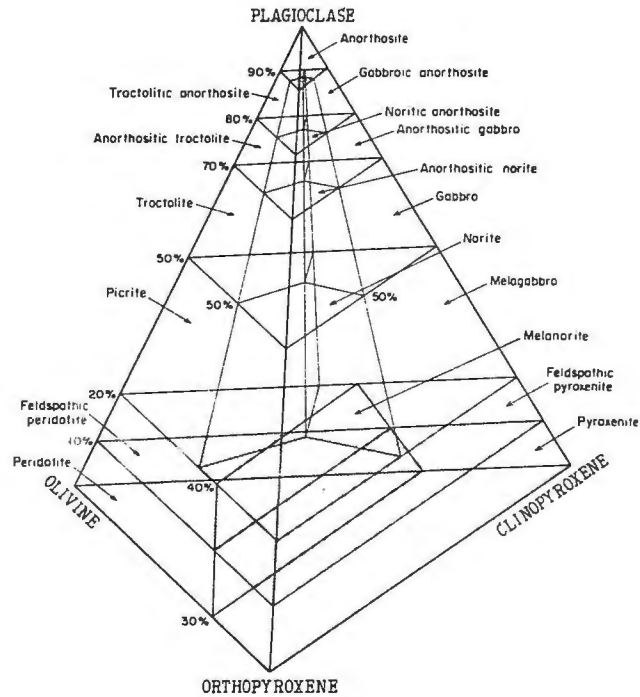


Figure 20. CLASSIFICATION SCHEME FOR MAFIC IGNEOUS ROCKS (from Phinney, 1972).

plagioclase laths up to 7 cm long. The rocks consist primarily of cumulus plagioclase feldspar (45 to 91%), and variable amounts of intercumulus olivine (0 to 17%), hypersthene (2 to 40%), and augite (tr. to 20%) (Figure 21). The plagioclase ( $An_{60-75}$ ) forms randomly oriented, zoned, subhedral to euhedral laths which contain carlsbad, pericline, and albite twinning. Schiller inclusions of minute ilmenite needles are common in cores of the laths. Locally, the laths are deformed with distinct tension fractures. Minor amounts of interstitial, adcumulus plagioclase are common. The Mg-rich olivine is anhedral to subhedral and commonly subpoikilitic to poikilitic with plagioclase embayments and inclusions. Reaction rims of hypersthene are common at contacts of the olivine with plagioclase, as are symplectite intergrowths of plagioclase and hypersthene (Figure 21). The hypersthene is primarily interstitial and an-

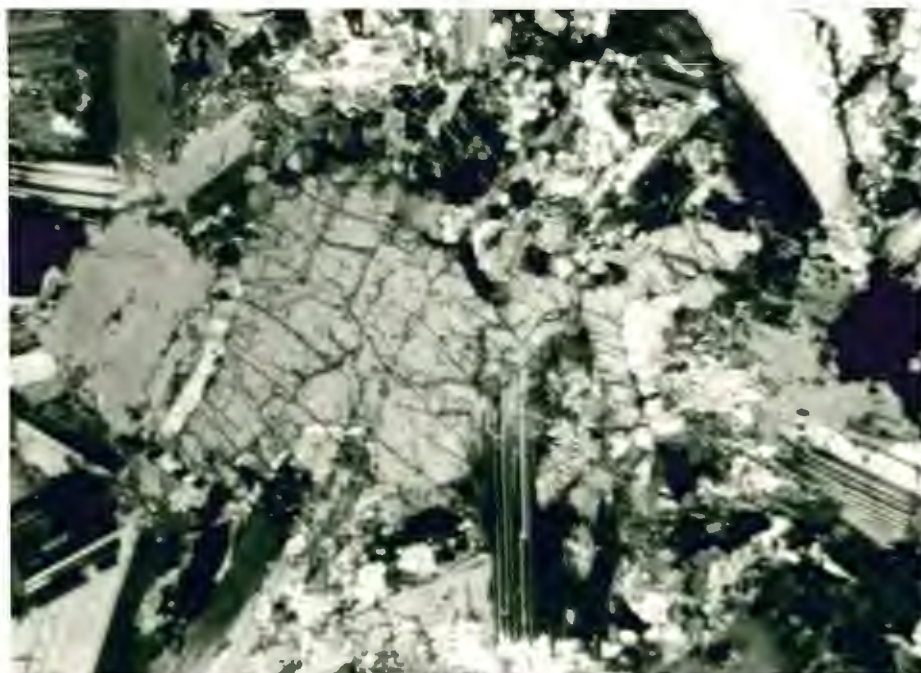
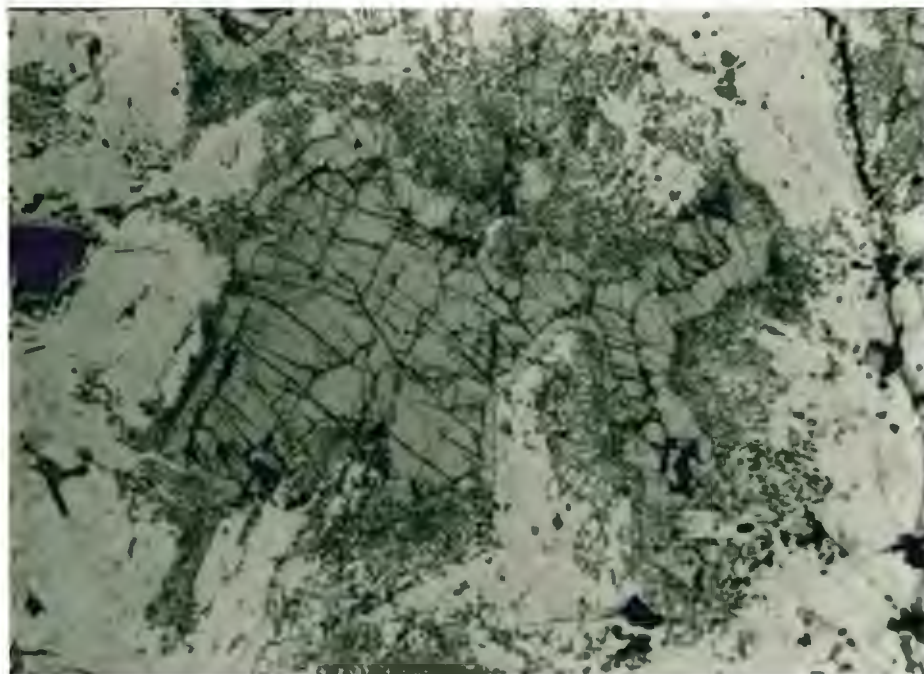


Figure 21. PHOTOMICROGRAPH OF SULFIDE-BEARING NORITE. Note intercumulus olivine rimmed by hypersthene, hypersthene-symplectite intergrowths, and plagioclase feldspar laths. Opaque (to left) is sulfide mantled by biotite. Sample MM-A-14. Transmitted light, uncrossed polars (top) and crossed polars (bottom). 6.25 mm across.

hedral to subhedral, and commonly it is subophitic to ophitic. The hypersthene also forms fine-grained, granoblastic aggregates which mantle olivine, and in some norite samples appears to have entirely replaced the olivine. It contains no inclusions, and is locally altered to cumingtonite (tr. to 5%), which occurs along cleavages in the hypersthene and as radiating, fibrous clusters. The interstitial augite is commonly subophitic to ophitic, and displays well-developed cleavage (Figure 22). Minute, oriented ilmenite and red to brown biotite inclusions are abundant in the augite. Biotite (tr. to 9%) also forms epitaxial straps at contacts between the augite and plagioclase which parallel the augite cleavage, and mantles sulfides and oxides. Interstitial orthoclase (0 to 4%) occurs locally. Minute, euhedral apatite inclusions (tr. to 3%) are ubiquitous. Ragged graphite blades (tr.) occur locally. Subhedral to euhedral ilmenite (1 to 7%) is common.

#### Gabbro to Peridotite Xenoliths

Xenoliths, upwards of 100 feet in maximum dimension, occur in the sulfide-bearing troctolitic rocks in the A drift (Plate 1). The xenoliths range in composition from gabbro to peridotite, and consist primarily of cumulus olivine and plagioclase feldspar and intercumulus augite. Modes of selected samples (Table 2) show the variations in composition of the xenoliths.

Contacts between the xenoliths and the sulfide-bearing troctolitic rocks are sharp and regular to highly irregular (Figure 23). Apophyses of sulfide-bearing troctolitic rocks cut the xenoliths (Figure 24). Plagioclase laths in the sulfide-bearing troctolitic rocks nucleated on the xenoliths and grew outward into the magma, a phenomenon also noted in the Skaergaard intrusion by Wager and Brown (1967) (Figure 25).

The picrites and peridotites are dark olive green, fine to medium

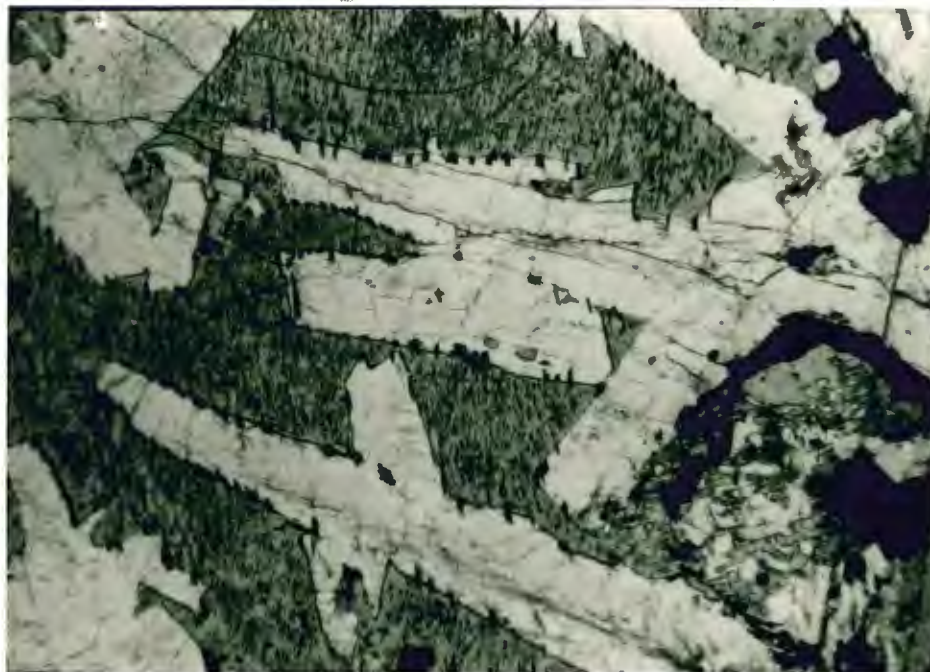


Figure 22. PHOTOMICROGRAPH OF OPHITIC AUGITE. Note the abundant minute ilmenite and biotite inclusions and epitaxial biotite (black) - all are aligned with the augite cleavage. Plagioclase feldspar laths are white. Sample AX-32. Transmitted light, uncrossed polars. 6.25 mm across.

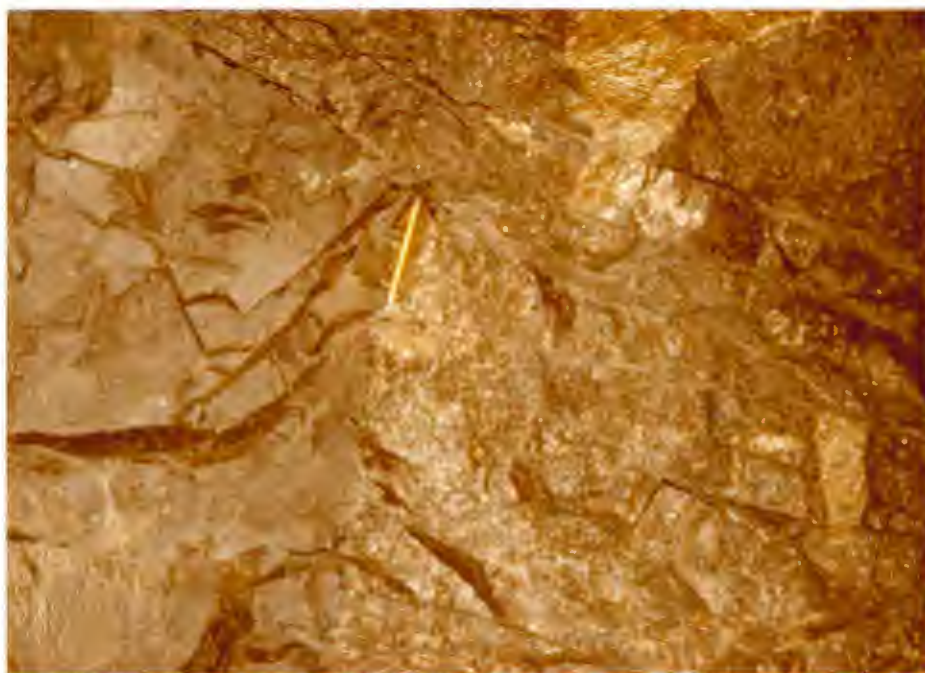


Figure 23. CONTACT BETWEEN SULFIDE-BEARING GABBRO AND A TROCTOLITE XENOLITH. The xenolith (left) forms a sharp contact with the gabbro (right). Sulfides are yellow. A drift-460 feet.

SAMPLES	Oliv.	Plag.	Aug.	Hyp.	Opaq.	Serp.	Biot.	Apat.	Rock Type
MM-A-49	42.7	9.4	2.3	-	9.7	35.7	tr.	tr.	peridotite
AX-12	12.8	17.1	0.6	-	10.6	58.4	0.5	-	feldspathic peridotite
AX-13	39.3	13.6	2.1	-	8.9	37.3	0.7	-	feldspathic peridotite
MM-A-43	24.3	32.4	0.3	-	11.0	31.7	0.3	tr.	picrite
MM-A-45	19.8	22.4	1.7	-	16.8	38.7	0.6	-	picrite
MM-A-42	39.5	57.8	0.5	-	0.2	16.0	0.4	-	troctolite
AX-17	24.0	68.8	4.1	0.6	0.8	0.5	1.2	-	troctolite
MM12	25.5	67.9	4.1	0.5	0.8	-	1.3	-	troctolite
MM-A-41	25.0	71.0	1.6	0.3	1.5	0.4	0.3	tr.	anorthositic troctolite
AX-11	21.4	52.9	25.1	0.4	0.2	tr.	-	tr.	olivine gabbro

Table 2. MODAL ANALYSES (VOLUME PERCENT) OF PERIDOTITE TO GABBRO XENOLITHS. 1000 points were counted per thin section. Serpentine and opaques are considered alteration products of the olivine for purposes of rock nomenclature.



Figure 24. DIKE OF SULFIDE-BEARING TROCTOLITE IN FELDSPATHIC PERIDOTITE XENOLITH. Note the sulfide vein (yellow) at the center of the dike. A drift-635 feet.

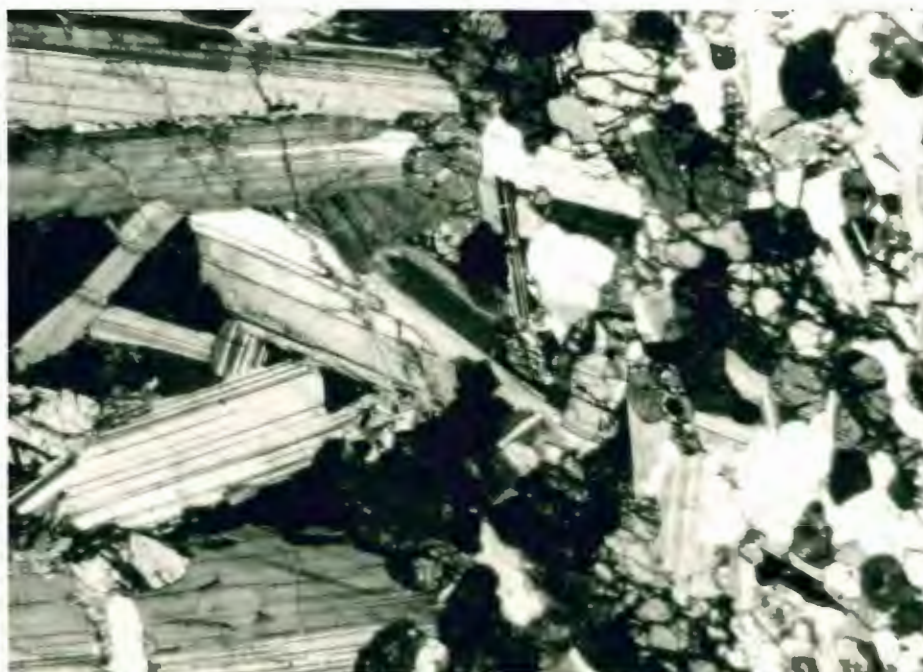


Figure 25. PHOTOMICROGRAPH OF CONTACT BETWEEN SULFIDE-BEARING GABBRO AND PICRITE XENOLITH. Note the plagioclase feldspar laths in the gabbro (left) oriented perpendicular to the contact. Sample MM-A-44. Transmitted light, crossed polars. 6.25 mm across.

grained, and panidiomorphic (Figure 26). They consist primarily of Mg-rich olivine (45 to 88%), plagioclase feldspar (9 to 50%), and augite (tr. to 30%). The olivine is equant and commonly exhibits a bimodal grain size distribution, with medium to coarse grains (4 to 10 mm) in a fine-grained (0.5 to 1 mm) matrix. The olivine crystals are commonly serpentinized to antigorite and magnetite along abundant fractures, producing a net texture. The serpentine veinlets are closely spaced, thin (less than 0.5 mm wide), and subparallel, imparting a foliation to the rock (Figure 26). Biotite occurs in trace amounts as an alteration of olivine and its serpentinization products, and cuts the serpentine foliation. The plagioclase ( $An_{60-73}$ ) forms subhedral laths with ilmenite schiller inclusions, and carlsbad, albite, and pericline twinning. Typically the laths are randomly oriented, but locally they are foliated. The laths commonly occur in fine-grained aggregates that form lenses 2 to 5 mm across. The plagioclase is resistant to fracturing with respect to the olivine, but in many samples subparallel fractures in the olivine continue through the plagioclase laths. The plagioclase is unaltered. The plagioclase forms inclusions in olivine and contains inclusions of olivine, and embays and is embayed by olivine. This textural evidence indicates that the olivine and plagioclase formed simultaneously as cumulus phases in the magma. Locally, symplectite intergrowths of plagioclase and augite occur at contacts of the plagioclase and olivine. The interstitial augite is commonly subpoikilitic, and contains abundant, minute ilmenite and biotite inclusions. In some samples, the augite contains exsolution lamellae of hypersthene.

The troctolites and gabbros are dark gray and fine to medium grained. They consist primarily of cumulus Mg-rich olivine (20 to 45%) and plagioclase feldspar ( $An_{68-72}$ ) (50 to 71%), and intercumulus augite



Figure 26. PHOTOMICROGRAPH OF A PERIDOTITE XENOLITH. Note the equant, interlocking grains of olivine, and the abundant subparallel veinlets of serpentine and magnetite. Sample MM-A-49. Transmitted light, uncrossed polars (top) and crossed polars (bottom). 6.25 mm across.

(tr. to 25%) (Figure 27). They are similar in mineralogy and texture to the peridotites and picrites with the following differences. The plagioclase content increases at the expense of olivine. Some samples are classified as "anorthositic troctolite" and "olivine gabbro" (Figure 20). The augite commonly forms a significant portion of the rocks. Samples with abundant interstitial augite have hypidiomorphic textures (Figure 28), in contrast to the panidiomorphic textures of samples composed primarily of cumulus plagioclase and olivine. The plagioclase laths are commonly foliated (Figure 27), but are randomly oriented in the augite-rich samples. The olivine does not form oikocrysts and is relatively fresh, with only minor serpenitization along fractures.

#### Interpretation

The common occurrence of sulfide-bearing norites near the Virginia Formation contact suggests that the magma was contaminated. Hypersthene in the norites increases at the expense of olivine, which it has replaced. An explanation for this relationship is that silica, introduced into the magma by assimilation of the Virginia Formation, reacted with the olivine to produce hypersthene. Other minerals whose occurrence can be explained by magma contamination are interstitial orthoclase ( $K_2O$ ), trace amounts of graphite, and ubiquitous biotite ( $K_2O, H_2O$ ).

The sulfide-bearing troctolitic rocks appear to have been emplaced as a crystal mush. The plagioclase laths are commonly deformed. Deformation of the Virginia Formation is greater than would be expected if the basaltic magma was liquid. However, the magma was sufficiently fluid to form narrow apophyses, and to incorporate and raft xenoliths of footwall material. The presence of plagioclase laths which nucleated on the gabbro to peridotite xenoliths, and the absence of this relationship at contacts of the sulfide-bearing troctolitic rocks and Virginia Forma-

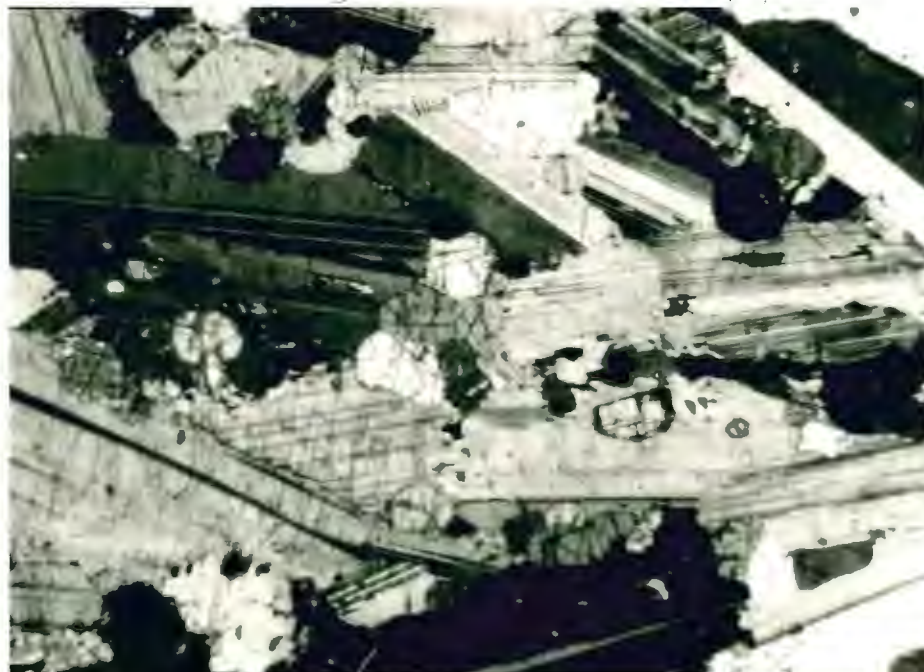


Figure 27. PHOTOMICROGRAPH OF AN ANORTHOSITIC TROCTOLITE XENOLITH. Note the equant, cumulus olivine and the sub-parallel plagioclase feldspar laths. Sample MM-A-41. Transmitted light, crossed polars. 6.25 mm across.

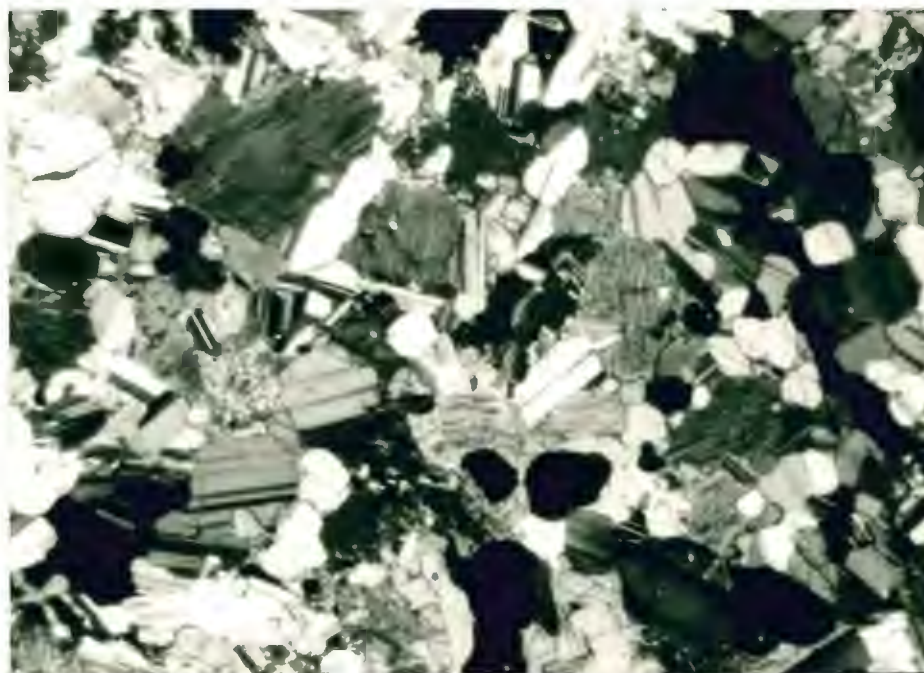


Figure 28. PHOTOMICROGRAPH OF AN OLIVINE GABBRO XENOLITH. Note the abundant interstitial augite with hypersthene exsolution lamellae, and the randomly oriented plagioclase feldspar laths. Sample AX-10. Transmitted light, crossed polars. 6.25 mm across.

tion xenoliths, suggests that the medium of the magma changed prior to its emplacement. The absence of chilled margins on the troctolitic rocks shows that the contact rocks were at high temperatures during emplacement.

The xenoliths of gabbro to peridotite are similar in mineralogy, texture, and paragenesis. Their confinement to an area of the A drift suggests that they may have come from the same intrusion. The rocks are cumulates which formed in a stable magma chamber. Differentiation produced the wide spectrum of igneous rock compositions. The cumulate rocks were incorporated as xenoliths by the sulfide-bearing troctolitic magma and rafted to their present positions.

#### Granite to Diorite Dikes

Granite to diorite dikes occur sporadically in both the Virginia Formation and the Duluth Complex. Commonly the dikes occur within sulfide veins. Modes of selected samples (Table 3) show the variations in composition of the dikes. In the A drift a granite dike, 10 feet wide, contains angular inclusions of the host sulfide-bearing troctolite (Figure 29). The dike material rims some calc-silicate pods and metadiabase bodies.

The dikes are typically white to pink with a medium to coarse grained granitic texture (Figure 30). Locally they are pegmatitic. The granitic rocks typically contain graphic intergrowths of mesoperthite (30 to 65%) and quartz (15 to 35%) (Figures 31 and 32). The mesoperthite is weakly to moderately kaolinitized. Biotite (tr. to 13%) is dark red brown to light green, and forms plates and thin books. Inclusions of stubby, fine-grained plagioclase laths occur in the mesoperthite. Locally plagioclase laths, which contain carlsbad and albite twinning, comprise up to 84% of the dikes. These plagioclase-rich rocks, which are

SAMPLES	Plag.	Orth.	Mpth.	Qtz.	Hyp.	Biot.	Opaq.	Apat.	Carb.	Chlor.	Ser.	Kaol.	Rock Type
MM-B-11	1.3	-	61.3	34.3	-	0.5	2.4	-	tr.	tr.	-	tr.	granite
MM-B-14	2.0	-	64.4	32.4	-	1.3	-	-	-	-	-	tr.	granite
MM-D-6	0.3	-	64.7	33.8	-	12.8	tr.	tr.	tr.	tr.	tr.	tr.	granite
MM-C-13	55.8	32.3	-	7.5	3.4	0.4	tr.	tr.	-	tr.	tr.	tr.	monzonite
MM-A-8	83.7	10.9	-	0.1	4.6	0.6	tr.	tr.	tr.	tr.	-	-	diorite
MM-D-1	79.3	12.2	-	0.2	6.4	0.1	0.9	1.0	tr.	tr.	tr.	tr.	diorite

Table 3. MODAL ANALYSES (VOLUME PERCENT) OF GRANITE TO DIORITE DIKES. 1000 points were counted per thin section.



Figure 29. GRANITE DIKE IN SULFIDE-BEARING TROCTOLITE. Note angular inclusions of the host troctolite (dark gray) in the granite (white). A drift-150 feet.

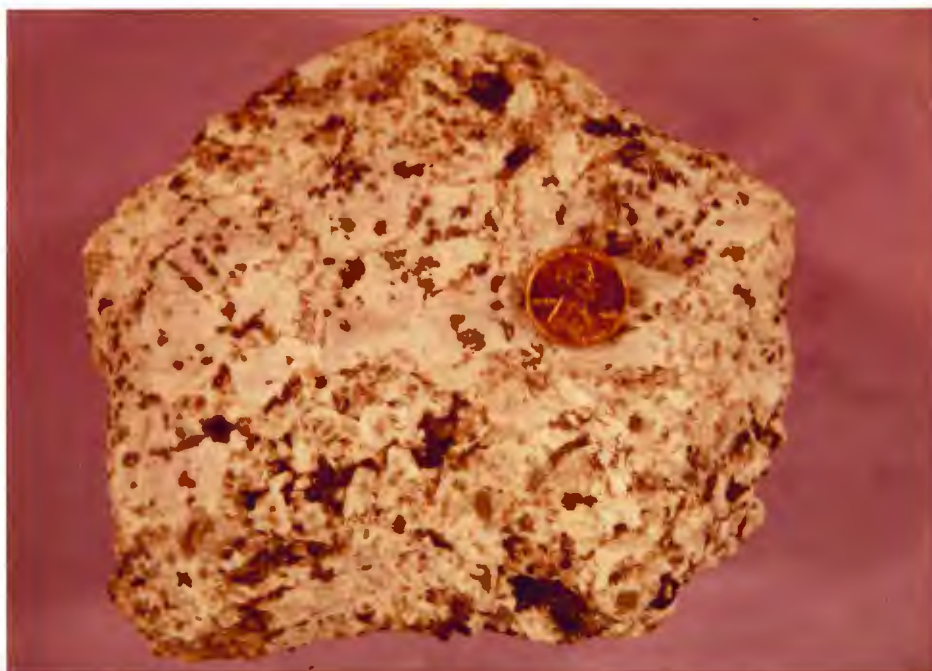


Figure 30. GRANITE DIKE SPECIMEN consisting of quartz (clear), orthoclase (white), and chloritized biotite (black to green). Irregular, dark, recessed areas are miarolitic cavities. A drift-150 feet.



Figure 31. PHOTOMICROGRAPH OF GRAPHIC GRANITE. Graphic intergrowths are of quartz (white) and mesoperthite (black). Sample MM-B-11. Transmitted light, crossed polars. 6.25 mm across.



Figure 32. PHOTOMICROGRAPH OF MESOPERTHITE IN A GRANITE DIKE. The granite consists of quartz (light gray), mesoperthite (white to dark gray), and biotite (gray blade to right). Sample MM-B-14. Transmitted light, crossed polars. 6.25 mm across.

deficient in quartz and mesoperthite, typically contain poikilitic orthoclase (11 to 30%) enclosing the plagioclase, and moderately uralitized, equant hypersthene (3 to 6%). The plagioclase compositions range from  $An_{34}$  to  $An_{50}$ , with calcium content increasing with the percentage of plagioclase in the rock. Weak to moderate sericitization of the plagioclase is ubiquitous. Minute patches of carbonate occur locally in the feldspars. Mirolitic cavities were observed in one granite dike (Figure 30). Generally the dikes are quite variable in composition and texture, and exhibit weak hydrothermal alteration.

#### Interpretation

The dikes probably represent a late differentiate of the Duluth Complex. They are later than the sulfide-bearing troctolitic rocks, as shown by inclusions of the troctolitic rocks within the dikes, and dikes within the troctolitic rocks. Pegmatitic textures, mirolitic cavities, and abundant ubiquitous biotite indicate that the dikes formed from a magma which contained a vapor phase.

## SULFIDE MINERALIZATION

### General Occurrence and Distribution

The sulfide mineralogy of the contact zone is simple, consisting primarily of pyrrhotite, pentlandite, chalcopyrite, and cubanite. Minor minerals include bornite, rammelsburgite, violarite, and native copper.

Sulfides are primarily disseminated in the troctolitic rocks. On a broad scale the sulfide mineralization forms a continuous low-grade zone 400 to 1000 feet thick along the contact (Figure 5). On a mining scale the mineralization is erratic due to variations in sulfide concentration in the troctolitic rocks, and abundant barren xenoliths of the Duluth Complex and the Virginia Formation.

Fe-Cu-Ni sulfide veins fill fractures and breccia zones in both the Duluth Complex and the Virginia Formation. Pelitic hornfels adjacent to the veins and the sulfide-bearing troctolitic rocks commonly contains interstitial sulfides. While the Virginia Formation and the metadiabase typically are barren of sulfides, the veins and associated interstitial sulfides are locally sufficiently concentrated to form economically interesting high-grade zones, the most significant of which is the Local Boy deposit.

Relatively minor occurrences of sulfides include stratiform sulfides in the pelitic hornfels, interstitial sulfides in the calc-silicate pods, and late stage veins along post-Duluth Complex fractures.

### Disseminated Sulfides in the Troctolitic Rocks

Sulfides disseminated in the troctolitic rocks are hexagonal pyr-

rhodite (43% of sulfides), cubanite and chalcopyrite (54% of sulfides), and pentlandite (3% of sulfides) (Stevenson et al, 1979). Cubanite to chalcopyrite ratios average 2 to 1 in the basal troctolites, but are 6 to 1 in the underground workings (Watowich, pers. comm.). This reflects higher iron content of the sulfides immediately at the contact. Copper to nickel ratios average 4.3 to 1, and range between 3.0 to 1 and 5.5 to 1 (Watowich, 1978). Model ore compositions for the basal troctolitic rocks are shown in Table 4.

E L E M E N T	BASAL SULFIDE-BEARING TROCTOLITIC ZONE OF THE DULUTH COMPLEX				HIGH-GRADE SULFIDE ZONES	
	Wt. % of Rock		Wt. % of Cu+Fe+S		Wt. % of Rock	Wt. % of Cu+Fe+S
	M1	M2	M1	M2		
Fe	1.834	1.693	42.7	49.4	7.335	43.9
Cu	0.800	0.516	18.6	15.1	2.849	17.0
Ni	0.185	0.031	-	-	0.318	-
S	1.658	1.215	38.6	35.5	6.528	39.1

Table 4. MODEL ORE COMPOSITIONS FOR THE BASAL SULFIDE-BEARING TROCTOLITIC ROCKS AND FOR Fe-Cu-Ni SULFIDE VEIN-RICH ZONES (from Stevenson et al, 1979).

M1: Determined by chemical analyses.

M2: Determined by modal analyses of polished sections. Calculations assume a 2 to 1 cubanite to chalcopyrite ratio, and use the mineral compositions presented in Table 5.

The sulfides are typically interstitial to silicates and finely disseminated, forming 2 to 4% of the rock. They are paragenetically later than the silicates, thus the size and form of the sulfide grains are controlled by the silicates (Figure 33). The sulfides have triangu-

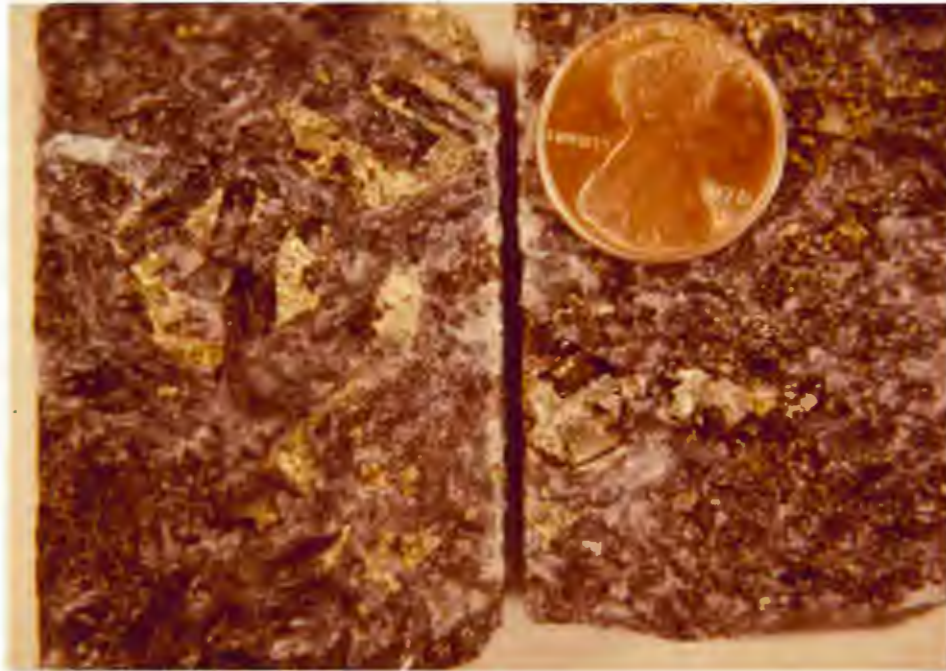


Figure 33. TEXTURES OF DISSEMINATED SULFIDE MINERALIZATION IN THE TROCTOLITIC ROCKS. The sulfides are typically interstitial to plagioclase feldspar laths (left) and are commonly mantled by biotite (right).

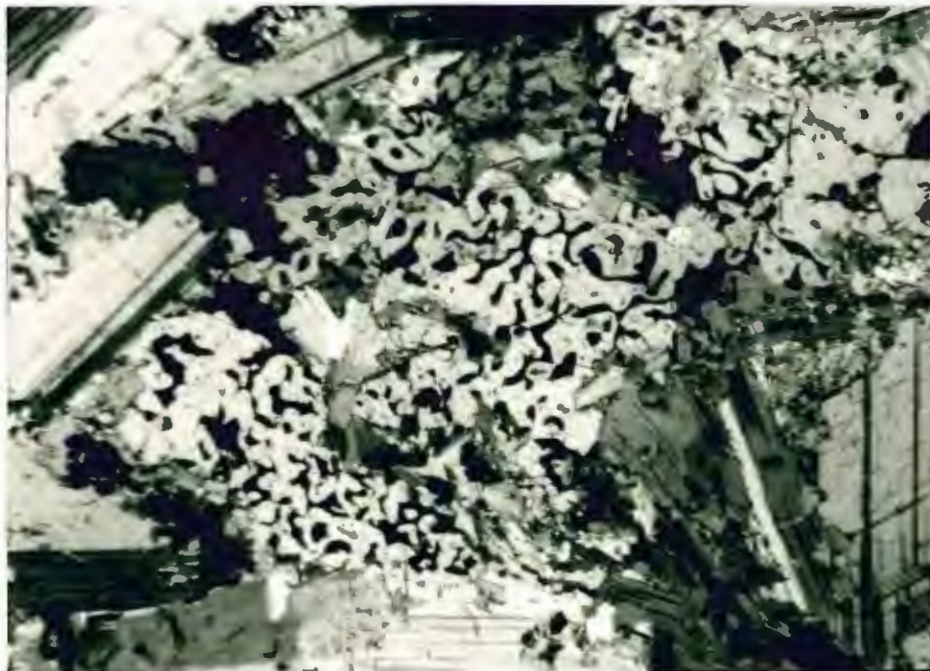


Figure 34. PHOTOMICROGRAPH OF A MYRMEKITIC INTERGROWTH OF CUBANITE-CHALCOPYRITE AND HYPERSTHENE IN TROCTOLITE. Sample AX-30. Transmitted light, crossed polars. 6.25 mm across.

lar forms between enclosing plagioclase laths, and are coarse-grained in pegmatitic rocks. Locally the interstitial sulfides coalesce to form knots up to several centimeters in diameter. Trace amounts of the sulfides fill fractures in silicates, and form myrmekitic intergrowths with hypersthene (Figure 34). Biotite commonly mantles the sulfides (Figure 33). Generally silicate minerals adjacent to the sulfides are unaltered, but minor sericitization of plagioclase, serpenitization of olivine, uralitization of pyroxenes, and carbonate occur locally.

### Sulfide Veins

Sulfide veins in the contact zone are of two types:

1. Fe-Cu-Ni sulfide veins similar in sulfide and silicate mineralogy to the sulfide-bearing troctolitic rocks.
2. late stage veins which occur along post-Duluth Complex fractures.

### Fe-Cu-Ni Sulfide Veins

Fe-Cu-Ni sulfide veins fill fractures and breccia zones, up to 30 feet wide, in both the Duluth Complex and the Virginia Formation (Figures 35, 36, and 37). The veins are in sharp contact with the host lithologies. Interestingly, some veins cut the xenoliths but do not extend into the adjacent sulfide-bearing troctolitic rocks. This suggests that some veins formed before the troctolitic rocks could be fractured. Veins offset other veins, which suggests that deformation occurred during formation of the veins.

Veins in the Duluth Complex and the Virginia Formation are distinctly different in sulfide mineralogy. In the Duluth Complex the veins consist of hexagonal pyrrhotite (45 to 70% of sulfides) and cubanite (16 to 40% of sulfides), with minor amounts of chalcopyrite (tr. to 4% of sulfides) and pentlandite (5 to 14% of sulfides). Veins in the Virginia Formation consist mainly of chalcopyrite (5 to 100% of sulfides) and cu-



Figure 35. CHALCOPYRITE-CUBANITE VEIN filling a breccia zone in the pelitic hornfels of the Virginia Formation. C drift-127 feet.



Figure 36. Fe-Cu-Ni SULFIDE VEIN IN THE SULFIDE-BEARING TROCTOLITE. Note the sharp contact of the vein with the troctolite (dark gray) and the granite dike (white to pink) within the vein. B drift-1120 feet.

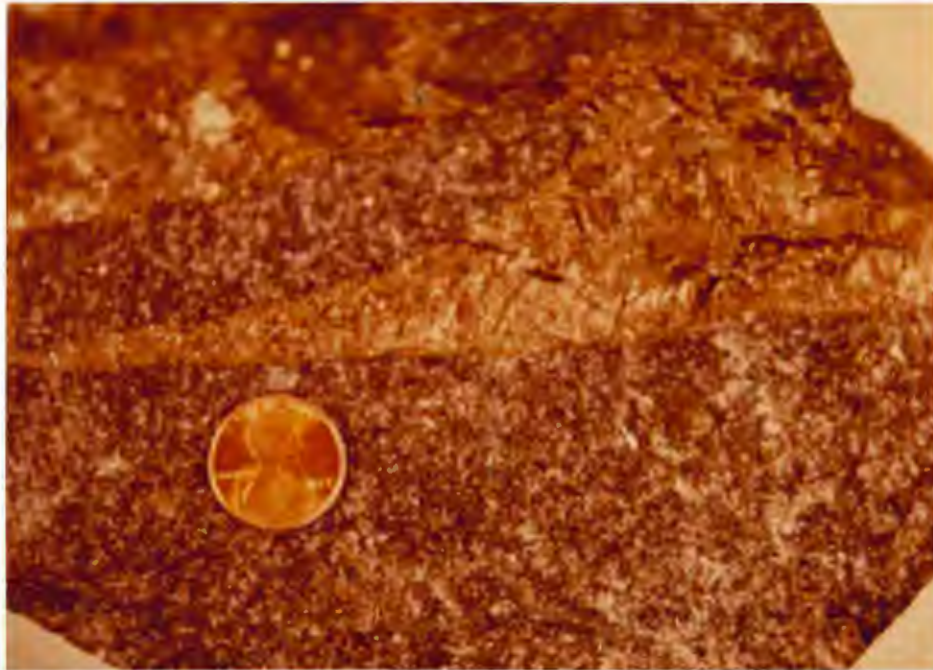


Figure 37. Fe-Cu-Ni SULFIDE VEIN IN SULFIDE-BEARING TROCTOLITE.  
Note sharp contacts of the vein with the host troctolite.  
End of B drift.

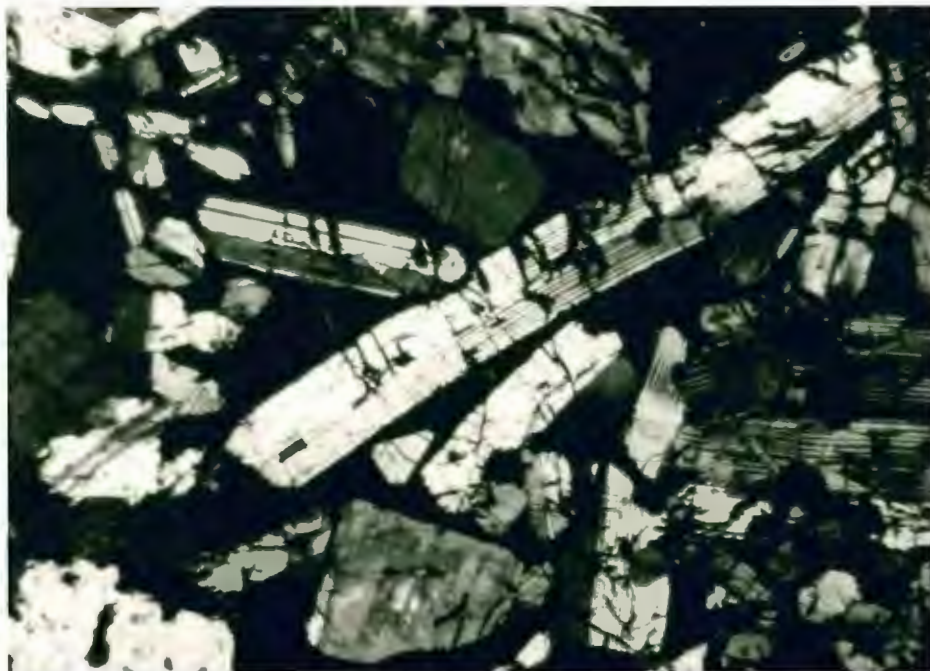


Figure 38. PHOTOMICROGRAPH OF CHALCOPYRITE-CUBANITE VEIN.  
The chalcopyrite-cubanite encloses deformed plagioclase  
laths and fills tension fractures in the laths. Sample  
MM-C-2. Transmitted light, crossed polars. 6.25 mm  
across.

banite (0 to 65% of sulfides), together forming 70 to 100% of the vein sulfides. Minor constituents are hexagonal pyrrhotite (0 to 25% of sulfides), pentlandite (0 to 17% of sulfides), and bornite (0 to 30% of sulfides). The abundance of copper-sulfides (particularly chalcopyrite) in veins in the Virginia Formation is fundamental to the high-grade copper mineralization in the Local Boy deposit. In some drill cores, pyrrhotite is concentrated at the lower margins of copper-rich veins, a relationship noted by Abel et al (1979) in copper-rich veins in the foot-wall of the Strathcona mine, Sudbury, Ontario.

The vein sulfides form a matrix to: plagioclase feldspar, olivine, and hypersthene - all are similar to minerals in the sulfide-bearing troctolitic rocks. The plagioclase ( $An_{58+}$ ) forms fine to medium grained, deformed laths (Figure 38). The hypersthene is fine to medium grained, anhedral to subhedral, and commonly subpoikilitic. The olivine is fine-grained and equant, and commonly is rimmed by hypersthene (Figure 39). Subhedral poikilitic orthoclase is common. Trace amounts of ilmenite and magnetite occur locally. Biotite is intergrown and contemporaneous with the sulfides, forming up to 20% of some samples (Figure 40), and locally mantles the sulfides. Olivine is commonly serpentized along contacts with the sulfides. Uralitization of the hypersthene and sericitization of the plagioclase are minor to absent. Trace amounts of carbonate occur locally.

Granite to diorite dikes commonly occur within the veins. The dikes are relatively barren of sulfides and are in sharp contact with the vein sulfides (Figure 36). Olivine and pyroxene within the veins are strongly altered along these contacts, forming distinct reaction rims (Figure 41).

#### Late Stage Veins

Late stage vein mineralization occurs along post-Duluth Complex

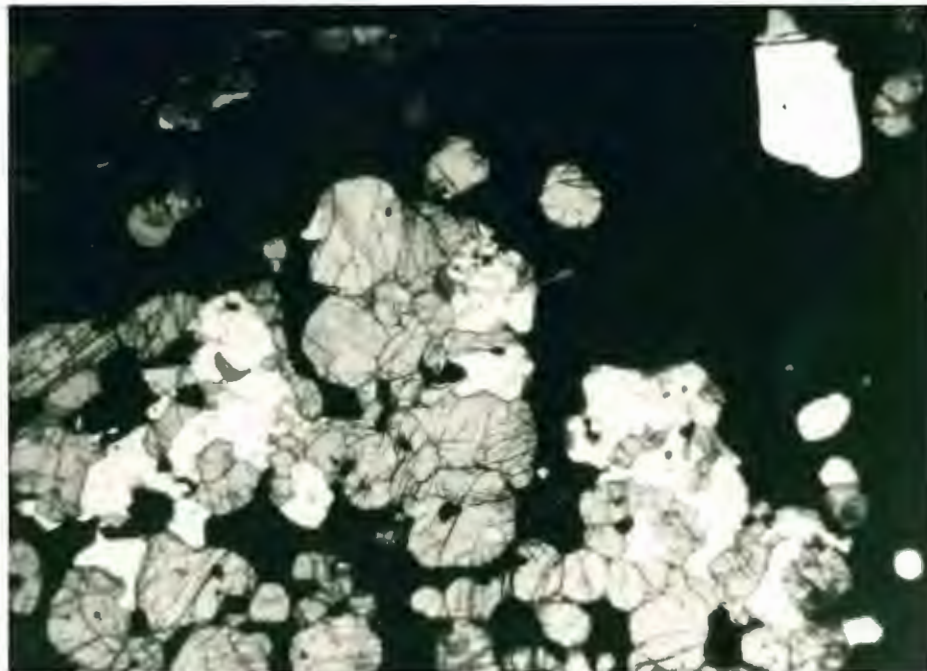


Figure 39. PHOTOMICROGRAPH OF AN Fe-Cu-Ni SULFIDE VEIN. Note the sulfides (primarily pyrrhotite and cubanite) (black) interstitial to and enclosing olivine (gray, high relief) and plagioclase feldspar (white, low relief). Sample MM-B-16d. Transmitted light, uncrossed polars. 6.25 mm across.

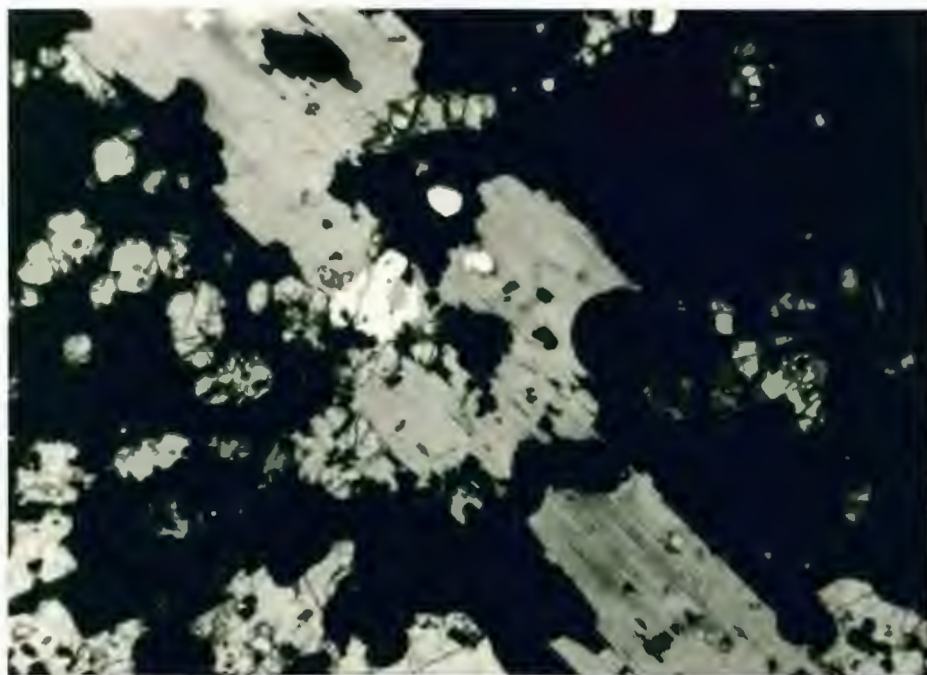


Figure 40. PHOTOMICROGRAPH OF A BIOTITE-RICH Fe-Cu-Ni SULFIDE VEIN. Note the poikiloblastic texture of the biotite. Sample MM-B-15c. Transmitted light, uncrossed polars. 6.25 mm across.

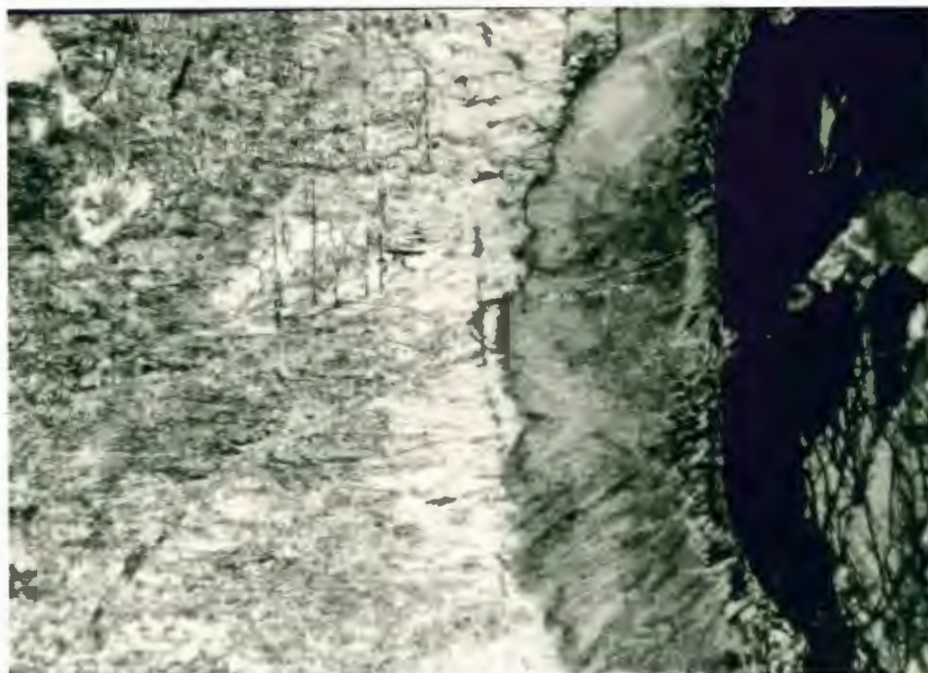


Figure 41. PHOTOMICROGRAPH OF THE CONTACT BETWEEN AN Fe-Cu-Ni SULFIDE VEIN AND A GRANITE DIKE. Note the reaction zone between the granite (light gray) and the sulfides (black). Olivine (high relief) in the sulfides is strongly altered. Sample MM-B-16a. Transmitted light, uncrossed polars. 6.25 mm across.



Figure 42. CHALCOPYRITE-RICH LATE STAGE VEIN along a post-Duluth Complex shear zone in the Virginia Formation. C drift-280 feet.

fractures (Figure 42). The veins are up to 3 feet thick and transect all lithologies. They consist mainly of chalcopyrite, bornite, chalcocite, quartz, and calcite (Figure 43). Acicular laumontite is common. Euhedral pyrite and quartz crystals were observed along some fracture surfaces. Where along faults, the veins also contain gouge and breccia.

#### Interstitial Sulfides in the Virginia Formation

Interstitial sulfides in the Virginia Formation are of three types:

1. stratiform sulfides in the pelitic hornfels.
2. sulfides in the pelitic hornfels adjacent to the Fe-Cu-Ni sulfide veins and the sulfide-bearing troctolitic rocks.
3. sulfides in the calc-silicate pods.

#### Stratiform Sulfides

Interstitial sulfides form stratiform bands, 1 to 10 mm thick, in the pelitic hornfels. The silicate mineralogy of the host pelitic hornfels is typically homogeneous, and graphite is abundant. The sulfide in the bands is monoclinic pyrrhotite; copper and nickel sulfides are absent. This sulfide assemblage is unique in the contact zone.

#### Sulfides in Pelitic Hornfels Adjacent to the Sulfide-bearing Troctolitic Rocks and Fe-Cu-Ni Sulfide Veins

Sulfides are locally concentrated in the pelitic hornfels adjacent to the sulfide-bearing troctolitic rocks and the Fe-Cu-Ni sulfide veins. The sulfides are interstitial to granoblastic, unaltered silicates, and commonly enclose spherical individual crystals and granoblastic aggregates (Figure 44). Biotite, which is typically poikiloblastic, is intergrown with and mantles the sulfides, indicating that biotite formation and emplacement of the sulfides are coeval.



FIGURE 43. LATE STAGE VEIN MINERALIZATION IN FAULT BRECCIA. The mineralization consists primarily of bornite (blue), quartz (white), and calcite (white). B drift-300 feet.

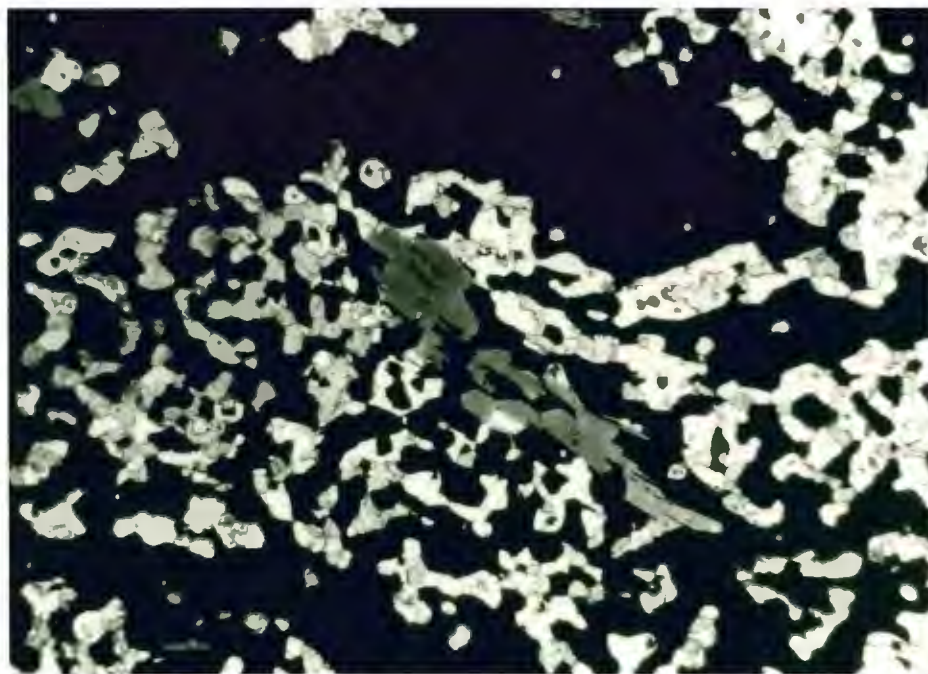


Figure 44. PHOTOMICROGRAPH OF INTERSTITIAL SULFIDES IN THE PELITIC HORNFELS. The sulfides (black) are interstitial to granoblastic hypersthene (gray, high relief), plagioclase feldspar (white, low relief), and cordierite (white, low relief). Note the poikiloblastic biotite. Sample MM-A-38. Transmitted light, uncrossed polars. 6.25 mm across.

The sulfides are primarily hexagonal pyrrhotite (40 to 70% of sulfides) and cubanite (20 to 28% of sulfides), with chalcopyrite (0 to 30% of sulfides), pentlandite (tr. to 10% of sulfides), and bornite (0 to 4% of sulfides) present locally. Thus, the sulfide assemblage is relatively high in iron. Trace amounts of ilmenite occur locally in the sulfides.

One sample of mafic hornfels contains chalcopyrite which is interstitial to granoblastic augite and strongly sericitized plagioclase feldspar (Figure 45). The chalcopyrite is rimmed and cut by minute chlorite veinlets, and occurs with trace amounts of carbonate.

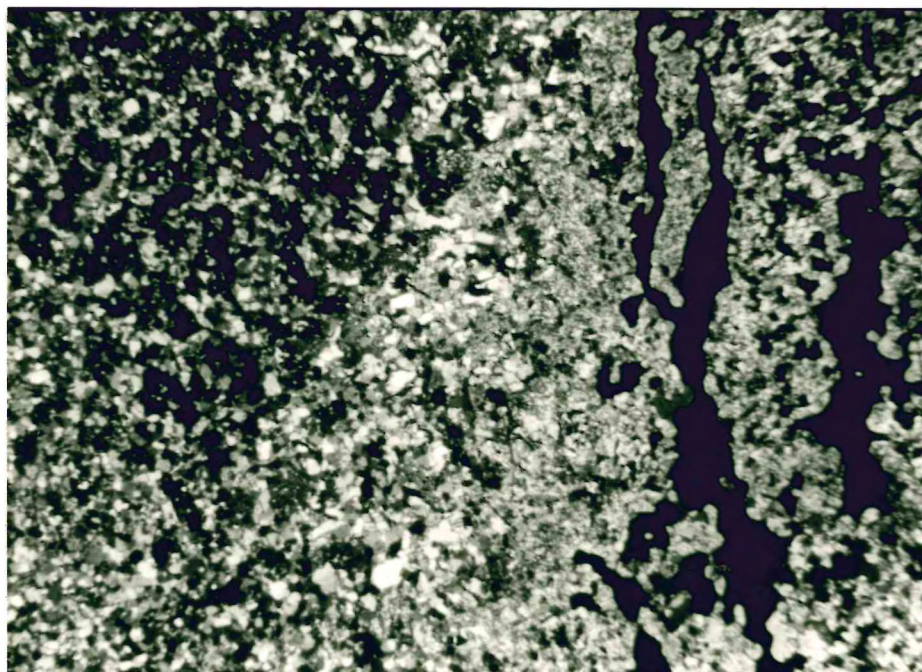


Figure 45. PHOTOMICROGRAPH OF INTERSTITIAL CHALCOPYRITE IN MAFIC HORNFELS. The hornfels contains augite, highly sericitized plagioclase feldspar, and chalcopyrite (black). Sample MM-C-5. Transmitted light, crossed polars. 6.25 mm across.

### Sulfides in the Calc-silicate Pods

Calc-silicate pods within the sulfide-rich pelitic hornfels are relatively barren of sulfides (Figure 46). However, some pods contain copper-sulfides and associated gangue mineralization (Figure 47). The principal minerals are chalcopyrite with exsolved cubanite, and poikiloblastic calcite, quartz, and apophyllite, which combined form up to 20% of the pods. Associated minerals (0 to 5% combined) are anhydrite, fluorite, heulandite, laumontite, and prehnite. The anhydrite forms interstitial aggregates of radiating crystals and euhedral crystals up to 1 cm long. In some samples it appears to have replaced wollastonite. The fluorite forms purple, subhedral inclusions in quartz. The prehnite occurs in fractures in anorthite (Kirstein, 1979).

### Mineragraphy

#### Pyrrhotite

Pyrrhotite ( $\text{Fe}_{1-x}\text{S}$ ) (Table 5) is characteristically hexagonal, though magnetic, monoclinic pyrrhotite occurs in the stratiform sulfides in the Virginia Formation. The pyrrhotite forms fine to coarse grained crystals up to 10 mm across that occur as anhedral interlocking grains, as islands in optical continuity within cubanite-chalcopyrite (Figure 48), and as rounded inclusions with chalcopyrite in silicates. In the Fe-Cu-Ni sulfide veins and in interstitial sulfides in the pelitic hornfels, the pyrrhotite commonly contains wavy exsolution intergrowths of troilite which produce a basketweave texture (Figure 49). The pyrrhotite is embayed and replaced by cubanite-chalcopyrite (Figure 48), and locally contains blade-like inclusions of chalcopyrite-cubanite.

#### Pentlandite

Pentlandite ( $(\text{Fe,Ni})_9\text{S}_8$ ) (Table 5) forms equant, anhedral crystals which are fine to coarse grained with a distinct hackly fracture (Figure



Figure 46. SULFIDE-RICH ZONE IN THE PELITIC HORNFELS. The sulfides surround barren calc-silicate pods (light gray) and "reaction rims" (dark gray). Red is paint. C drift-250 feet.



Figure 47. SULFIDE MINERALIZATION IN A CALC-SILICATE POD. The surrounding pelitic hornfels is sulfide-rich. B drift-562 feet.

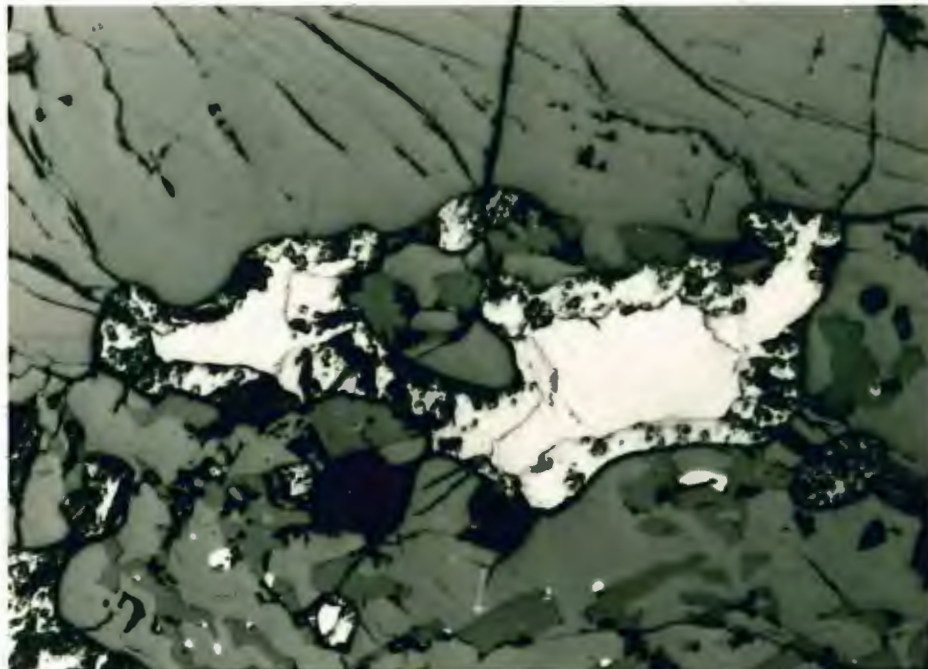


Figure 48. PHOTOMICROGRAPH OF PYRRHOTITE REPLACED BY CUBANITE. The pyrrhotite (white, smooth) forms islands in optical continuity in the cubanite (light gray, weakly hackly). The medium to dark grays are silicates. Sample MM-D-14. Reflected light, uncrossed polars. 1.5 mm across.



Figure 49. PHOTOMICROGRAPH OF AN EXSOLUTION INTERGROWTH OF TROILITE AND PYRRHOTITE. Note the basketweave texture of the troilite (light gray) and the pyrrhotite (gray). Sample MM-A-17. Reflected light, crossed polars. 1.5 mm across.

E L E M E N T	PYRRHOTITE		PENTLANDITE		CUBANITE		CHALCOPYRITE	
	Wt. %	Atm. Prop.	Wt. %	Atm. Prop.	Wt. %	Atm. Prop.	Wt. %	Atm. Prop.
Fe	63.3	1.015	31.9	0.572	41.1	0.696	30.6	0.520
Cu					23.2	0.345	34.4	0.514
Ni			31.3	0.534				
Co			3.3	0.056				
S	35.8	1.000	32.0	1.000	33.9	1.000	33.8	1.000

Table 5. COMPOSITIONS OF THE MAJOR SULFIDE MINERALS determined by electron microprobe. Values shown are averages for the underground workings; only slight variations in composition exist. (Information provided courtesy of AMAX Exploration, Inc.)

\* Atm. Prop.: atomic proportion on basis of 1 sulfur atom.

50). It typically occurs at contacts between chalcopyrite-cubanite and pyrrhotite grains. The pentlandite commonly is replaced by chalcopyrite-cubanite along cleavages, leaving islands and skeletal crystals of pentlandite in a chalcopyrite-cubanite matrix (Figure 51).

#### Cubanite-Chalcopyrite

Cubanite ( $\text{CuFe}_2\text{S}_3$ ) (Table 5) and chalcopyrite ( $\text{CuFeS}_2$ ) (Table 5) typically are anhedral and fine to medium grained. Commonly they occur together, with cubanite lamellae exsolved along the (111) cleavage of chalcopyrite (Figure 52). Either cubanite or chalcopyrite can predominate in these grains. Locally the chalcopyrite forms blade-like crystals in pyrrhotite and basket-weave intergrowths with pentlandite. In the sulfide-bearing troctolitic rocks, chalcopyrite and cubanite form round inclusions in silicates and myrmekitic intergrowths with hypersthene

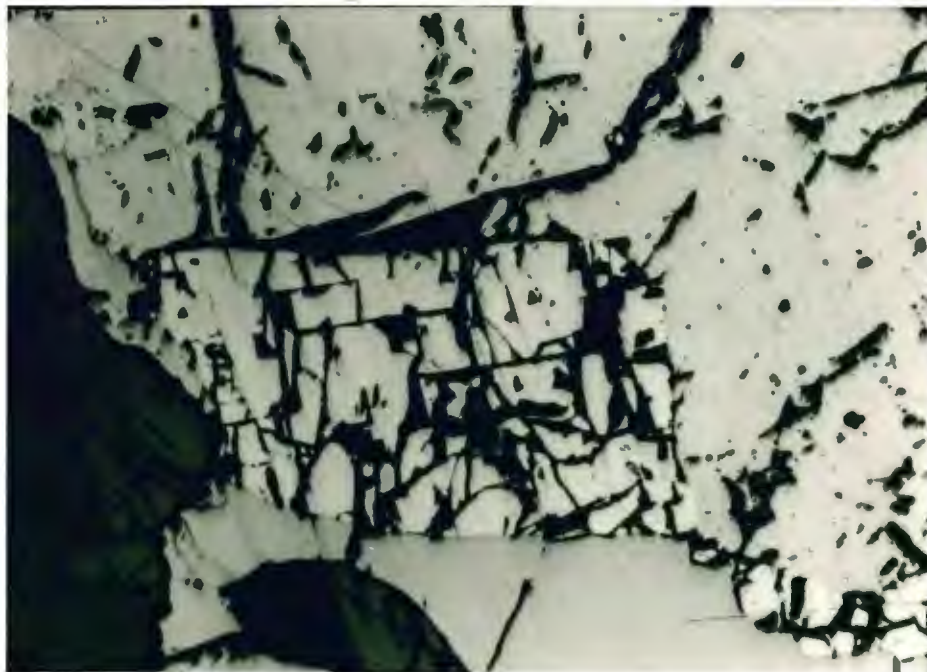


Figure 50. PHOTOMICROGRAPH OF PENTLANDITE (equant, white, hackly) bordered by cubanite (light gray, weakly hackly) above, by pyrrhotite (light gray, smooth) below, and by silicates (medium to dark gray) to left. Sample MM-D-14. Reflected light, uncrossed polars. 1.5 mm across.

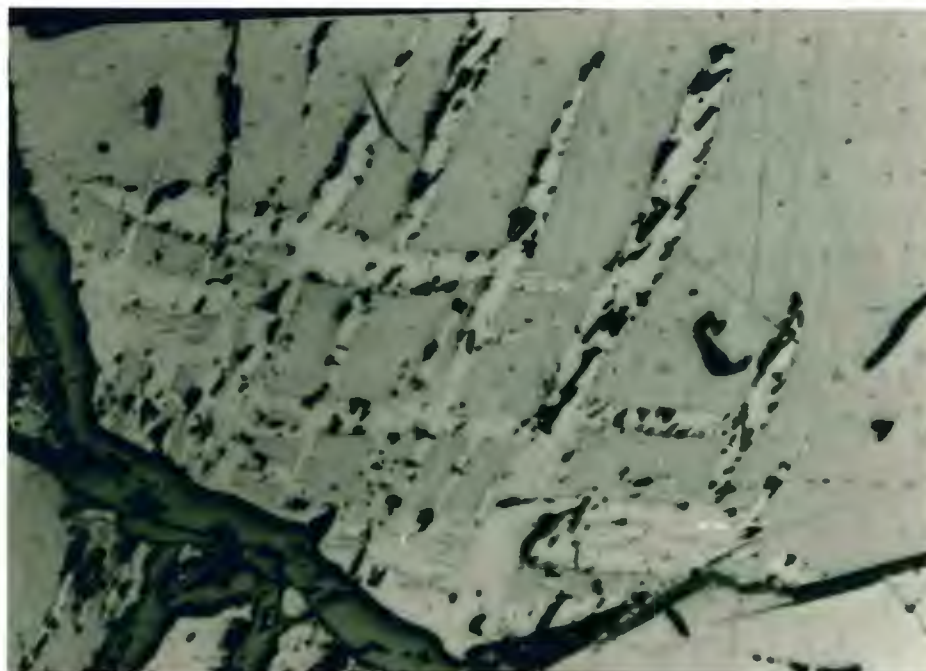


Figure 51. PHOTOMICROGRAPH OF PENTLANDITE REPLACED BY CHALCOPYRITE. The skeletal pentlandite (white, hackly) was replaced along cleavages by the chalcopyrite (light gray). Medium gray to lower left is silicate. Sample MM-B-5. Reflected light, uncrossed polars. 1.5 mm across.

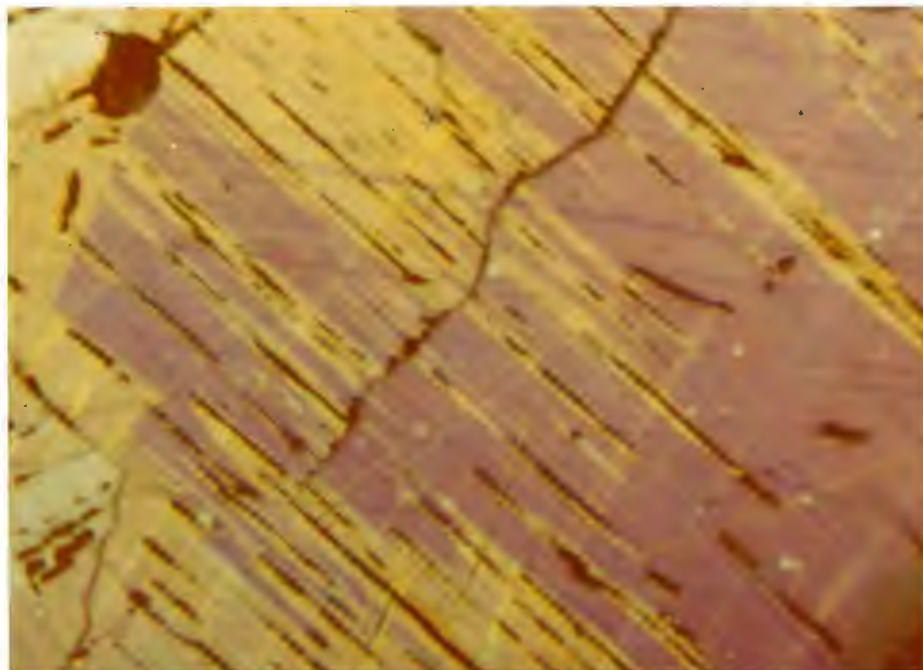


Figure 52. PHOTOMICROGRAPH OF EXSOLVED CUBANITE-CHALCOPYRITE. The cubanite (purple) exsolved along the (111) cleavage of the chalcopyrite (yellow). Sample MM-C-1. Reflected light, crossed polars. 1.5 mm across.

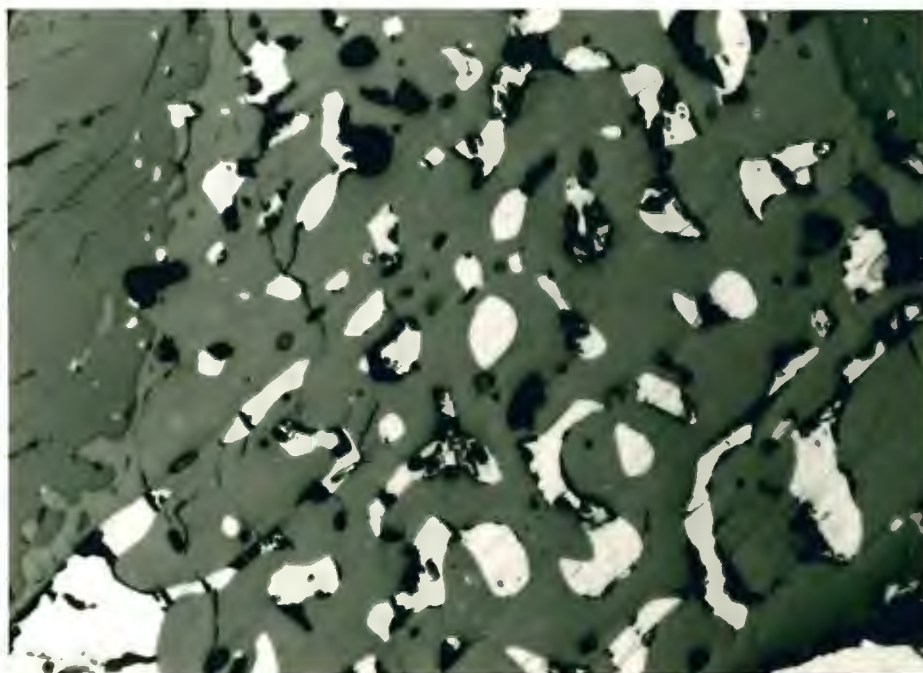


Figure 53. PHOTOMICROGRAPH OF A MYRMEKITIC INTERGROWTH OF PYRRHOTITE AND HYPERSTHENE IN TROCTOLITE. The pyrrhotite is white. Sample AX-30. Reflected light, uncrossed polars. 1.5 mm across.

(Figure 53), and cut silicates along fractures. The chalcopyrite and cubanite cut and replace both pyrrhotite and pentlandite, thus, the cubanite and chalcopyrite are paragenetically later. Locally bornite ( $\text{Cu}_5\text{FeS}_4$ ) has replaced the chalcopyrite in amounts up to 30% of the sulfides (Figure 54).

#### Ilmenite and Magnetite

Ilmenite ( $\text{FeTiO}_3$ ) and magnetite ( $\text{Fe}_3\text{O}_4$ ) commonly occur with the sulfides. Ilmenite is ubiquitous and relatively abundant in the sulfide-bearing troctolitic rocks, where it forms fine to medium grains which are equant, skeletal, and rod-like (4 mm) (Figure 55). The ilmenite appears to have formed prior to the crystallization of the sulfide phases. Trace amounts of magnetite occur locally as round, anhedral grains in the sulfides and as veinlets cutting the sulfides. Thus two generations of magnetite are present.

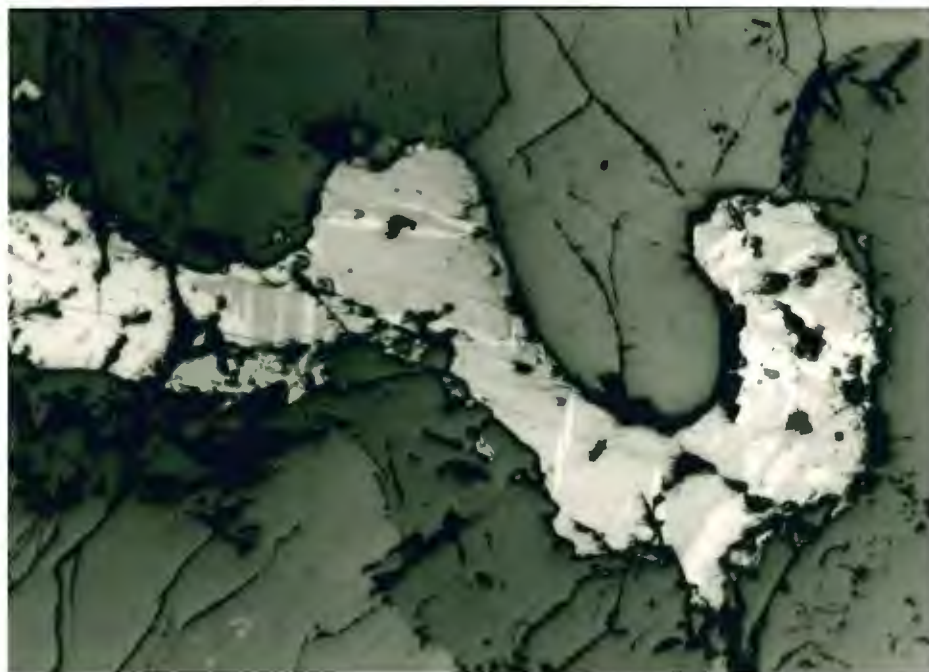


Figure 54. PHOTOMICROGRAPH OF INTERGROWN CHALCOPYRITE AND BORNITE IN NORITE. The chalcopyrite is white, the bornite is light gray, and silicates are darker grays. Sample MM-D-14. Reflected light, uncrossed polars. 1.5 mm across.

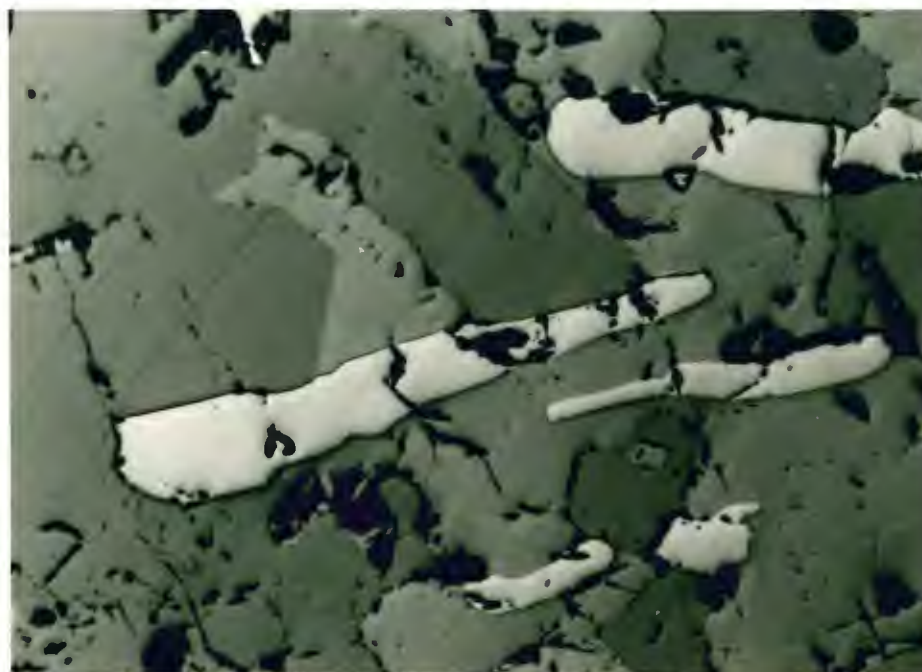


Figure 55. PHOTOMICROGRAPH OF ILMENITE IN SULFIDE-BEARING NORITE. The ilmenite (light gray) forms rods within the silicates (darker grays). Sample MM-A-11. Reflected light, uncrossed polars. 1.5 mm across.

## GENESIS OF THE SULFIDE MINERALIZATION

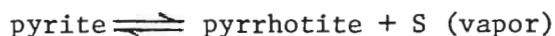
Sulfides in the contact zone appear to be of three genetic types:

1. syngenetic, sedimentary sulfides in the Virginia Formation.
2. magmatic sulfides in the troctolitic rocks and the veins, and magmatic sulfide replacement of the pelitic hornfels.
3. hydrothermal sulfides in the late stage veins and the calc-silicate pods.

### Syngenetic, Sedimentary Sulfides in the Virginia Formation

The stratiform sulfides in the Virginia Formation appear to be syngenetic with the host pelitic sediments. The bedded nature of the sulfides can not be explained by selective replacement since the silicate mineralogy of the rocks is homogeneous. The absence of copper and nickel sulfides suggests that the stratiform sulfides were isolated from the magmatic sulfides.

The stratiform sulfides appear to have formed by the deposition of pyrite in a carbonaceous (now graphitic) sediment. Bedded pyrite in carbonaceous sediments is common in less metamorphosed portions of the Virginia Formation. During metamorphism the pyrite recrystallized to form interstitial monoclinic pyrrhotite by the reaction:



The sulfur released by this reaction may have diffused into the troctolitic magma.

### Magmatic Sulfides

The magmatic sulfides are assumed to have formed from an immiscible

sulfide liquid in the troctolitic magma. The copper to nickel ratios and the interstitial nature of the sulfides in the basal troctolitic rocks are consistent with this interpretation. The absence of basin-like sulfide bodies in depressions of the footwall contact, such as occur at Sudbury, Ontario, can be explained by the dynamic, turbulent emplacement of the magma as a viscous crystal mush. The question of the extent to which the sulfur was orthomagmatic or assimilated from the Virginia Formation is beyond the scope of this study.

The Fe-Cu-Ni sulfide veins appear to have formed by filter-pressing of sulfide liquids from the troctolitic magma into fractures. The olivine and deformed plagioclase laths in the veins, and similar sulfide assemblages in the veins and the troctolitic rocks support this interpretation. The paucity of ilmenite in the veins, in contrast to its abundance in sulfides in the troctolitic rocks, may be due to crystallization of the ilmenite before filter-pressing. The local abundance of biotite and orthoclase in the veins represents concentrations of  $K_2O$ .

Sulfides in the veins show evidence of considerable mobilization. The veins extend over 100 feet into the Virginia Formation from the sulfide-bearing troctolitic rocks. Where the veins occur in the troctolitic rocks, the adjacent host rocks form sharp contacts with the veins and are not depleted in sulfides. Some veins which cut the xenoliths abut against the sulfide-bearing troctolitic rocks, suggesting that these veins formed before the troctolitic rocks could be fractured. The occurrence of granite to diorite dikes within the veins is attributed to dilatant fractures which reopened the veins to form conduits for the dike emplacement.

Copper-rich sulfide veins are fundamental to the high-grade copper mineralization of the Local Boy deposit. The veins appear to have form-

ed by separation of a copper-rich liquid from a pyrrhotite solid solution at magmatic temperatures. Concentrations of pyrrhotite at the base of some large copper-rich veins suggests relatively unrestricted movement of the pyrrhotite solid solution in the liquid. The pyrrhotite concentrations may have formed by flow mechanisms or by gravitational settling.

Sulfides in the pelitic hornfels adjacent to the sulfide-bearing troctolitic rocks and the Fe-Cu-Ni sulfide veins have an interstitial, replacement texture. The sulfides appear to have formed by diffusion along grain boundaries and replacement of the silicates. The disseminated to massive concentrations of these sulfides reflect the degree of replacement.

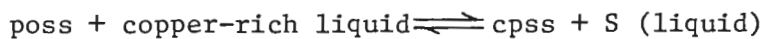
The abundance of sulfide veins and associated replacement sulfides in the pelitic hornfels with respect to the other lithologies is due to the susceptibility of the hornfels to brittle deformation and to replacement by the magmatic sulfide fluids.

Experimental work in the Cu-Fe-S (Kullerud, Yund, and Moh, 1969) and Cu-Fe-Ni-S (Craig and Kullerud, 1969) systems determined the stability fields of phase assemblages in isochemical magmatic sulfide systems. Results of this work are consistent with the sulfide paragenesis and sulfide assemblages observed at Minnamax \*. Of particular significance is that the "M2" model ore composition for the basal troctolitic rocks (Table 4) lies within the pyrrhotite solid solution-copper rich liquid field in the Cu-Fe-S system at  $1000^{\circ}$  C. (Figure 56), and near the chalcopyrite-cubanite-hexagonal pyrrhotite field in the Cu-Fe-S system at  $200^{\circ}$  C. (Figure 59), which is the common sulfide assemblage at Minnamax.

---

\* The model ore compositions for the basal troctolitic rocks (Table 4) are assumed to approximate the bulk composition of sulfides in the troctolitic rocks in the underground workings.

Using results of the experimental work, and field and microscopic observations, the following paragenesis is proposed for the magmatic sulfides at Minnamax. Pyrrhotite solid solution (poss) began to crystallize from a sulfide liquid at approximately 1180° C. In equilibrium with the poss was a copper-rich liquid, proposed to have formed the chalcopyrite-cubanite rich veins. Chalcopyrite solid solution (cpss) began to crystallize from the copper-rich liquid at approximately 970° C. A copper-rich liquid phase persisted until the reaction (at approximately 860° C.):



At approximately 610° C., pentlandite formed from the solid state reaction of poss and previously formed  $(\text{Ni,Fe})_{3+x}\text{S}_2$ , followed at slightly lower temperature by the exsolution of cubanite solid solution from the cpss. The approximate 1 to 1 ratio of metal to sulfur in the microprobed chalcopyrite (Table 5) indicates re-equilibrium of the chalcopyrite at temperatures as low as 200° C. (Yund and Kullerud, 1966). The hexagonal pyrrhotite exsolved troilite at approximately 140° C.

#### Hydrothermal Sulfides

Sulfide and gangue mineralization in the late stage veins and the calc-silicate pods is similar to that formed by hydrothermal solutions. The abundant calcite, quartz, and copper-sulfides (chalcopyrite, bornite, chalcocite) indicate that the solutions were relatively rich in silica, CO<sub>2</sub>, and copper. The presence of laumontite indicates that some solutions were below 350° C. (assuming 2 kb of pressure) (Liou, 1971). The euhedral quartz and pyrite growing outward from surfaces, and confinement of the mineralization to fractures and cavities in the calc-silicate pods indicate deposition in open spaces.

## SUMMARY AND CONCLUSIONS

The Minnamax deposit occurs at the contact of the Duluth Complex and the Virginia Formation. The Virginia Formation consists of pelitic hornfels with locally abundant calc-silicate pods and contains diabase intrusions - all have been deformed and metamorphosed to the pyroxene hornfels facies by the Duluth Complex. Mineral assemblages in the calc-silicate pods indicate temperatures of 650 to 750<sup>o</sup> C. (Kirstein, 1979). The Duluth Complex, emplaced as a crystal mush, consists of sulfide-bearing troctolitic rocks which are commonly norites, and contain orthoclase, biotite, and graphite. These features suggest assimilation of the Virginia Formation by the magma. Barren gabbro to peridotite xenoliths within the sulfide-bearing troctolitic rocks are similar in mineralogy and texture, and may have come from one differentiated cumulate body. The Duluth Complex - Virginia Formation contact is highly irregular, characterized by numerous Duluth Complex apophyses and Virginia Formation xenoliths. Granite to diorite dikes cut all lithologies.

The sulfides are primarily magmatic. Minor stratiform, sedimentary sulfides occur in the Virginia Formation, and hydrothermal sulfides and associated gangue occur along post-Duluth Complex fractures and in the calc-silicate pods. The magmatic sulfide mineralization, consisting of pyrrhotite, pentlandite, cubanite, and chalcopyrite, is primarily disseminated in the troctolitic rocks within 1000 feet of the Virginia Formation contact. Emplacement of the magma as a crystal mush may have inhibited settling of the sulfide liquid into depressions of the contact. Fe-Cu-Ni sulfide veins fill fractures and breccia zones, up to 30 feet

wide, in both the Duluth Complex and the Virginia Formation. Pelitic hornfels adjacent to the veins and the sulfide-bearing troctolitic rocks commonly is replaced by the sulfides. In one area the veins are sufficiently concentrated to form a high-grade copper zone, the Local Boy deposit. The veins probably formed by filter-pressing sulfide liquid from the troctolitic rocks into fractures. Some distinctly chalcopyrite-cubanite rich veins appear to have formed by separation of a copper-rich liquid from a pyrrhotite solid solution at magmatic temperatures. The abundance of sulfide veins and associated replacement sulfides in the pelitic hornfels with respect to other lithologies is due to the susceptibility of the hornfels to brittle deformation and to replacement by the magmatic sulfide fluids.

## APPENDIX I

## SAMPLES

This section lists by underground drift samples examined petrographically in thin section (T) and/or in polished section (P). Locations of the samples are given in the form A-B where:

A = the location within the drift (in feet)

B = the left (l) or right (r) rib of the drift  
(moving away from the shaft area)

The samples are identified by rock type and/or sulfide mineralization type. Essential minerals (>10%) are listed in order of abundance. For polished sections, only the essential sulfide-oxide minerals (>10% of the sulfide-oxide assemblage) are given. Abbreviations for the minerals are:

ap = apatite	il = ilmenite
aug = augite	mp = mesoperthite
bio = biotite	ol = olivine
bn = bornite	or = orthoclase
cp = chalcopyrite	pt = pentlandite
cord = cordierite	plag = plagioclase
cb = cubanite	po = pyrrhotite
gr = graphite	qtz = quartz
hyp = hypersthene	sulf = undifferentiated sulfides

SHAFT AREA

SAMPLE	LOCATION	ROCK-SULFIDE TYPE	ESSENTIAL MINERALS
MM6 (T)		metadiabase	plag, ol, hyp
MM7 (T)		metadiabase	plag, ol, hyp

A DRIFT

SAMPLE	LOCATION	ROCK-SULFIDE TYPE	ESSENTIAL MINERALS
MM-A-7 (T)	22-1	sulfide-bearing norite	plag, hyp
MM-A-4 (T)	25-1	biotite-rich pelitic hornfels	plag, cord, bio, hyp
MM-A-5 (T)	26-1	biotite schist	plag, cord, or, bio
MM-A-3 (T)	31-1	sulfide-bearing norite	plag, hyp, aug
MM-A-10 (T)	40-1	sulfide-bearing norite	plag, hyp, aug
MM-A-8 (T)	51-1	diorite dike	plag, or
MM-A-11 (T)	56-1	sulfide-bearing norite	plag, hyp
MM-A-11 (P)	56-1	disseminated sulfides in norite	cb, il, cp
MM-A-12 (T)	68-1	metadiabase	plag, hyp
MM-A-16 (T)	100-1	sulfide-bearing norite	plag, hyp, aug
MM-A-14 (T)	105-r	sulfide-bearing norite	plag, hyp
MM-A-17 (P)	132-1	interstitial sulfides in pelitic hornfels	po, cb
MM8 (T)	151-1	granite dike	mp, qtz, plag
MM-A-20 (T)	183-1	biotite schist	plag, bio, cord
AX-30 (P)	208-1	disseminated sulfides in troctolitic rock	po, pt, cb
MM20 (P)		disseminated sulfides in troctolitic rock	cb, cp, il
MM-A-23 (T)	244-1	sulfide-bearing anorthositic troctolite	plag, ol
MM-A-23 (P)	244-1	disseminated sulfides in anorthositic troctolite	cb, cp
MM-A-24 (T)	250-1	sulfide-bearing anorthositic troctolite	plag, sulf, ol
MM-A-24 (P)	250-1	disseminated sulfides in anorthositic troctolite	po, pt, cb
MM-A-26 (T)	253-1	biotite-rich pelitic hornfels	plag, or, hyp, cord, bio
MM-A-27 (T)	261-1	pelitic hornfels	plag, hyp, cord
MM-A-29 (T)	314-1	biotite-rich pelitic hornfels	or, plag, bio, cord, hyp
MM-A-30 (T)	320-1	sulfide-bearing norite	plag, hyp, aug
MM-A-32 (T)	336-1	metadiabase	plag, aug, hyp
MM9 (T)	338-1	metadiabase	plag, hyp
MM-A-33 (T)	351-1	pelitic hornfels	sulf, plag, hyp, cord
MM-A-33 (P)	351-1	interstitial sulfides in pelitic hornfels	po, cb
MM-A-34 (T)	353-1	pelitic hornfels	plag, hyp, cord, sulf
AX-32 (T)	376-1	sulfide-bearing gabbro	plag, aug, sulf
AX-32 (P)	376-1	disseminated sulfides in gabbro	po, cb, il, cp
MM-A-38 (T)	394-1	pelitic hornfels	sulf, plag, hyp, cord, bio
MM-A-38 (P)	394-1	interstitial sulfides in pelitic hornfels	po, cb

A DRIFT (continued)

SAMPLE	LOCATION	ROCK-SULFIDE TYPE	ESSENTIAL MINERALS
MM12 (T)	396-1	troctolite xenolith	plag, ol
MM-A-40 (T)	410-1	troctolite xenolith	plag, ol
AX-17 (T)	419-1	troctolite xenolith	plag, ol
AX-16 (T)	435-1	troctolite xenolith	plag, ol, aug
MM-A-41 (T)	439-r	anorthositic troctolite xenolith	plag, ol
MM-A-42 (T)	474-1	troctolite xenolith	plag, ol
MM-A-43 (T)	481-1	picrite xenolith	ol, plag
MM-A-44 (T)	483-1	picrite xenolith	ol, plag
AX-14 (T)	493-1	sulfide-bearing gabbro	plag, aug, ol
AX-14 (P)	493-1	disseminated sulfides in gabbro	cb, cp
MM-A-45 (T)	520-1	picrite xenolith	ol, plag
AX-12 (T)	521-1	feldspathic peridotite xenolith	ol, plag
AX-13 (T)	524-1	feldspathic peridotite xenolith	ol, plag
MM-A-46 (T)	528-1	feldspathic peridotite xenolith	ol, plag
MM-A-47 (T)	569-r	melagabbro xenolith	plag, aug, ol
AX-11 (T)	577-1	olivine gabbro xenolith	plag, aug, ol
AX-10 (T)	580-1	troctolite xenolith	plag, ol, aug
AX-8 (T)	603-1	sulfide-bearing troctolitic anorthosite	plag
AX-7 (T)	629-r	picrite xenolith	ol, plag
MM-A-48 (T)	644-1	feldspathic peridotite xenolith	ol, plag
AX-5 (P)	649-1	disseminated sulfides in troctolitic rock	cb, cp, po
AX-1 (T)	653-r	sulfide-bearing anorthosite	plag
AX-1 (P)	653-r	disseminated sulfides in anorthosite	po, il, cb, pt, cp
AX-3 (T)	657-r	sulfide-bearing anorthositic troctolite	plag, ol
MM-A-49 (T)	662-1	peridotite xenolith	ol

B DRIFT

SAMPLE	LOCATION	ROCK-SULFIDE TYPE	ESSENTIAL MINERALS
AX-20 (T)	42-1	metadiabase	plag, hyp
AX-21 (T)	70-1	metadiabase	plag, hyp, aug
AX-22 (T)	370-r	metadiabase	plag, hyp
AX-23 (T)	400-r	metadiabase	plag, hyp
AX-24 (T)	425-r	metadiabase	plag, hyp, ap
MM-B-1 (T)	534-1	metadiabase	plag, hyp
MM-B-3 (T)	563-r	graphite schist	sulf, plag, or, hyp, cord
MM-B-3 (P)	563-r	interstitial sulfides in graphite schist	po, cb, pt

B DRIFT (continued)

SAMPLE	LOCATION	ROCK-SULFIDE TYPE	ESSENTIAL MINERALS
MM-B-4 (P)	567-r	interstitial sulfides in pelitic hornfels	po, cp, cb
AX-26 (T)	580-1	mafic hornfels	aug, plag, hyp
MM-B-5 (P)	803-1	sulfide vein in pelitic hornfels	cp, pt
X-5 (T)	812-1	biotite schist	or, bio, hyp, plag, cord
MM-B-6 (P)	862-1	sulfide vein in troctolitic rock	po, cb
MM-B-7 (T)	869-1	sulfide-bearing norite	plag, hyp
MM-B-20c (T)	1046-1	sulfide vein in troctolitic rock	ol, plag, sulf
MM-B-20c (P)	1046-1	sulfide vein in troctolitic rock	po, cb
MM-B-20b (T)	1064-1	sulfide vein in troctolitic rock	sulf, ol
MM-B-20a (T)	1079-1	sulfide vein in troctolitic rock	sulf, plag, ol
MM-B-18 (T)	1092-1	sulfide vein in troctolitic rock	plag, sulf, ol
MM-B-18 (P)	1092-1	sulfide vein in troctolitic rock	po, cb
MM-B-16d (T)	1110-r	sulfide vein in troctolitic rock	sulf, ol, plag
MM-B-16d (P)	1110-r	sulfide vein in troctolitic rock	po, cb
MM-B-16e (P)	1110-r	sulfide vein in troctolitic rock	po, cb
MM-B-16c (P)	1110-r	sulfide vein in troctolitic rock	po, cb
MM-B-16b (P)	1110-r	sulfide vein in troctolitic rock	po, cb, cp
MM-B-16a (P)	1110-r	sulfide vein in troctolitic rock	pt, po, cb
MM-B-15c (T)	1118-1	sulfide vein in troctolitic rock	sulf, bio, ol, plag
MM-B-15c (P)	1118-1	sulfide vein in troctolitic rock	po, cb
MM-B-15b (P)	1118-1	sulfide vein in troctolitic rock	cb, po, pt
MM-B-15a (P)	1118-1	sulfide vein in troctolitic rock	cb, pt, po
MM-B-13a (T)	1115-1	granite dike	mp, qtz
MM-B-13b (T)	1115-1	quartz monzonite dike	mp, plag, qtz
MM-B-14 (T)	1117-r	granite dike	mp, qtz
MM-B-12 (T)	1207-r	granite dike	mp, qtz
MM-B-11 (T)	1220-r	granite dike	mp, qtz

C DRIFT

SAMPLE	LOCATION	ROCK-SULFIDE TYPE	ESSENTIAL MINERALS
MM-C-10 (T)	45-r	metadiabase	plag, hyp
MM-C-11 (T)	58-1	pelitic hornfels	plag, or, cord, hyp
MM-C-1a (P)	64-r	sulfide vein in pelitic hornfels	cb, cp, bn
MM-C-1b (P)	64-r	sulfide vein in pelitic hornfels	cb, cp, pt
MM-C-2 (T)	125-1	sulfide vein in pelitic hornfels	sulf, plag, hyp
MM-C-2 (P)	125-1	sulfide vein in pelitic hornfels	cp
MM-C-13 (T)	128-1	monzonite dike	plag, or
MM-C-14 (T)	143-1	graphite schist	plag, hyp, cord, gr
MM-C-3 (T)	218-1	sulfide vein in pelitic hornfels	sulf, plag, hyp
MM-C-3 (P)	218-1	sulfide vein in pelitic hornfels	cb, po, cp
MM-C-4 (T)	223-1	pelitic hornfels	sulf, plag, hyp, or, cord
MM-C-4 (P)	223-1	interstitial sulfides in pelitic hornfels	po, cb, pt
MM-C-5 (T)	225-1	mafic hornfels	plag, hyp, aug
MM-C-5 (P)	225-1	interstitial sulfides in mafic hornfels	cp, pt
MM-C-22 (T)	271-1	pelitic hornfels	plag, hyp, sulf
MM-C-22 (P)	271-1	sulfide vein in pelitic hornfels	cb, cp, pt
MM-C-23 (T)	275-1	sulfide-bearing troctolite	plag, ol
MM-C-23 (P)	275-1	disseminated sulfides in troctolite	cb, cp, po
MM-C-25 (T)	279-1	sulfide-bearing norite	plag, hyp
MM-C-27 (T)	362-1	pelitic hornfels	plag, hyp, or, cord
MM-C-30 (T)	500-r	graphite schist	plag, or, cord, gr
MM-C-32 (T)	572-1	biotite-rich pelitic hornfels	or, bio, hyp, plag, cord

D DRIFT

SAMPLE	LOCATION	ROCK-SULFIDE TYPE	ESSENTIAL MINERALS
MM-D-1 (T)	68-1	diorite dike	plag, or
MM-D-4 (T)	174-r	graphite schist	plag, gr, hyp, cord, sulf, qtz
MM-D-2 (T)	182-r	anorthositic norite	plag, hyp
MM-D-5 (P)	225-r	sulfide vein in pelitic hornfels	cb, po
MM-D-6 (T)	235-r	granite dike	mp, qtz, bio
MM-D-7 (T)	276-r	graphite schist	plag, gr, cord
AX-33 (T)	293-1	metadiabase	plag, hyp, aug
MM-D-10 (T)	330-r	biotite schist	plag, cord, hyp, bio

D DRIFT (continued)

SAMPLE	LOCATION	ROCK-SULFIDE TYPE	ESSENTIAL MINERALS
MM-D-10 (P)	330-r	sulfide vein in biotite schist	cp
MM-D-11 (T)	360-r	norite	plag, hyp, il
MM-D-12 (P)	365-r	sulfide vein in pelitic hornfels	cb, bn, po
X-1 (T)	371-1	mafic hornfels	aug, plag
MM-D-13 (T)	376-r	sulfide-bearing norite	plag, hyp
MM-D-14 (T)	401-r	sulfide-bearing norite	plag, hyp, ol
MM-D-14 (P)	401-r	disseminated sulfides in norite	il, po, cb, cp
MM-D-16 (T)	407-r	sulfide-bearing norite	plag, hyp
MM-D-17 (T)	455-r	metadiabase	plag, hyp, aug
MM-D-19 (T)	470-r	metadiabase	plag, hyp
MM-D-20 (T)	480-1	metadiabase	plag, hyp, aug

APPENDIX II  
EXPERIMENTAL WORK IN THE Cu-Fe-S AND Cu-Fe-Ni-S  
SYSTEMS AND ITS APPLICATION TO THE SULFIDES  
AT MINNAMAX

This section summarizes the results of experimental work in the Cu-Fe-S and Cu-Fe-Ni-S systems by Kullerud, Yund, and Moh (1969) and by Craig and Kullerud (1969), respectively. The experiments were conducted under isochemical conditions with composition, temperature, and pressure the intensive variables. At fixed compositions, variations in pressure affect the stability fields of sulfide phase assemblages in these systems by less than  $10^{\circ}$  C. Thus, the stability fields are primarily temperature and composition dependent. The sulfide phase assemblages which exist at specific compositions and temperatures are shown in Figures 56, 57, 58, and 59. The model ore compositions for the basal troctolitic rocks (Table 4) at Minnamax are shown by "M1" and "M2" on the phase diagrams. In the Cu-Fe-S system, the "M2" composition lies in the 2 phase field of pyrrhotite solid solution and copper-rich liquid at  $1000^{\circ}$  C. (Figure 56), and near the hexagonal pyrrhotite-chalcopyrite-cubanite field at  $200^{\circ}$  C. (Figure 59). This composition would permit the separation of copper-rich liquids to form the chalcopyrite-cubanite veins at Minnamax, and upon cooling it forms the hexagonal pyrrhotite-cubanite-chalcopyrite assemblage which is the predominant sulfide assemblage at Minnamax.

The experimental work suggests the following paragenesis and tem-

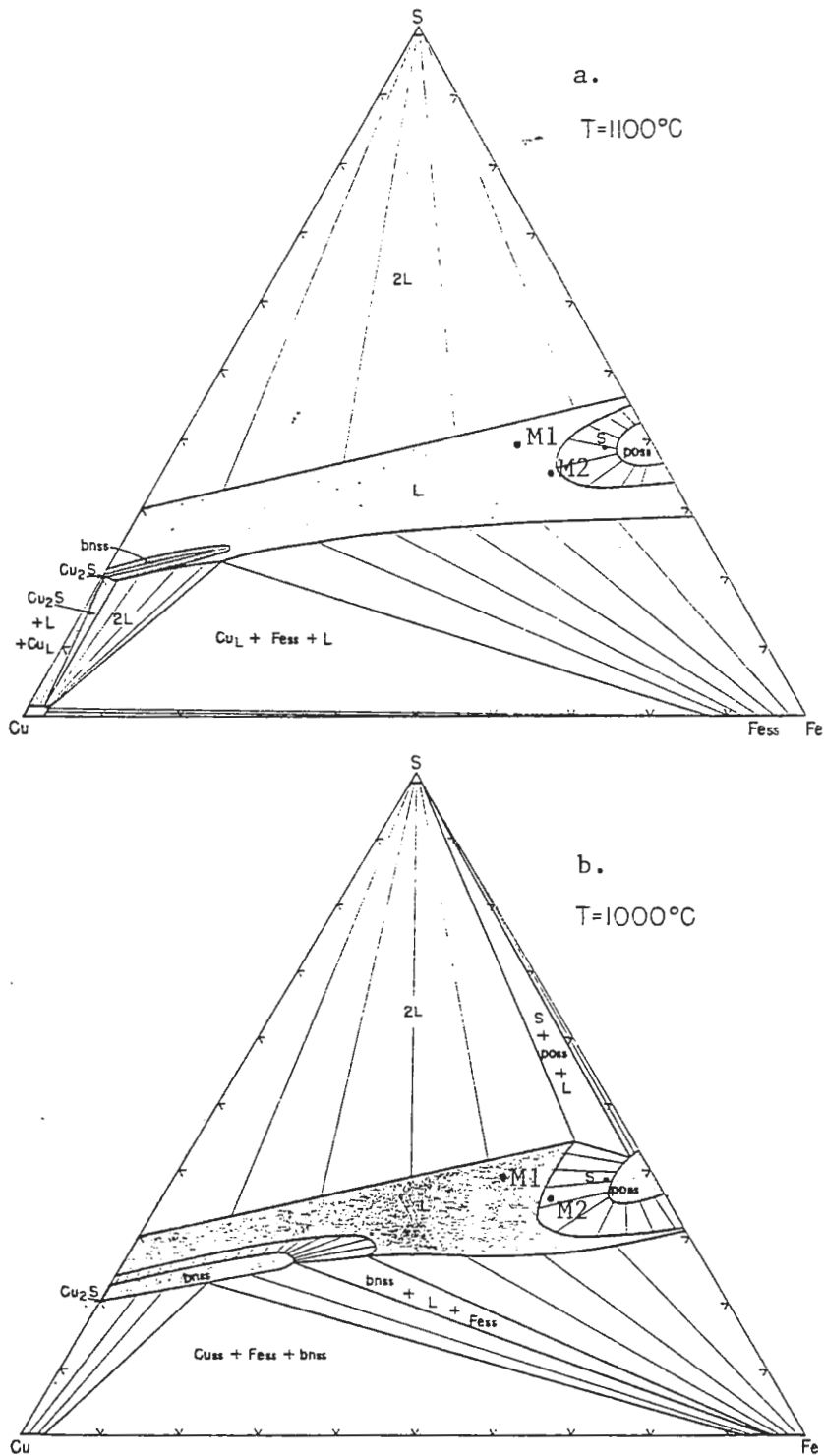


Figure 56. PHASE RELATIONS IN THE Cu-Fe-S SYSTEM. Model ore compositions for the basal troctolitic rocks (Table 4) are shown by "M1" and "M2". (a) Phase relations at  $1100^{\circ}\text{C}$ . Note that the ore compositions lie within the liquid field. (b) Phase relations at  $1000^{\circ}\text{C}$ . Note that "M2" lies within the field of pyrrhotite solid solution and copper-rich liquid. (from Kullerud, Yund, and Moh, 1969).

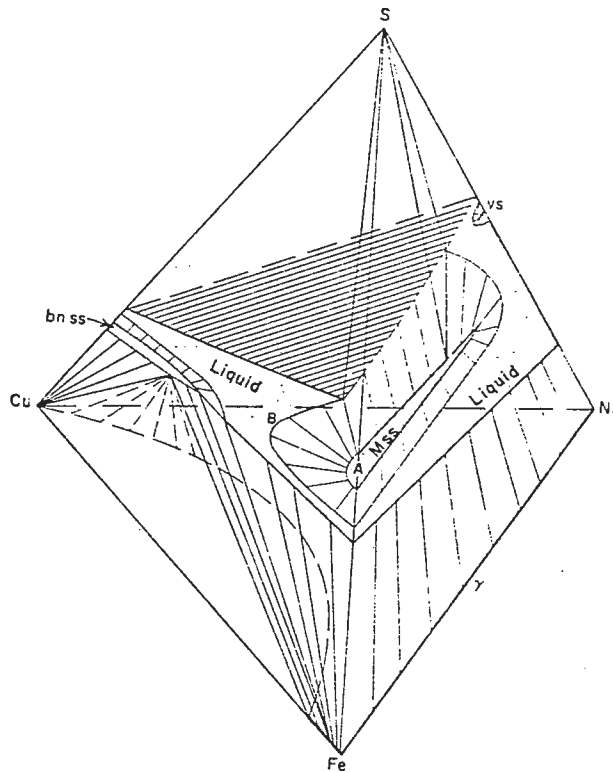


Figure 57. PHASE RELATIONS IN THE Cu-Fe-Ni-S SYSTEM AT 1000° C. The diagram is schematic; tie lines to S (liquid) are omitted for clarity. Note that pyrrhotite solid solution (mss) can stably coexist with copper-rich liquid. (from Craig and Kullerud, 1969)

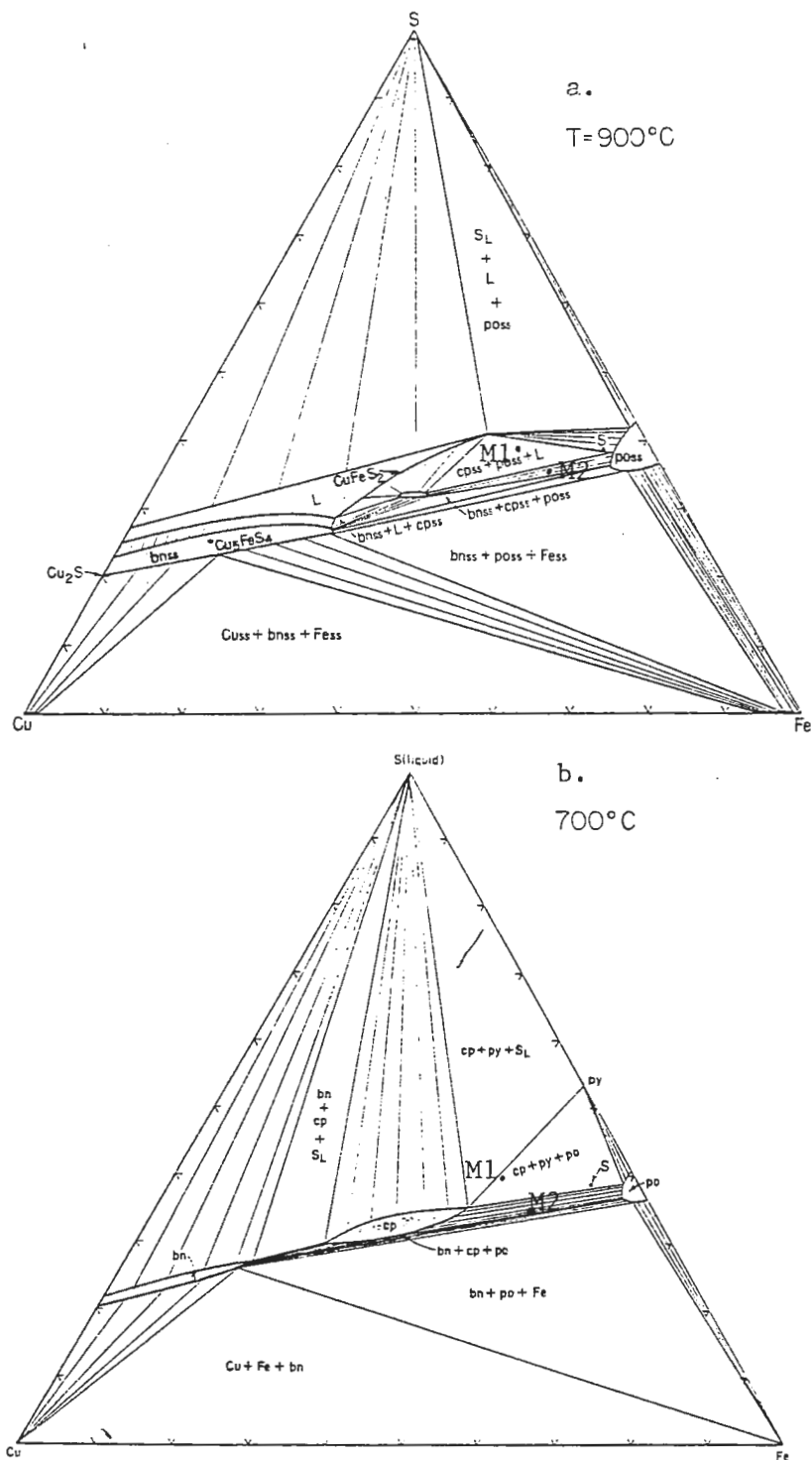


Figure 58. PHASE RELATIONS IN THE Cu-Fe-S SYSTEM. Model ore compositions for the basal troctolitic rocks (Table 4) are shown by "M1" and "M2". (a) Phase relations at 900°C. (b) Phase relations at 700°C. (from Kullerud, Yund, and Moh, 1969)

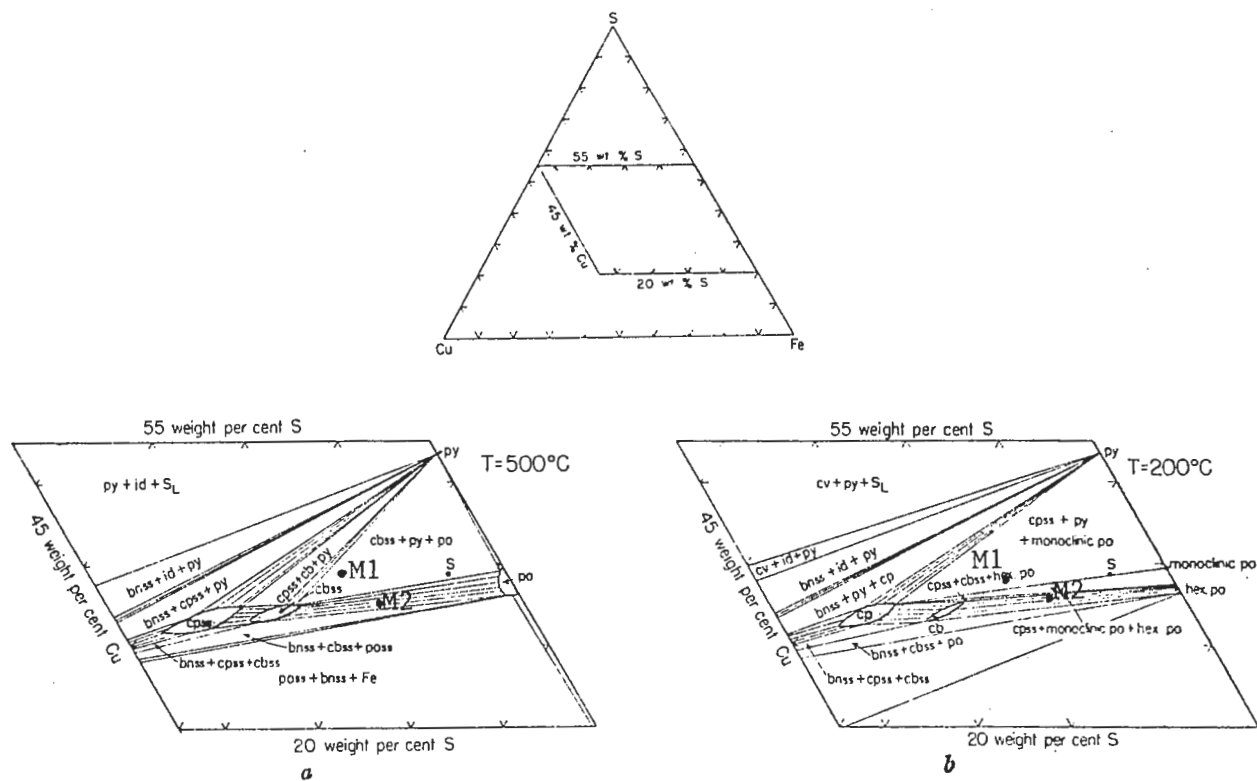


Figure 59. PHASE RELATIONS IN THE Cu-Fe-S SYSTEM. Model ore compositions for the basal troctolitic rocks (Table 4) are shown by "M1" and "M2". (a) Phase relations at 500<sup>o</sup> C. (b) Phase relations at 200<sup>o</sup> C. Note that "M2" lies near the hexagonal pyrrhotite-chalcopyrite-cubanite field. (from Kullerud, Yund, and Moh, 1969)

peratures of formation for sulfides of the ore composition and mineralogy observed at Minnamax.

TEMPERATURE (°C.)	PHASE RELATIONS
1000++	an immiscible sulfide phase occupied interstitial voids between crystalline silicates and oxides (Figure 56a).
1000+	pyrrhotite solid solution (poss) begins to crystallize in equilibrium with a relatively copper-rich liquid (Figures 56b and 57).
970	chalcopyrite solid solution (cpss) begins to crystallize from the copper-rich liquid (Figure 58a).
860	(Ni,Fe) <sub>3+X</sub> S <sub>2</sub> forms, and the reaction: copper-rich liquid + poss $\rightleftharpoons$ cpss + poss places a lower temperature limit on the existence of the copper-rich liquid (Figure 58b).
610	pentlandite forms from the solid state reaction of the poss and (Ni,Fe) <sub>3+X</sub> S <sub>2</sub> .
590	cpss exsolves to form cpss and cubanite solid solution (cbss).
200	the approximate 1:1 sulfur to metal ratio in the chalcopyrite at Minnamax (Table 5) indicates re-equilibrium at low temperatures, possibly as low as 200° C. (Yund and Kullerud, 1966).
140	hexagonal pyrrhotite inverts to low temperature pyrrhotite and exsolves troilite.

## REFERENCES CITED

- Abel, A. K. et al, 1979, Copper mineralization in the footwall complex, Strathcona Mine, Sudbury, Ontario: Canadian Mineralogist, v. 1, pp. 275-285.
- Anderson, G. E., 1956, Copper-nickel mineralization at the base of the Duluth Gabbro: Unpublished M.S. thesis, Univ. of Minnesota - Mpls., 74 pp.
- Bonnichsen, B., 1968, General geology and petrology of the metamorphosed Biwabik Iron Formation, Dunka River area, Minnesota: PhD. dissertation, Univ. of Minnesota - Mpls., 240 pp.
- \_\_\_\_\_, 1971, Hornfelses in the southern part of the Duluth Complex, Minnesota (abstract): 17th Annual Inst. of Lake Superior Geol. Proc., pp. 11-12.
- \_\_\_\_\_, 1972, Southern part of the Duluth Complex: in Geology of Minnesota: A centennial volume (P. K. Sims and G. B. Morey, eds.), Minn. Geol. Survey, pp. 361-387.
- \_\_\_\_\_, 1975, Geology of the Biwabik Iron Formation, Dunka River area, Minnesota: Econ. Geol., v. 70, pp. 319-340.
- Boucher, M. L., 1975, Copper-nickel mineralization in a drill core from the Duluth Complex of northeastern Minnesota: U. S. Bureau of Mines, Rept., Invest. 8084, 55 pp.
- Craig, J. R. and G. Kullerud, 1969, Phase relations in the Cu-Fe-Ni-S system and their application to magmatic ore deposits: in Magmatic ore deposits (H. D. B. Wilson, ed.), Econ. Geol. Mon. 4, pp. 344-358.
- French, B. M., 1968, Metamorphism of the Biwabik Iron Formation: Minn. Geol. Survey Bull. 45, 103 pp.
- Grosh, W. A. et al, 1955, Investigation of copper-nickel mineralization in the Kawishiwi River area, Lake County, Minnesota: U. S. Bureau of Mines, Rept. Invest. 5177, ii, 18 pp.
- Grout, F. F. and T. M. Broderick, 1919, The magnetite deposits of the eastern Mesabi range, Minnesota: Minn. Geol. Survey Bull. 17, 58 pp.
- Gundersen, J. N. and G. M. Schwartz, 1962, The geology of the metamorphosed Biwabik Iron Formation, Eastern Mesabi district, Minnesota: Minn. Geol. Survey Bull. 43, 139 pp.

- Hardyman, R. F., 1969, The petrography of a section of the basal Duluth Complex, St. Louis County, northeastern Minnesota: Unpublished M.S. thesis, Univ. of Minnesota - Mpls., 132 pp.
- Heinrich, E. W., 1965, Microscopic identification of minerals: McGraw-Hill Book Co., New York, 414 pp.
- Kirstein, M. H., 1979, Contact metamorphism of the Virginia Formation in the Minnamax deposit, St. Louis County, Minnesota: Unpublished M.S. thesis, Univ. of Minnesota - Duluth, 60 pp.
- Kullerud, G., R. A. Yund, and G. H. Moh, 1969, Phase relations in the Cu-Fe-S, Cu-Ni-S, and Fe-Ni-S systems: in Magmatic ore deposits (H. D. B. Wilson, ed.), Econ. Geol. Mon. 4, pp. 323-343.
- Liou, J. G., 1971, P-T stabilities of laumontite, wairwakite, lawsonite, and related minerals in the system  $\text{CaAl}_2\text{Si}_2\text{O}_8\text{-SiO}_2\text{-H}_2\text{O}$ : Jour. Pet., v. 12, pp. 379-409.
- Mainwaring, P. R. and A. J. Naldrett, 1977, Country-rock assimilation and the genesis of Cu-Ni sulfides in the Water Hen intrusion, Duluth Complex, Minnesota: Econ. Geol., v. 72, pp. 1269-1284.
- Mancuso, J. D. and J. D. Dolence, 1970, Structure of the Duluth Gabbro Complex in the Babbitt area, Minnesota (abstract): 16th Annual Inst. of Lake Superior Geol. Proc., p. 27.
- Perry, E. C., Jr. and B. Bonnicksen, 1966, Quartz and magnetite: Oxygen-18 oxygen-16 fractionation in metamorphosed Biwabik Iron Formation: Science, v. 513, pp. 528-529.
- Perry, E. C., Jr., F. C. Tan, and G. B. Morey, 1973, Geology and stable isotope geochemistry of the Biwabik Iron Formation, northern Minnesota: Econ. Geol., v. 68, pp. 1110-1125.
- Pfleider, E. P., G. B. Morey, and R. L. Bleifuss, 1968, Mesabi deep-drilling project, progress report no. 1: 41st Ann. Meeting, Minn. Section, A. I. M. E., pp. 59-92.
- Phinney, W. C., 1969, The Duluth Complex in the Gabbro Lake quadrangle, Minnesota: Minn. Geol. Survey Rept. Inv. 9, 20 pp.
- \_\_\_\_\_, 1972, Duluth Complex, history and nomenclature: in Geology of Minnesota: A centennial volume (P. K. Sims and G. B. Morey, eds.), Minn. Geol. Survey, pp. 333-334.
- Renner, J., 1969, The petrology of the contact rocks of the Duluth Complex, Dunka River area, Minnesota: Unpublished M.S. thesis, Univ. of Minnesota - Mpls.
- Ripley, E. M., 1978, Sulfur isotope studies of the Dunka Road Cu-Ni deposit, Duluth Complex, Minnesota (abstract): Econ. Geol., v. 73, pp. 1396-1397.

- Schwartz, G. M. and D. M. Davidson, 1952, Geologic setting of the copper-nickel prospect in the Duluth Gabbro near Ely, Minnesota: *Mining Eng.*, v. 4, no. 7, pp. 699-702.
- Sims, P. K. and S. Viswanathan, 1972, Giants Range batholith: in *Geology of Minnesota: A centennial volume* (P. K. Sims and G. B. Morey, eds.), Minn. Geol. Survey, pp. 120-139.
- Stevenson, R. J. et al, 1979, *Geology and mineralogy*, v. 3, chpt. 1: in *Regional copper-nickel study*, Minnesota Environmental Quality Board, open file report.
- Taylor, R. B., 1964, *Geology of the Duluth Gabbro Complex near Duluth, Minnesota*: Minn. Geol. Survey Bull. 44, 63 pp.
- Tyson, R. M. and L. L. Y. Chang, 1978, The petrology of the Partridge River troctolite and its importance to sulfide mineralization (abstract): *Econ. Geol.*, v. 73, p. 1399.
- Wager, L. R. and G. M. Brown, 1967, *Layered igneous rocks*: Freeman, San Francisco.
- Wager, R. E., R. Alcock, W. C. Phinney, and P. W. Weiblen, 1969, A comparison of the copper-nickel deposits of the Sudbury and Duluth basins (abstract): 13th Ann. Mining Symposium, 42nd Ann. Meeting, Minn. Section, A. I. M. E., pp. 95-96.
- Watowich, S. N., 1978, A preliminary geological view of the Minnamax copper-nickel deposit in the Duluth Gabbro: 39th Ann. Minn. Mining Symposium, 51st Ann. Meeting, Minn. Section, A. I. M. E., pp. 19: 1-11.
- Weiblen, P. W. and G. B. Morey, 1975, The Duluth Complex - A petrologic and tectonic summary: 36th Ann. Minn. Mining Symposium, pp. 72-95.
- White, D. A., 1954, Stratigraphy and structure of the Mesabi Range, Minnesota: Minn. Geol. Survey Bull. 38, 92 pp.
- Wolff, J. F., 1917, Recent geologic developments on the Mesabi Range, Minnesota: *Am. Inst. Mining Metall. Engineers Trans.*, v. 56, pp. 142-169.
- Yund, R. A. and G. Kullerud, 1966, Thermal stability of assemblages in the Cu-Fe-S system: *Jour. Pet.*, v. 7, pp. 454-488.